

**CFD HEAT TRANSFER SIMULATION OF THE HUMAN UPPER
RESPIRATORY TRACT FOR ORONASAL BREATHING CONDITION**

A Thesis
Submitted to the Graduate Faculty
of the
North Dakota State University
of Agriculture and Applied Science

By
Raghavan Srinivasan

In Partial Fulfillment of the Requirements
for the Degree of
MASTER OF SCIENCE

Major Department:
Industrial and Manufacturing Engineering

March 2011

Fargo, North Dakota

North Dakota State University
Graduate School

Title

CFD HEAT TRANSFER SIMULATION OF THE HUMAN UPPER RESPIRATORY

TRACT FOR ORONASAL BREATHING CONDITION

By

RAGHAVAN SRINIVASAN

The Supervisory Committee certifies that this *disquisition* complies with North Dakota State University's regulations and meets the accepted standards for the degree of

MASTER OF SCIENCE

North Dakota State University Libraries Addendum

To protect the privacy of individuals associated with the document, signatures have been removed from the digital version of this document.

ABSTRACT

Srinivasan, Raghavan, M.S., Department of Industrial and Manufacturing Engineering, College of Engineering and Architecture, North Dakota State University, March 2011. CFD Heat Transfer Simulation of the Human Upper Respiratory Tract for Oronasal Breathing Condition. Major Professor: Dr. Kambiz Farahmand.

In this thesis, a three dimensional heat transfer model of heated airflow through the upper human respiratory tract consisting of nasal, oral, trachea and the first two generations of bronchi is developed using computational fluid dynamics simulation software. Various studies have been carried out in the literature investigating the heat and mass transfer characteristics in the upper human respiratory tract, and the study focuses on assessing the injury taking place in the upper human respiratory tract and identifying acute tissue damage based on level of exposure. The model considered is for the simultaneous oronasal breathing during the inspiration phase with high volumetric flow rate of 90 liters/minute and a surrounding air temperature of 100 degrees centigrade. The study of the heat and mass transfer, aerosol deposition and flow characteristics in the upper human respiratory tract using computational fluid mechanics simulation requires access to a two dimensional or three dimensional model for the human respiratory tract. Depicting an exact model is a complex task since it involves the prolonged use of imaging devices on the human body. Hence a three dimensional geometric representation of the human upper respiratory tract is developed consisting of nasal cavity, oral cavity, nasopharynx, pharynx, oropharynx, trachea and first two generations of the bronchi. The respiratory tract is modeled circular in cross-section and varying diameter for various portions as identified in this study. The dimensions are referenced from the literature herein. Based on the dimensions, a simplified 3D model representing the human upper respiratory tract is

generated. This model will be useful in studying the flow characteristics and could assist in treatment of injuries to the human respiratory tract as well as help optimize drug delivery mechanism and dosages. Also a methodology is proposed to measure the characteristic dimension of the human nasal and oral cavity at the inlet/outlet points which are classified as internal measurements.

ACKNOWLEDGEMENTS

I dedicate the thesis work to my parents for their support and motivation they provided me throughout my MS degree.

I thank my advisor, Dr. Farahmand, because without his guidance it would have been not possible. I appreciate the support, suggestions and questions he had for me throughout the study.

I also want to thank Dr. Suzen (Mechanical Department) for his assistance with the CFD software.

I also want to thank Dr. Jun Zhang for suggestions and questions that assisted me in developing this thesis.

I thank Dr. Shi for his suggestions that motivated me to work on the thesis.

TABLE OF CONTENTS

ABSTRACT.....	iii
ACKNOWLEDGEMENTS	v
LIST OF TABLES	viii
LIST OF FIGURES.....	ix
CHAPTER 1. INTRODUCTION	1
1.1. Problem Definition	1
1.2. The Human Respiratory Tract (HRT)	1
CHAPTER 2. LITERATURE REVIEW	5
2.1. Mathematical Model and Numerical Simulation in the Respiratory Tract.....	6
2.1.1. Literature Review on Mathematical Models Generated	7
2.1.2. CFD Simulations in the HRT	13
2.2. Anthropometric Details of the HRT	24
CHAPTER 3. METHODOLOGY.....	30
3.1. Methodology.....	30
3.2. Other Significance	32
3.3. Assumptions and Limitations	33
3.4. A Three Dimensional Model of the Upper HRT	34
CHAPTER 4. CFD SIMULATION.....	40
4.1. Boundary Conditions.....	42
4.2. Simulation Run Setup.....	43
4.3. Scenarios Considered for Simulation	44
4.4. Simulation Results and Discussion.....	44

4.5. Nasal and Oral Breathing.....	52
4.6. Higher Temperature Inlet of 423 K.	60
4.7. Comparison Between Oronasal Breathing, Nasal Breathing and Oral Breathing	62
4.8. Comparison of the Model	64
CHAPTER 5. BURN EVALUATION.....	69
5.1. Fire and Fire Injury Statistics	70
5.2. Thermal Impact.....	71
5.3. Time for Thermal Injury to Occur in the Upper Human Respiratory Tract	73
5.4. Injury as a Result of Inhaling Hot Gas or Steam	74
CHAPTER 6. PROPOSED METHODOLOGY FOR ANTHROPOMETRIC DATA COLLECTION	77
6.1. Anthropometric Data	77
6.2. Current Methodology.....	78
6.3. Proposed Methodology	79
CHAPTER 7. CONCLUSION AND FUTURE RESEARCH.....	86
7.1. Conclusion	86
7.2. Future Research	86
REFERENCES.....	88
APPENDIX-1	97
APPENDIX-2.....	99

LIST OF TABLES

<u>Table</u>	<u>Page</u>
1. Simulation approaches. (Tang et al. 2004).....	19
2. Oral dimensions used by Grgic et al. (2004).....	27
3. Temperature range for degree of burn to occur.....	72
4. Temperature obtained at respiratory tract surface.....	72
5. Values for Henriques' constant (Lv et al. (2006)).....	73
6. Results solving equation 1.....	74

LIST OF FIGURES

<u>Figure</u>	<u>Page</u>
1. The Human Respiratory Tract.....	2
2. Simplified geometry used by Lv et al. (2006).....	12
3. Model of Trachea used by Ertbruggen et al. (2005)	13
4. The 17- generation Bronchial tree used by Gemci et al. (2002)	14
5. Nasal cavity geometry used by Inthavong et al. (2006).....	15
6. Nasal cavity geometry along with the mesh created by Lindemann et al. (2004) ..	16
7. Portion of the Respiratory Tract used by Luo et al. (2004).....	16
8. Three dimensional model of upper HRT developed by Martonen et al. (2001)	17
9. Three dimensional model of upper HRT used by Wang et al. (2009)	20
10. Simplified model used by Xi and Longest (2007)	21
11. Upper respiratory tract model. Yung-Sung et al. (1999).....	22
12. Upper respiratory tract model. Zhang and Kleinstreuer (2003).....	23
13. Nasal cavity geometry by Liu et al. (2009).....	24
14. Model generated by Cheng et al. (1996).....	25
15. Oral cavity dimensions determined by Robinson et al. (2009).....	26
16. Model of oral airway used by Grgic et al. (2004)	27
17. Dimensions determined by Mohebbi et al. (2008)	29
18. Geometry of the upper HRT for 3D analysis	35
19. Mesh generation	41
20. Temperature (K) variation inside the tract (A cross-sectional view).....	45
21. Temperature profile along the nasal, oral and tracheal region.....	46

22. Nasal temperature profile for mesh configuration 1	47
23. Nasal temperature profile for mesh configuration 2	47
24. Oral temperature profile for mesh configuration 1	48
25. Oral temperature profile mesh configuration 2	48
26. Tracheal temperature profile for mesh configuration 1	49
27. Tracheal temperature profile for mesh configuration 2	49
28. Velocity plot for mesh configuration 1	50
29. Velocity plot for mesh configuration 2	50
30. Temperature (K) plot for mesh configuration 1	51
31. Temperature (K) plot for mesh configuration 2	52
32. Pressure (Pa) plot for mesh configuration 1	53
33. Pressure (Pa) plot for mesh configuration 2	53
34. Streamline plot for mesh configuration 1	54
35. Streamline plot for mesh configuration 2	54
36. Velocity profiles for nasal breathing	55
37. Velocity profiles for oral breathing	56
38. Temperature profile along nasal cavity during nasal breathing	57
39. Temperature profile along nasal cavity during oral breathing	57
40. Temperature profile along oral cavity during nasal breathing	58
41. Temperature profile along oral cavity during oral breathing	58
42. Temperature profile along trachea during nasal breathing	59
43. Temperature profile along trachea during oral breathing	59
44. Velocity profile for inlet temperature of 423 K	60

45. Temperature profile along nasal cavity for inlet temperature of 423 K.....	61
46. Temperature profile along oral cavity for inlet temperature of 423 K.....	61
47. Temperature profile along trachea for inlet temperature of 423 K.....	62
48. Comparison between oronasal breathing, nasal breathing and oral breathing.....	63
49. Velocity contour at nasal inlet.....	64
50. Comparison between current simulation model and Lindemann et al. (2004).....	65
51. Temperature profile as reported by Lindemann et al. (2004).....	66
52. Temperature profile along nasal cavity for the simplified geometry.....	67
53. Cross-section at inlet (a) and towards the center (c, d). Subramanian et al. (1997)	67
54. Ω (Burn value) value at various time (seconds) level.....	75
55. Anterior portion of the Nasal cavity.....	80
56. Tool for measuring Nasal cavity dimension. (Patent number US6659963).....	80
57. Pictorial view of the tool (Patent number US6659963).....	81
58. Tool for measuring Oral cavity dimension.....	82
59. Top view of Oral cavity (mm).....	83
60. Oral cavity measuring instrument (All Dimensions in mm).....	84

CHAPTER 1. INTRODUCTION

1.1. Problem Definition

Industrial safety has top priority when designing a facility even though safety issues are dealt with in every aspect of the design, construction, and operation, mishaps do happen unexpectedly. Of these the injury due to inhalation of hot gas is commonly encountered posing a threat to human life when dealing with fire and combustible material. Various papers have been published in the literature studying the heat and mass transfer characteristics in the human respiratory tract. Most of these studies focus on the temperature and water vapor exchange through the respiratory tract. However studies related to evaluation of burn injury inside the Human Respiratory Tract (HRT) is also studied and very limited literature available. The 2D analysis of the burn injury evaluation has also been performed. These evaluations help in determining the degree of injury and the possible type of remedy provided.

1.2. The Human Respiratory Tract (HRT)

The human respiratory tract consists of the nasal and oral cavity, pharynx, larynx, trachea, bronchi (only first two generations of the bronchi) and lungs (not included in this study) as shown in Figure 1. The human respiratory system as a whole consists of the respiratory tracts and the respiratory muscles that help in the air movement and heat exchange in and out of the human body. The primary function of the human respiratory system is to deliver or supply oxygen to the tissues and the heart. Besides oxygen supply and olfaction (sense of smell), there is another important function that takes place in the human respiratory tract which consists of cleaning, filtering, heating cooling and

humidifying the inhaled air. The upper respiratory tract consisting of the nasal cavity, pharynx and larynx contributes to the inhalation process.

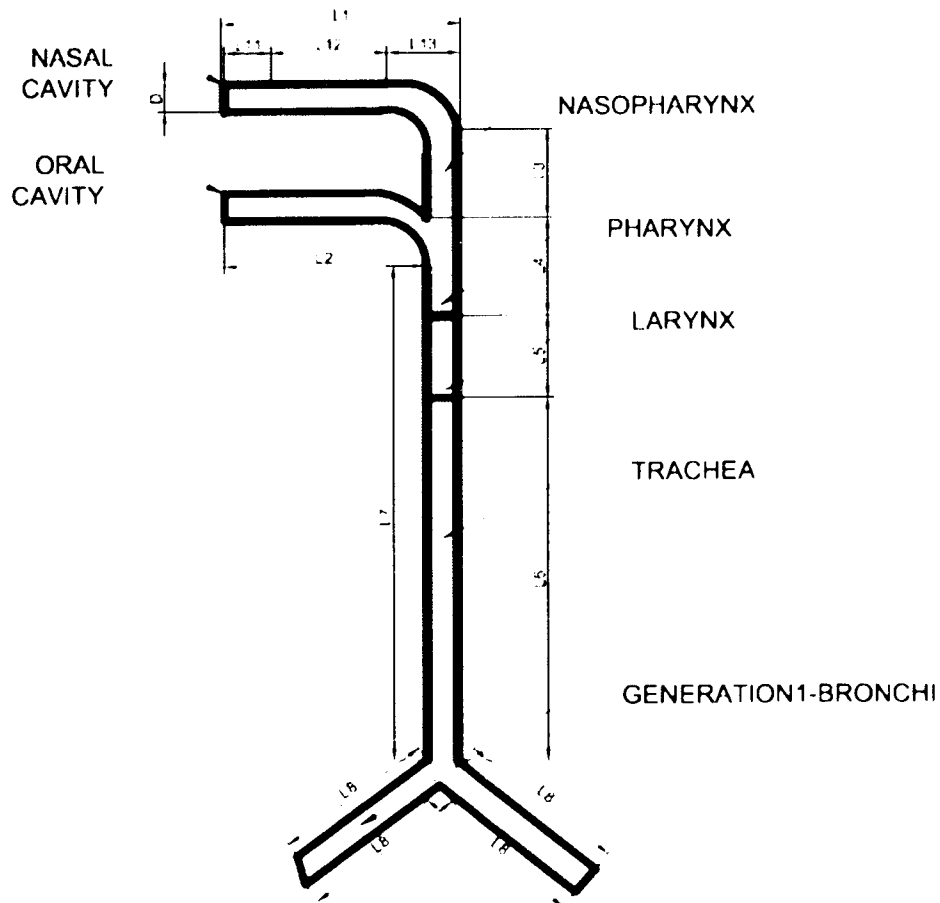


Figure 1. The Human Respiratory Tract

Various Studies have investigated the heat and mass transfer in the human respiratory tract. The inspired air is heated to normal body temperatures and the expired air is cooled to regain the heat back in the body. These measurements of the heat and water transport were carried out by the use of thermocouples. Mathematical models depicting the heat and water transport phase by McCutchan et al., Tsu et al. and Tsai et al. were used for numerical simulation and to determine the heat transfer characteristics of the

region. Recent trends include, generating a three dimensional model of the respiratory tract into CFD software such as Ansys CFX. The model generation is based on the magnetic resonance imaging (MRI) or computed axial tomography (CAT) scan of the respiratory tract obtained from a healthy volunteer. Most models use the Navier-Stokes equation for the CFD simulation. The simulation performed in the above cases analyzed the heat transfer at room temperature. Lv et al. performed a 2D simulation to analyze the injury taking place in the respiratory tract during inhalation of hot air. The study of the heat and mass transfer, aerosol deposition and flow characteristics in the upper human respiratory tract using computational fluid mechanics simulation requires access to a 2D or 3D model for the human respiratory tract. An exact model is a complex task to obtain since it involves use of imaging devices on human body. Hence a simplified 3D geometry representing the upper human respiratory tract is developed here consisting of nasal cavity, oral cavity, nasopharynx, pharynx, oropharynx, trachea and first two generations of the bronchi.

A study of the heat transfer mechanism of the human respiratory tract would help asses any heat, smoke and fire related injury affecting the human respiratory tract. The design of respirator systems used by people working in extreme environments like fire fighters exposed to forest fire, chemical and biological exposure or hazardous material exposure can be better improved by comprehensive study of the thermal profile. This can help in better occupational health and safety in case of firefighter's and emergency responders. These emergency responders are exposed to extreme temperatures and do have protection equipment, like a respirator for oxygen supply, but still the inhaled air is heated because of the extreme temperature in the surrounding atmosphere. Lv et al. evaluated the

burn injury due to inhalation of hot gas. The evaluation was based on a two dimensional model of heat transfer normal respiration characteristics were taken into account (nasal breathing, cycle duration 3 seconds and respiration frequency 20 breaths/minute). In emergency situations there is bound to be chaos and confusion in addition to the physical load, the increased heart rate and respiration rate dictate a high possibility of oronasal breathing (simultaneous breathing via oral and nasal cavity) taking place expectedly when under physical stress. A 3D heat transfer study is performed here to identify the temperature obtained at the surface of the tissue during the inspiration phase. Various works are available in the literatures that study the temperature profile in the respiratory tract which includes the nasal and the oral respiratory tract separately.

CHAPTER 2. LITERATURE REVIEW

Lv et al. analyzed the degree of burn in the respiratory tract, but their model had some limitations 1) was a 2 dimensional model; and 2) it analyzed only the nasal tract. Other's have also investigated cases under normal breathing conditions but lacked in providing a 3D heat transfer study specifically for oronasal breathing. This cannot be the case in every situation, for instance, during a fire hazard it is more likely that there is oronasal breathing so it would be appropriate to analyze both respiratory tracts simultaneously with alternate breathing pattern such as hyperventilated conditions than normal breathing so as to satisfy the oronasal breathing pattern.

To study the characteristics like particle deposition, burn injury, heat and mass transfer in the upper human respiratory tract (HRT) various models were developed. These models were based on the images obtained from computed tomography (CT) scans, MRI and or acoustic rhinomanometry (AR). These procedures are complex, and access to these images is limited. The cost involved with obtaining and using these types of data is also too high. Hence simplified airway geometry of the HRT consisting of nasal airway, oral airway, pharynx, larynx, trachea and first two generations of the bronchi is developed based on the data available from the literature herein.

Simplified model of the respiratory tract were used to study the desired phenomena in the HRT. Ertbruggen et al. used an anatomically based three dimensional model consisting of trachea up to the segmental bronchi to simulate flow and particle transport. The model is based on the morphometric data available in the literature. Gemci et al. used a simple model of a straight tube that depicts the human larynx and the trachea to study the

dispersion of the drugs spray droplet using CFD simulation. Grgic et al. used an idealized mouth and throat geometry to study the aerosol deposition and flow characteristics. The geometric model created here was with reference from CT scans, MRI and direct observations. Luo et al. used a simple airway model to study the flow characteristics, a simple geometric model representing the trachea and the first two generations of the bronchi. The dimensions of the model are based on data available and these are used by the authors here to develop the geometry. Yu et al. used the parameters from the Wiebel's lung model. The geometry consisted of the first two generations of the bronchi applied for the simulation. Zhang et al. studied the heat and mass transfer characteristics in the human oral cavity, pharynx, larynx, trachea and up to the third generation of the bronchi. Xi and Longest used simplified geometry for the oral cavity, pharynx, larynx and tracheal region, using CT scans and available data to develop a realistic model of the oral airway with nasopharynx.

2.1. Mathematical Model and Numerical Simulation in the Respiratory Tract

The literature review is divided into two sections. The section one sub divided into two subsections where first part focuses on the analysis of the heat and mass transfer characteristics using mathematical model and numerical simulations. The second part discusses the use of Computational Fluid Dynamics (CFD) and other fluid dynamics software used for the study of the heat and mass transfer characteristics in the Human Respiratory Tract (HRT). The second section focuses on the Anthropometric data measurements for the HRT. A methodology is proposed in chapter 6 for determining the dimensions of the preliminary portion in the HRT for both the nasal and the oral cavity.

2.1.1. Literature Review on Mathematical Models Generated

Daviskas et al. (1990) have derived a time dependent model based on the single differential equation with an analytical solution to predict the heat and mass transfer in the human respiratory tract. The modeling of the airflow within the human oral cavity was assumed to be laminar in nature. This model was run in the software FORTRAN and then the results were compared with the data recorded from the experiment which involves the measurement of the parameters in the human oral cavity. The authors concluded with the fact that the air equilibrates with the wall before it reaches body conditions, the respiratory conditions affect the conditioning of the inspired air and the walls of the upper airways being unsaturated.

Enkhbaatar and Traber (2004) have emphasized on the pathophysiological aspects of lung injuries as the injury rate due to the burn caused by inhalation of smoke is high. The authors have explained the factors affecting the mechanism which is due to the injury in the human lungs attributed to inhalation of nitric oxide.

Farahmand and Kaufman (2001) measured the response time of fine thermocouple in air. The conditions for the experimental purposes were similar to that of the human respiratory system. This method also takes into account the mass transfer characteristics like measuring the relative humidity. Also Farahmand and Kaufman (2006) have developed a method to measure the response time of wet bulb thermocouples (wire diameter 0.005 cm) in air simulating the human respiratory conditions. An experimental setup was put up to measure the response time of the thermocouple arrangement. During the theoretical analysis of the thermocouple temperature responses were considered as step change. The analysis of the experiment found that there were no significant difference in

the response times considering the two different conduits used for the experiment. Thus a method for repeatable and reliable measures of the response time of the thermocouples is concluded above.

Kaufman and Farahmand et al. (2006) have demonstrated a method of measuring the heat and mass transfer characteristics of the human oral cavity. This was done by measuring the multiple airstream and surface temperatures simultaneously with the help of a thermocouple arrangement (7 numbers of thermocouple). The relative humidity in this case was computed psychometrically. The airflow was modeled in the pipe flow and this data was compared with the data obtained from the oral temperature measurements. This was done by correlating the Nusselt's number to Reynolds number. The experiment concludes that the Nu measured in the pipe differs from that of the oral cavity which questions the basic assumption regarding the shape of the conduit.

Saidel et al. (1983) developed a mathematical model describing the heat and mass transfer characteristics in both radial and axial directions of a cylinder which represents an trachea. The mass and energy balance equations here are expressed as a function of radial, axial positions and time. The above model used a alteration-direction algorithm to solve the two finite difference equations.

Hanna and Scherer et al. (1986) have proposed a new mathematical model to study the heat and water exchange in the human respiratory tract. This model is developed as a function of distance into the airways. The model is derived by applying mass, momentum and energy into the selected cross section. The model was solved numerically using the data available from the literature. Fourth order predictor-corrector numerical solution was

used to solve the equation. Chilton-Colburn j factor was used to analyze the mass transfer characteristics.

Hanna and Scherer et al. (1986) have demonstrated a different way to study the mass transfer coefficients in the upper respiratory tract (nasal) by using the acrylic cast model of the same using the naphthalene sublimation technique. The experimental results were found to be satisfactory with the physiological measurements and data available from the measurements take from the in-vitro systems of similar flow geometry.

Ingenito et al. (1986) have conducted a finite difference analysis based on a numerical control model using the integral formulation of the first law of thermodynamics. The derivation of the model was based on the data available from the literature. These equations were then solved by using a first order explicit finite difference scheme in both time and space. The data from the predicted and experimental values were compared and they have observed a positive correlation with the inspiration as well as the expiration temperatures.

Tsu et al. (1988) developed a one dimensional mathematical model describing the dynamic heat and gas exchange process taking place in the human airway. The development of the mathematical model takes into account the three factors, exchange of soluble gas between respired air and airway mucosa, mucous layer which expands and contract based on inspiration or expiration and the secretion of fluid from the tissue to the mucus. The mathematical modeling here analyzes the two approaches, one consisting of a detailed continuity and energy balance equation and the other by use of control volume analysis. Based on the advantages the control volume analysis provides, this was used for the modeling purposes. The development of mathematical model was performed

considering a section respiratory tract and this can be applied to any part of the respiratory tract. The control volume description of the airway is dividing into three regions consisting of airway lumen, a mucous layer and an underlying nonperfused tissue layer. A total of 17 equations based on the control volume analysis were derived and solved by using LSODE, a time integration software package which solves differential equations. The boundary layer conditions were also defined. These results obtained were compared with the data available in the literature. Two different papers for nasal and oral data were referred. The predicted temperature profiles generated from the data were found to having good correlation for both nasal and oral.

McCutchan and Taylor (1951) studied temperature, humidity and enthalpy of the inspired and expired air. The goal here was to study the characteristic in high temperatures, high humidity and to extrapolate the data which can help detect critical temperatures that exceed human tolerance.

McFadden et al. (1985) have conducted an experiment to study the thermal profile of the heat transfer in the human intrathoracic airways. This experiment consisted of inserting a thermocouple arrangement designed and calibrated into the human nasal cavity. The distance of the nasal probe and the nose surface was constantly recorded. The subjects were made to perform eucapnic hyperventilation and the temperature within the airways which was recorded continuously. The data obtained was analyzed using paired t-tests and one factor ANOVA. The results were studied and was concluded that there is continuous change in temperature both during inspiration as well as expiration phase. This was in agreement to the work previously available in the literature.

Naftali et al. (1998) conducted a 2 dimensional computational model study of transport phenomenon considering the transverse cross section of the human nose. The Navier-Stokes equations for the laminar and incompressible air flow are taken into account. The initial and boundary conditions are also defined here. These equations are non-linear which are solved by using the finite element method. The local rates of water vapor and heat from the nasal tissue are defined here. The experiments are performed on criteria such as normal breathing, breathing during exercise, abnormal nasal cavities and extreme environments. It was concluded that in all the above cases inhaled air was warmed and humidified to suit the body conditions.

Varene et al. (1986) compared the heat and mass transfer characteristics in the human mouth and nose breathing. This comparison was concluded by the facts that expired air is not saturated with water, latent heat constitutes the larger part of heat transfer, countercurrent heat recovery is imperfect and that there exists no large difference between oral and nasal breathing considering the heat and mass transfer phenomena.

Keck et al. (2000) measured the temperature during the respiration phase of 50 volunteers. These values based on the experiment were correlated with that obtained with a rhinomanometry. The increases in temperatures based on the geometry of the nasal cavity were studied. It was concluded here that the increase in the nasal temperature can be compared to the logarithmic model curve of air temperature passing through a heated cylinder.

Niinimaa et al. (1981) determined the oronasal distribution of the respiratory airflow experimentally by collecting data from 30 volunteers in normal and excited conditions. At rest, the majority of the subjects breathed nasally but as degree of exercise

increased the oronasal breathing commences and the volume of air intake increases in the oral and reduces at the nasal cavity.

Webb et al. (1951) studied the thermal changes taking place in the human nasal tract by measuring the temperatures with the use of thermocouples. The cold environment was taken into account if it damages the pulmonary airways but the results proved that even if in cold environment the inspired air is heated up and then delivered to the pulmonary airways.

Lv et al. (2006) derived a transient 2 D model to study the heat and mass transfer characteristics, and this was further used to predict the impact of inhaled hot gas during early stages of fire. The model was developed based on the Pennes bioheat transfer equation. The Boundary conditions are specified for the same. The equations developed were solved by using a predictor-corrector numerical method. The values for the tissue and air properties are taken from available literature. The analysis part here involves the use of the individual's physiological and environmental variables. The burn evaluation is then performed based on the Henrique's model. The 2D model, a long right circular cylinder as shown in Figure 2 is used by the authors in their study.

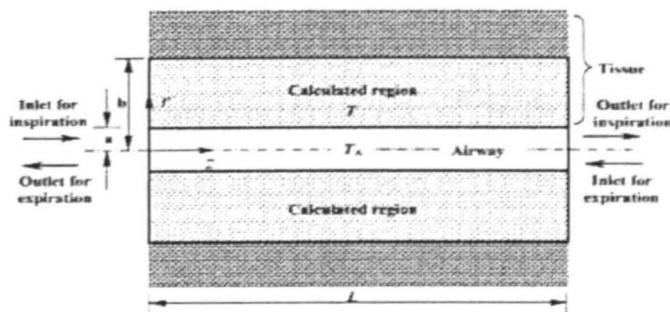


Figure 2. Simplified geometry used by Lv et al. (2006)

2.1.2. CFD Simulations in the HRT

Ertbruggen et al. (2005) studied the gas flow and particle deposition in a model based on the morphometric data available in the literature. The model used here is shown in Figure 3 consists of the tracheal and the bronchial region. The expansion caused in the walls of the airway during breathing was neglected in this model. The Reynolds number 2500 was based on the diameter of the tube.

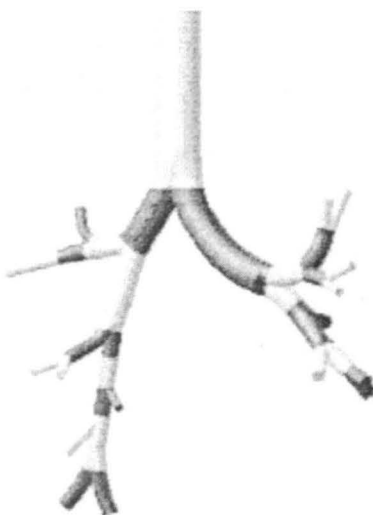


Figure 3. Model of Trachea used by Ertbruggen et al. (2005)

Gemci et al. (2002) used both, computational fluid dynamics simulation and experimentally by using phase doppler interferometry to study the inhalation of airflow containing dispersed drug spray droplets. The cross-section used here was of a straight tube of circular cross-section depicting the larynx and the trachea. Gemci et al. (2008) have also performed a CFD analysis of airflow in the upper 17 generations of the human respiratory tract. The authors performed the computational model on the 17 generations of the human lung available in literature as shown in Figure 4. The governing equations used here were the Navier-Stokes and the continuity equations with appropriate boundary

conditions. Turbulence model and large eddy simulation was also taken into account. Air was assumed to be incompressible. The pressure drops observed along the flow agree with that in the existing literature. Secondary swirling flows resulting from the airways curvature was also observed.

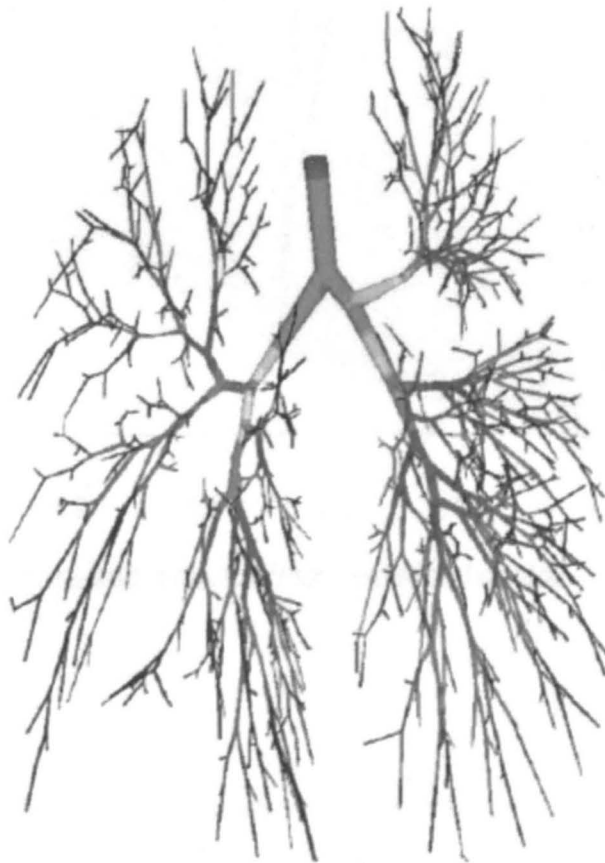


Figure 4. The 17- generation Bronchial tree used by Gemci et al. (2002)

Inthavong et al. (2006) performed a numerical study of the spray particle deposition in the human nasal cavity. The authors here considered simulated conditions with added insertion angle for the drugs into the nasal cavity and the injected particle velocity to capture its flow properties along the nasal cavity. The geometry simulated here is shown in the Figure 5. The model used also provides the length of the nasal cavity. Similar kind of

geometry was used by Zhang et al. (2008), Lindemann et al. (2004) and Pless et al. (2004) for performing the numerical simulation.

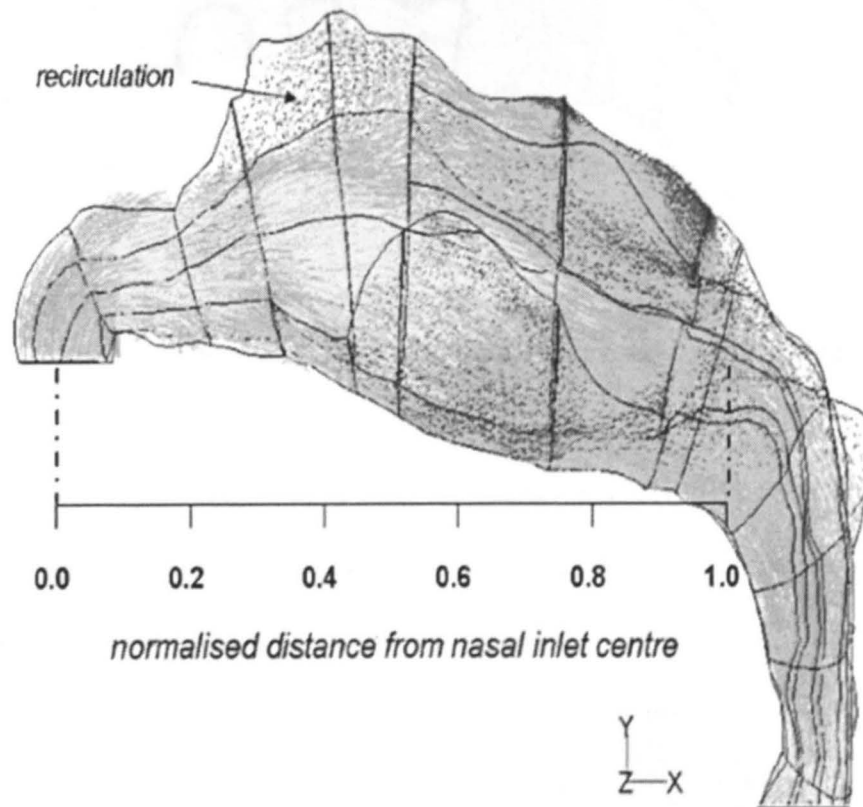


Figure 5. Nasal cavity geometry used by Inthavong et al. (2006)

Lindemann et al. (2004) have studied the temperature distribution along the nasal cavity during the inspiration phase. The 3 dimensional model of the human nasal cavity shown in Figure 6 was developed based on the CT scan of a healthy adult volunteer. Mesh optimization algorithms were used to optimize the quality of the mesh. Navier-Stokes equation for 3 dimensional and incompressible fluid flows and viscous fluids were employed. The intranasal temperatures were also practically measured by the use of thermocouples. The results in both cases were compared and found to be satisfactory.

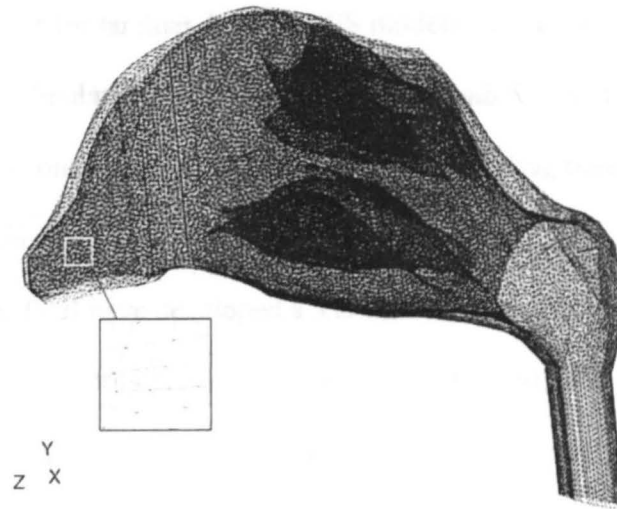


Figure 6. Nasal cavity geometry along with the mesh created by Lindemann et al. (2004)

Luo et al. (2004) performed a large eddy simulation model (LES) using a simple airway model for the trachea and the bronchi as shown in Figure 7. The dimensions for the trachea and the bronchi were determined from that available in literature.



Figure 7. Portion of the Respiratory Tract used by Luo et al. (2004)

Numerical methods for laminar, $k-\epsilon$ and LES models were used for the above simulation purpose. The simulation results were compared with the existing $k-\epsilon$ models for verification. The authors concluded that LES is capable of modeling transitional/turbulent flows in the upper human respiratory tract.

Martonen et al. (2002) have developed a 3 D numerical simulation of the human upper respiratory tract. The extrathoracic airways (head and throat) were also considered. The simulations were based on the 1:1 scale of the medical school model used for instructional purposes. This reconstructed by CFX mesh build continued by flow simulations. The governing equations are based on the Navier-Stokes equations. Inspiration and expiration was assumed to be via the nasal cavity. This analysis studied the air flow during inspiration, expiration and the pressure differences during the respiration cycle. This simulation performed was based on the three dimensional model developed by Martonen et al. (2001) shown in Figure 8.

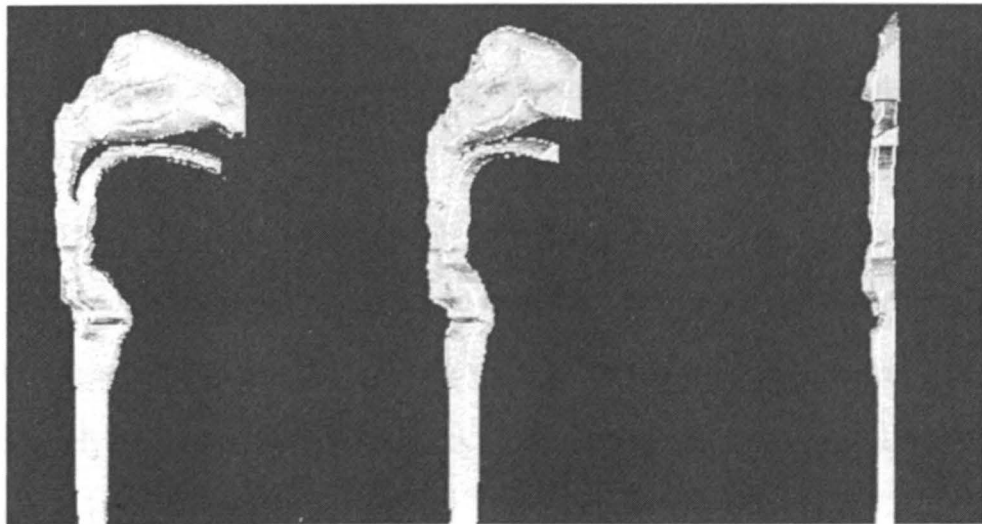


Figure 8. Three dimensional model of upper HRT developed by Martonen et al. (2001)

Pless et al. (2004) have simulated the flow of the air in the human respiratory tract to study the characteristics during the expiration phase. A three dimensional model was developed based on the CT scan of a male volunteer. The numerical simulation was based on the Navier-Stokes equation for 3-D incompressible and viscous fluids. The authors concluded the paper by demonstrating a close relationship between the heat exchange during expiration and the airflow pattern. This emphasizes the fact that nasal air conditioning takes place in both inspiration and expiration.

Srinivasan et al. (2011) conducted a three dimensional heat transfer simulation using a CFD software to study the temperature profile through the upper human respiratory tract consisting of nasal, oral, trachea and the first two generations of bronchi. The model developed is for the simultaneous oronasal breathing during the inspiration phase with high volumetric flow rate of 90 liters minute and the inspired air temperature being 100 degrees Centigrade. The geometric model depicting the upper human respiratory tract is generated based on the data available (literature cited). The results of the simulation give the temperature distribution along the center of the respiratory tract and the surface tissue of the respiratory tract.

Tang et al. (2004) in their study outline the various simulation approaches for the breathing conditions other parameters as shown in Table 1. Simulation approaches. (Tang et al. 2004). The author here concludes that the drug delivery mechanism in the cavity is influenced largely by the airflow characteristics and numerical simulation being a good tool to study the characteristics of the airflow.

Table 1. Simulation approaches. (Tang et al. 2004)

Breathing conditions		Behavior and Symptoms	Related locations	Main flow features	Simulation approaches	
1	Normal: -quiet -resting -sleeping	Inspiration Expiration Flow rate of 125-200 ml/s	a. nasal cavity b. larynx c. trachea d. bronchi	Periodic flow, Laminar flow, Gap flow, small deformation at the junction of b and c	Sinusoidal velocity profiles, single phase approach	
2	Abnormal: -exertion -sickness -physical exercise	-asthma -nasal polyp -heavy vibrissae -foreign-body -sneezing Flow rate of 200-625 ml/s		a. nasal cavity b. larynx c. trachea d. bronchi	Constriction flow, obstruction flow, extra mucus flow, high flow rate, turbulent flow, deformation at the junction of a to d	single phase approach, multiphase approach, turbulent model, frees surface model, Fluid-Structure interaction (FSI) approach
		-morbid surface			excessive dry/secretion of the mucosal surface permeation flow	liquid film flow model, specific boundary model, porous media model
		-cough -snore -yawn	a-d e. mouth	high flow rate with deformations and vibrations in c or d-e	FSI approach acoustic approach	
3	Drug delivery: -inhaler -collunarium	Therapy spray	a. nasal cavity b. larynx c. trachea d. bronchi	aerosol flow droplet flow free surface flow permeation flow biological reaction	multiphase approach, FSI approach porous media model	
4	Air pollutions: -dust air: inorganic dust, organic dust, synthetic material dust -chemical gas	Silicosis Asbestosis chronic obstructive pulmonary diseases, COPD				

Wang et al. (2009) studied the respiratory airflow in the human upper airway considering the human upper respiratory tract except the oral tract and up to three generations of bronchi in the lower respiratory tract. The model shown in Figure 9 was based on the CT scan of a healthy volunteer reconstructed in Ansys data available in literature which was used in the study. Analysis was based on the turbulent model available in the CFD.

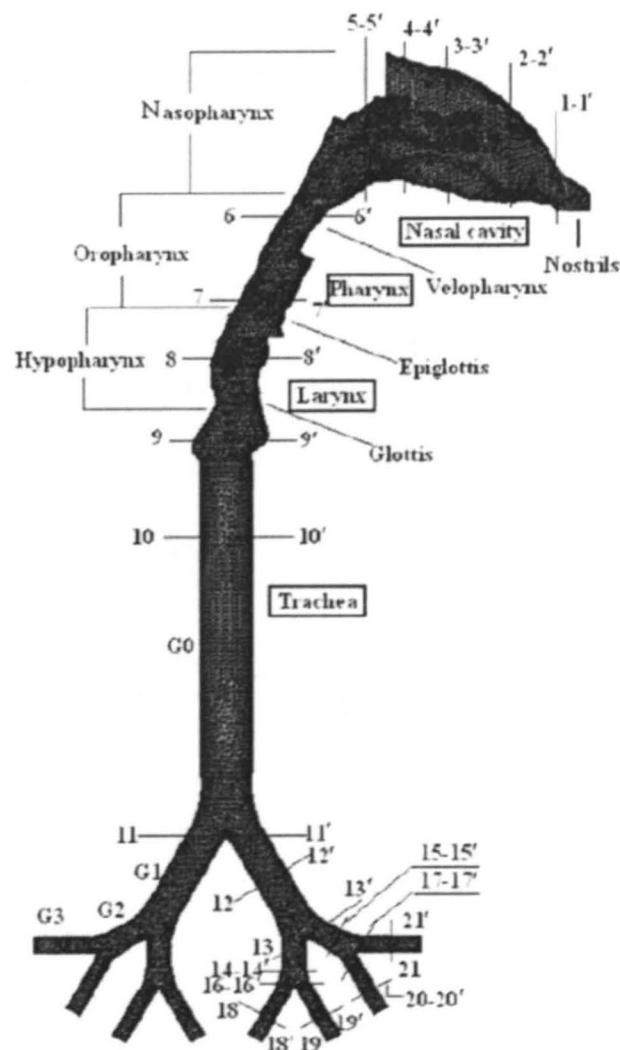


Figure 9. Three dimensional model of upper HRT used by Wang et al. (2009)

Wen et al. (2008) also perform a numerical simulation by using CFD to study the airflow dynamics in the human nasal cavity. The nasal cavity geometry used here is similar to that used by Inthavong (2006). The geometry was obtained through a CT scan of a volunteer.

Xi and Longest et al. (2007) used simplified models shown in Figure 10 of the respiratory tract to study the aerosol transport and deposition. The objective here is to study the effect of the geometry simplifications on the aerosol deposition along the respiratory tract. The simulations were performed by using a low Reynolds number (LRN) $k-\epsilon$ turbulence model.

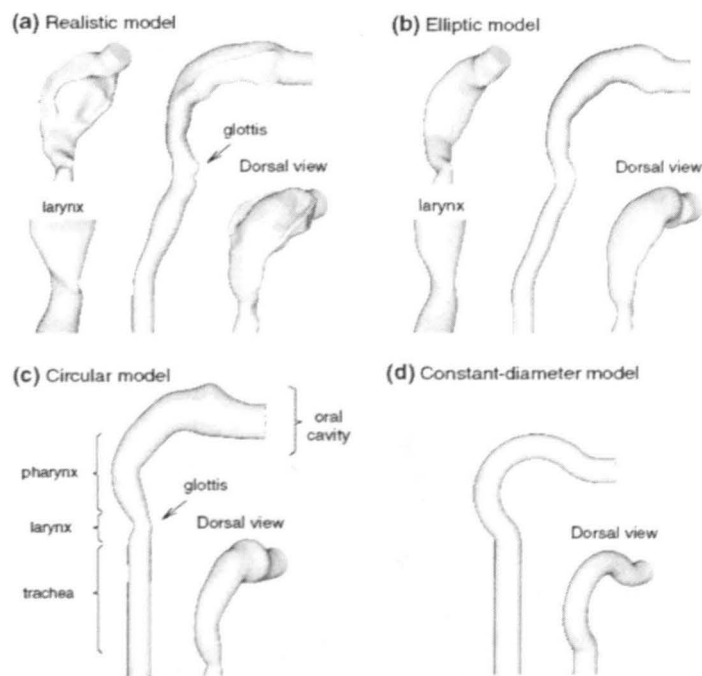


Figure 10. Simplified model used by Xi and Longest (2007)

Yu et al. (1998) studied the particle flow deposition in the human upper respiratory tract up to the first two generations in the bronchi in the lower respiratory tract. A medical school teaching model was used to re build the geometry using the CFD software. Velocity profiles for three patterns was analyzed i.e. nasal, oral and simultaneous nasal and oral along the human respiratory tract under normal room conditions.

Yung-Sung et al. (1999) study the effects of the drug deposition influenced by the respiration rate and the particle diameter via the oral cavity. An airway replica consisting of the oral cavity, pharynx, larynx, trachea and three generations of bronchi shown in Figure 11 is developed with data available from the dental cast of a volunteer, for human oral cavity and remaining referred from literature.

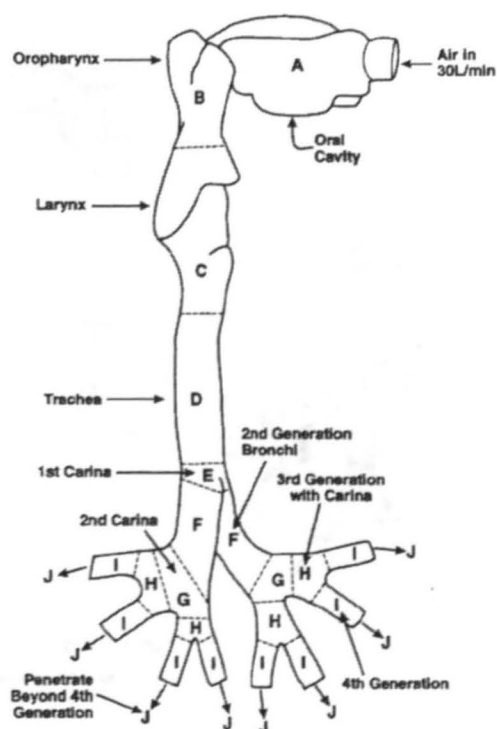


Figure 11. Upper respiratory tract model, Yung-Sung et al. (1999)

Zang et al. (2008) studied the airflow in the human nasal respiratory tract. A three dimensional model was made and was analyzed based on the Navier-Stokes and the continuity equation for airflow using finite element method under steady state inspiratory condition. The model generated in Ansys was based on CT scan of the thirty volunteers. The airflow characteristics and pressure distribution at various points were studied. It was concluded that the airflow in the nasal tract have different distribution models i.e. path of the air flowing varies with subject. This is based on the geometry of the nasal tract which varies with individuals.

Zhang and Kleinstreuer et al. (2003) used the geometric model show in Figure 12 to study the heat and mass transfer in the human upper respiratory tract.

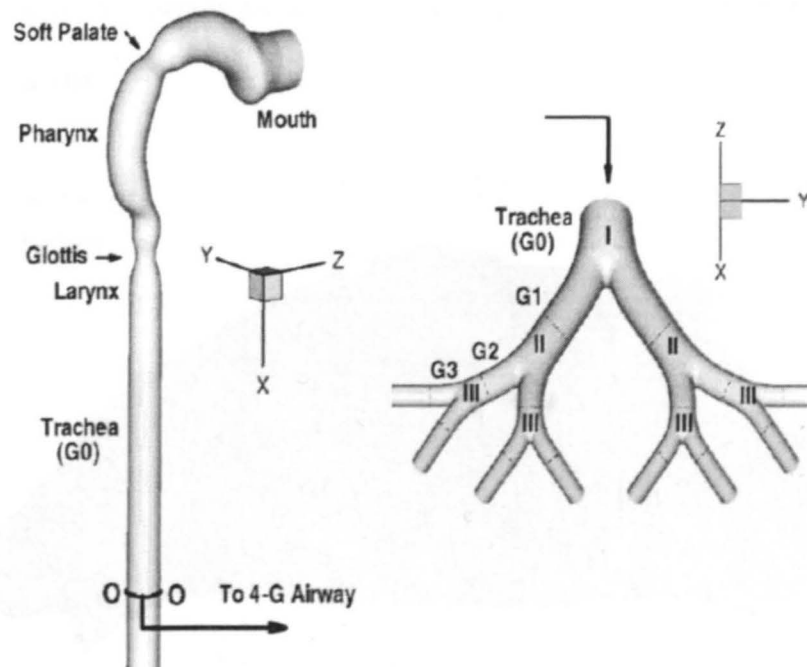


Figure 12. Upper respiratory tract model, Zhang and Kleinstreuer (2003)

The model was analyzed for both laminar and locally turbulent flow conditions. The model dimensions were imported from the literature to develop the oral tract and the first four generations of the bronchi.

2.2. Anthropometric Details of the HRT

Liu et al. (2009) developed a geometric model of the human nasal cavity using CT scan images. This was done in collaboration with a hospital's Otolaryngology department and a subject size of 30 volunteers was used in the study. The model created here was then compared with that available in the literature and a satisfactory model for the nasal cavity was obtained. The CT scan available was first converted into 2D coronal cross-sectional slices as shown in Figure 13 and with this as a reference a new 3D geometry was developed. The model completely focuses on the nasal cavity until the posterior region just above the nasopharynx.

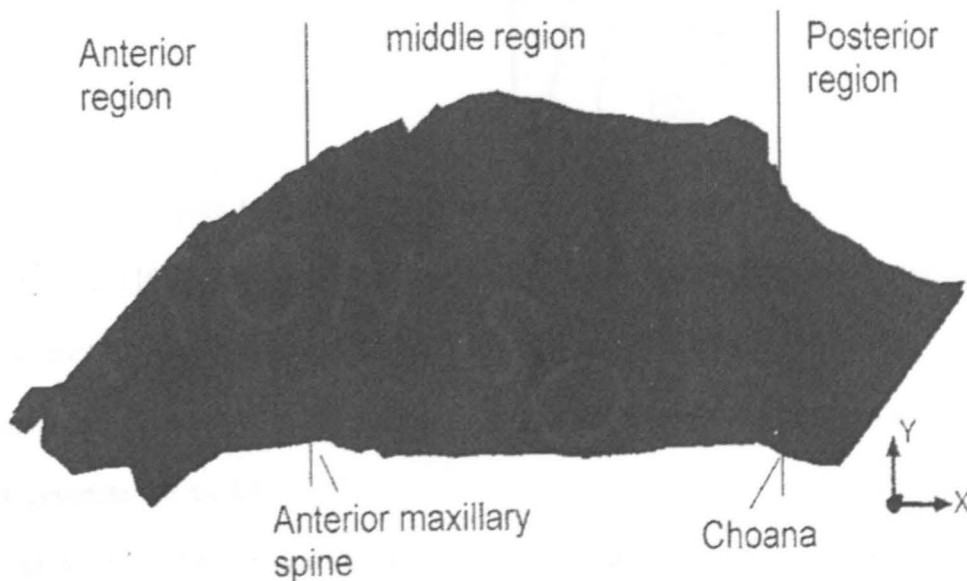


Figure 13. Nasal cavity geometry by Liu et al. (2009)

Cheng et al. (1996) emphasize the fact that the deposition along the respiratory tract is influenced by the three major factors: physical, physiological and morphological. To study the aerosol deposition in the human nasal and oral cavity the authors here measured in vivo nasal cavity dimensions using both MRI and AR. Cheng et al. (1997) have outlined some of the measurements of the oral region extending up to the mid trachea as shown in Figure 14.

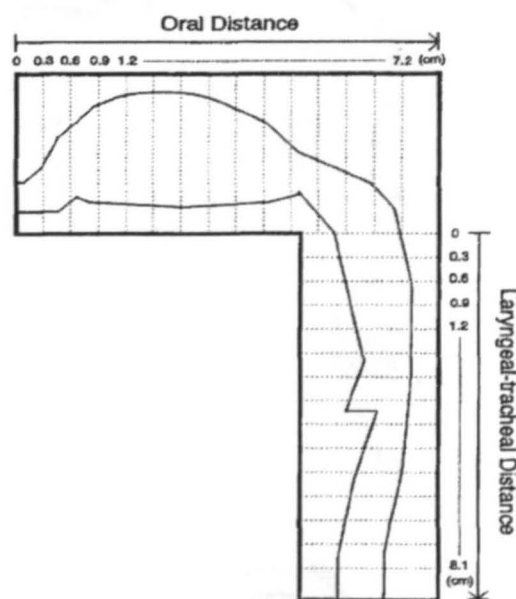


Figure 14. Model generated by Cheng et al. (1996)

Cheng et al. (1997) measured the characteristics of the oral cavity until the trachea. These characteristics were then related to the dimensionless parameters to study the ultrafine particulate deposition. Adult-Nasal-Oral-Tracheal head airway cast was used in the study to generate the model.

Robinson et al. (2009) reconstructed a 3D model using dimensions of oral cavity and the throat model using casting procedures summarized in Figure 15. The authors here

implemented the casting method instead of the MRI citing that accurate geometry is not obtained due to the movement of the vocal folds during breathing. These values are used in determining the oral cavity measurement tool in chapter 8.

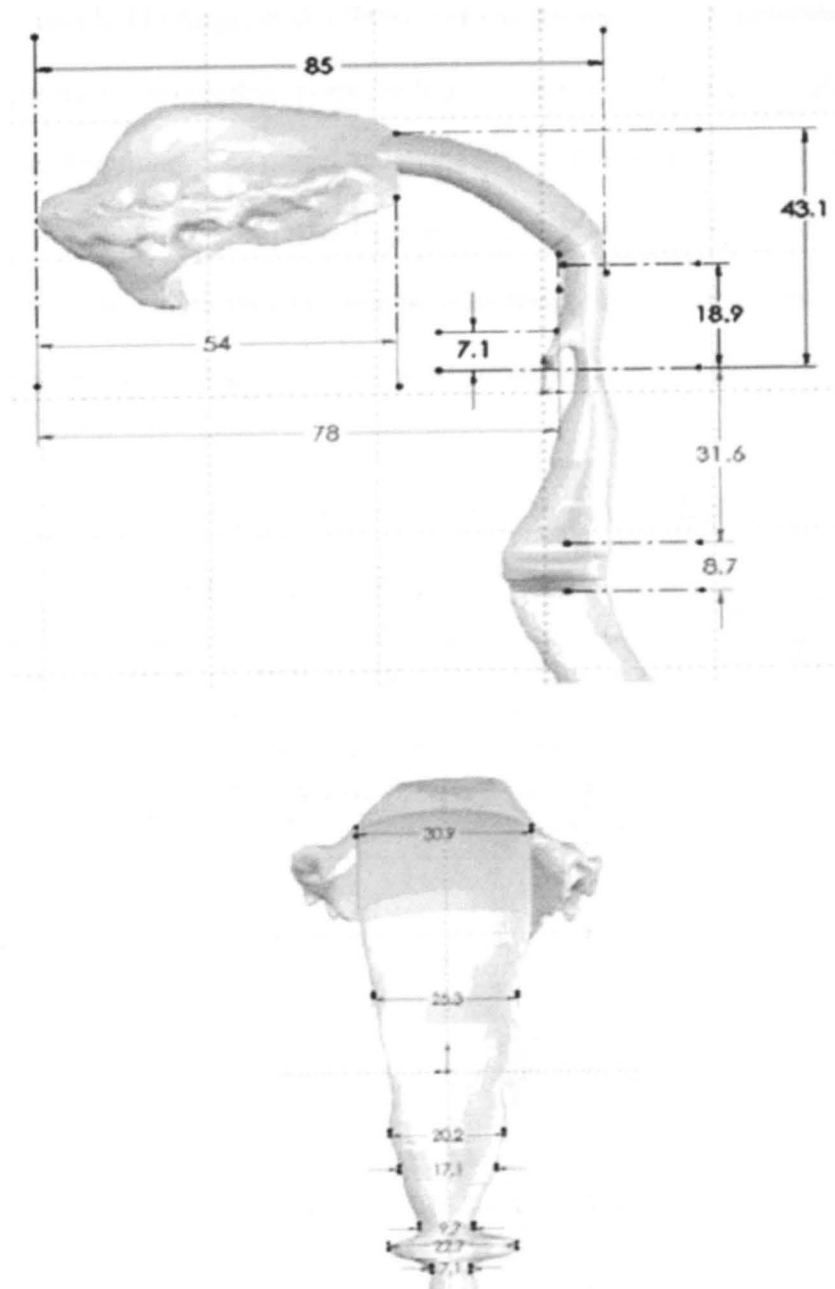


Figure 15. Oral cavity dimensions determined by Robinson et al. (2009)

Grgic et al. (2004) studied the aerosol deposition and flow measurements using a human mouth and throat replica shown in Figure 16. The mouth piece angle and dimension were selected from that available in the literature for straight tubes as summarized in Table 2. Oral dimensions used by Grgic et al. (2004). The extrathoracic model generated here was generated using the information available from CT scans, MRI scans and observation of subjects during breathing. The model generated here consisted of the oral cavity, oropharynx, larynx and the trachea. Also Grgic et al. (2004) study the inter-subject and intra-subject in realistic mouth-throat geometries including mouth, oropharynx, larynx and trachea. The models used for these purposes were obtained using MRI scans of seven geometries.

Table 2. Oral dimensions used by Grgic et al. (2004)

Model	Idealized	S1a	S1b	S2	S4	S5a	S5b	S3
D_{inlet} (cm)	1.7	1.3	1.3	2.3	2.3	2.3	2.3	1.4
Volume (cm ³)	73.8	50.0	33.8	99.3	82.6	96.9	117.3	57.6
Length (cm)	21.1	19.1	18.5	19.7	18.9	18.4	18.9	18.2
D_{mean} (cm)	2.1	1.8	1.5	2.5	2.4	2.6	2.8	2.0



Figure 16. Model of oral airway used by Grgic et al. (2004)

Hilberg et al. (1989) studied the nasal cavity geometry using acoustic reflection (AR). These results were compared with the geometry obtained from the CT scans. Terheyden et al. (2000) validated the results obtained from the AR from 3D reconstructed images from the CT scans. The results obtained were reasonably accurate for diagnostic use up to the turbinate head region.

Xi et al. (2008) used the CT scans of a volunteer to construct the realistic model for the respiratory tract. The authors here also considered the variations in the cross-section for various portions of the respiratory tract and the mesh generation also considered different mesh types. The anthropometric data here were based on that obtained from the CT scans. Sampson et al. described the optical coherence tomography (OCT) in lieu of the CT or MRI scans. The airway dimensions have been verified against that obtained from X-ray or CT scan.

Mohebbi et al. (2008) have conducted an experiment to measure the volume and oral cross-sectional area at different points along the tract shown in Figure 17. AR was used for this particular test. Gomes et al. (2008) also used the AR to study the nasal cavity dimensions. Malkoc et al. (2005) used the concept of lateral cephalometric radiographs in determining the airway characteristics. This test provided only the 2D images of the nasopharynx.

Tang et al. (2004) and Ertbruggen et al. (2005) use the CT scans to study the nasal cavity characteristics and the airway dynamics respectively. Tang et al. (2004) also suggests some of the possible simulation techniques depending upon the type of flow.

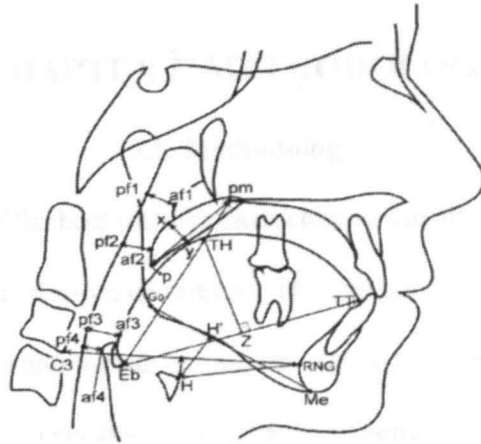


Figure 17. Dimensions determined by Mohebbi st al. (2008)

CHAPTER 3. METHODOLOGY

3.1. Methodology

Previous studies of the heat transfer characteristics available in the literature are mostly limited to only normal room conditions. This cannot be the case every time, adverse conditions do exist and human beings are exposed to varying environmental conditions almost routinely. This study is targeting challenges that human beings face while working in harsh environments, the effects on the respiratory system and how it can be protected. In a fire or chemical emergency, people are usually exposed to gases and smoke at various temperatures. The effect of hot gas/smoke on the internal tissue along the respiratory tract is unknown. Even a firefighter using a respirator for oxygen intake from a tank is exposed to various environmental temperatures. These environmental temperatures will influence the temperature of the oxygen tank which in turn affects the people working in the particular environment. For example, if we consider a scenario of forest fire then it is bound to be that the temperatures of the oxygen tanks will be high in equilibrium with the surrounding environment. The making of a respirator unit or a treatment therapy can be well defined.

Lv et al. (2006) analyzed the degree of burn in the respiratory tract but their model had some limitations, 1) It was a 2 D model, 2) It analyzed only the nasal tract, and 3) It assumed normal conditions and others also have investigated similar scenarios but ignored the oronasal breathing in the event of a hazard. In reality, during a fire hazard it is more likely that there is oronasal breathing in the human respiratory tract so it would be logical to analyze both the tracts simultaneously with alternate breathing pattern, such as

hyperventilated conditions, than normal breathing so as to satisfy the oronasal breathing pattern.

The methodology selected here consists of the defining the structure of the human respiratory tracts and explaining the model assumptions. For the analysis purpose, the portion of the human upper respiratory tract (URT) consisting of nasal cavity, oral cavity, pharynx and the larynx will be taken into consideration. The major part of the filtration and heat exchange takes place in the upper respiratory tract hence this portion is more prone to serious damage caused by burns. Understanding a more realistic pattern of flow of air during oronasal respiration will allow to study and recommend a more suitable treatment or even prevention methods when exposure causes internal burn injury to the upper respiratory tract. The next step will lead to the modeling of the selected geometry, 2D or a 3D model based on the selected parameters. This equation can be further solved by numerical methods. The degree of burn in the respiratory tract can be analyzed as done previously by using Henrique's model. Physiological status and environmental status can also be analyzed. Various software are available which can be used for the modeling and verification purposes based on the feasibility of the study.

The methodology proposed here consists of performing a 3-D heat transfer analysis for oronasal breathing using the geometry shown in Figure 18. This geometry simplifies the model due to the complex structure of the human nasal, oral and the respiratory tract. The model will be cylindrical in cross section and consisting of the nasal cavity, oral cavity, pharynx, larynx, trachea and the first two generations of the Bronchi.

The temperature profile of the air flow in the respiratory tract was studied for nasal, oral and oronasal breathing but is limited to the normal atmospheric conditions. This

analysis can be further extended by considering extreme conditions. Simulating a hazardous situation such as of fire or smoke where individual(s) may be exposed to heated or superheated gas or smoke or even steam. This simulation will allow the evaluation of burn injury under such elevated or extreme condition. The work done based on literature available is to study the airflow dynamics in the respiratory tract but the evaluation of burn injury is limited to the nasal cavity as performed by Lv et al. (2006). The proposed approach consists of simulating the simultaneous flow of fluid through the human nasal and oral cavity, known as oronasal breathing, to evaluate the burn injury in adverse conditions such as fire or smoke hazard. Hence the thermal profile of the oronasal breathing during extreme conditions has to be studied to suit the characteristics; geometry of respiratory tract generated here is based dimensions obtained from literature.

3.2. Other Significance

Injury caused due to accidents related to fire or smoke can be hazardous in nature. The degree of treatment also varies depending on the damage caused on the human respiratory tract. The burn impact or injury due to inhalation of hot gas is commonly encountered (Enkhbaatar and Traber, 2004) hence the treatment to the injury also has to be developed effectively. Various therapies like fluid resuscitation formula, nutritional support regimes etc are available and are based on the degree of injury for combined burn and smoke inhalation was performed by Lv et al. (2006). This analysis was 2D, and if this is extended into a 3D heat transfer study, the results would be helpful in developing engineering solutions or preventive measure along with effective treatment therapies. This study of the respiratory profile may be further extended up to the design of artificial respiratory system. Various parameters such as temperature of fluid, pressure and

measurements based on the anthropometric data can be used to design artificial portable respiratory systems which may have built in cooling system to reduce the temperature of inhaled gas in the case of civil or forest fire fighters. The results could bring an insight on the type and extent of injury expected in these types of exposures.

Particle deposition model which would be useful in optimizing drug delivery mechanism to the affected areas of the respiratory track would be developed based on the burn impact determined through the CFD mode. Burn injuries will most definitely effect both nasal and oral track and an understanding of the type of burn injury and the extent of it will allow healthcare professionals to make a more informed decision when it comes to drug dosage and duration of treatment.

3.3. Assumptions and Limitations

The human upper respiratory tract consisting of the nasal, oral, pharynx, larynx, trachea and the first two generations of the bronchi is highly complex and asymmetric in nature. The tissue structure around the human respiratory tract is also complicated to depict in a 3 D model. The surface of the tissues internally is highly variable. As highlighted the complexity of the procedure and high costs involved in developing a highly complex model which is beyond the scope of this project. Thus, a simplified model having a smooth internal surface and cylindrical cross-section with different diameters for each of the identified portions in the human upper respiratory tract is used for simulation.

The tissue structure within the human upper respiratory tract also differs widely, in this model it is assumed to be of circular cross-section along the circumference of the human upper respiratory tract model. The value of the thickness of tissue is referred to that

used by Lv et al. (2006). The body temperature here is assumed to be constant throughout the human upper respiratory tract.

This study will basically analyze the results based on the simulation performed for the inhalation of hot air. The temperature obtained at the surface of the human upper respiratory tract will be used for the analysis and Henrique's model will be used to determine if this temperature damages the tissue.

3.4. A Three Dimensional Model of the Upper HRT

The Human Respiratory System consisting of the nasal tract, oral tract, pharynx, larynx, trachea and bronchi is highly complex in structure and asymmetric in nature. The tissue structure within the respiratory tract also adds to the complexity. This structure has high variability among individuals in terms of measurable dimensions such as height, width, diameter and thickness. As observed in the literature various numbers of attempts have been made by use of models depicting the human respiratory tract. The three dimensional replica of the HRT were constructed by taking measurements from the actual HRT by use of scanning and imaging devices. Procedures such as Computed Tomography (CT) scan, Acoustic Rhinomanometric were used. Use of morphometric data was also a part of 3D reconstruction of the HRT. The models built for the purpose of CFD simulation was often referred to that of the morphometric data or data obtained from scanning and imaging when available. Due to the complexity and high cost of obtaining actual data, model generated using data available is one feasible option.

Simplified models which could be standardized for the purpose of CFD simulation were developed and used in this study. The model developed here is based on the data

available in literature cited herein, as measurement of real time data is a complex process and costly. Based on the measurement in the literature the three dimensional geometry of the upper HRT is developed. The proposed method here is to utilize the three dimensional model representing the upper HRT to simulate and study various flow characteristics leading to the estimation of the duration of exposure and temperatures causing first degree, second degree or third degree burn injuries inside the upper respiratory tract when inhaling hot gas or smoke. Figure 18 shows the structure of the HRT consisting of the nasal cavity, oral cavity, nasopharynx, pharynx, larynx, trachea, and first two generations of the bronchi. The geometry has varying diameter for nasal, oral, nasopharynx, pharynx, larynx, tracheal, and bronchi regions. The horizontal tract for simulation purpose is bent at an angle 90° .

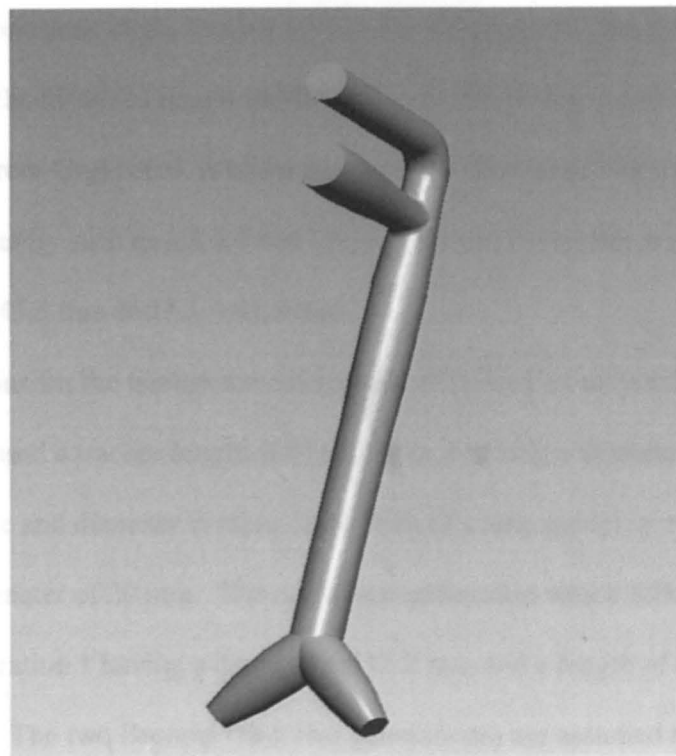


Figure 18. Geometry of the upper HRT for 3D analysis

Wen et al. and Inthavong et al. reported that the length of the nasal tract, the horizontal portion having a length L_1 to be in the range of 100 – 110 mm. Liu et al. reported the horizontal length of the middle region L_{12} to be on an average of 65.1 mm. It is assumed here that value for L_1 to be 105 - 110 mm and the portion nasopharynx L_3 being 35 mm. Cheng et al. reported the value of the shape factor for the irregular cross section of the nasal cavity to be 2.79. The mean minimum cross-section area reported here is 2.1 square cm having a mean shape factor of 2.5. Using this value for calculating the conduit diameter representing the nasal cavity is 16.35 mm extending down to the nasopharynx region L_3 , see appendix 1.

The dimensions for the oral cavity, pharynx and larynx are referenced from Grgic et al., Zhang et al., Johnstone et al., Robinson et al. and Cheng et al. For the oral cavity length and diameter the idealized length for the oral to larynx distance and of mean diameter of 21 mm from Grgic et al. is taken into account. The length for the various portions of the oral cavity such as L_2 , L_4 and L_5 are given in Johnstone et al. where $L_2 = 73.6 \approx 74$ mm, $L_4 = 43.5$ mm and $L_5 = 41.9$ mm.

The dimensions for the trachea are referred from Weibel's lung model, Wang et al. and Johnstone et al. used a trachea length (L_6) of 120 mm having a diameter of 18 mm. The Tracheal distance and diameter is taken from Weibel's lung model, a tracheal length of 120 mm and a diameter of 20 mm. The upper two generation which follows the trachea is referred to as generation 1 having a diameter of 12.2 mm and a length of 47.6 mm from Hlastlala and Berger. The two Bronchi (first two generations) are assumed to be at an angle of 45° . The left and right bronchi have varying lengths and diameters. For the purpose of simulation it is assumed to be constant. Summing up the above values it is determined that

the maximum horizontal distance is 110 mm and the vertical distance is approximately 240 mm until the end of trachea, see appendix 2.

The above defined dimensions were taken into account while developing the model in Pro-E. A constant diameter for the nasal cavity until the nasopharynx region was taken into account. The portion from the nasopharynx to larynx has a variable diameter of a tapering cross section towards the end of larynx. The oral cavity too follows a tapering cross section so as to merge with the oropharynx whose cross sectional diameter varies. The cross section for the first two generation of the bronchi varies from the tracheal region to the end of it. The irregularities in the surface smoothness in the internal portion of the respiratory tract are due to the varying geometries at points. These are considered with respect to the actual geometry whose internal surface is completely irregular. The oral cavity is merged into the tract as a straight pipe.

The dimensions considered here for the human respiratory tract are based on the anthropometric measurements available in the literature. There are three aspects which need to be addressed.

1. The change in the internal dimensions of the HRT during excited breathing conditions

When a normal cycle of respiration takes place, the human body is in a relaxed position without much stress to the body. The nasal respiration takes place usually with mouth being closed. When the respiration rate increases the oronasal breathing commences and a change in the expansion of the respiratory tract can be observed as the increase in volume of intake/exit air.

2. Increase/Decrease in Tidal volume

Increase in the respiration rate also increases the tidal volume as there is an expansion in the HRT. The tidal volume is the volume of air inspired or expired during normal breathing. Highly excited conditions of the human body during physical exercise also have high impact on the tidal volume. This not only impacts the frequency but also the cross-sectional shape of the HRT.

3. Expansion/Contraction of the HRT based on body posture.

The Human tissue is highly flexible; it contracts and expands based on the amount of pressure applied in the human Body. The pressure exerted by body posture also leads to the expansion or contraction of the internal organs including the HRT. For example when a person is lying backwards then there is expansion in the human body and while bending inwards there is a contraction of the muscles.

The above factors are complicated to address which adds to the complexity in defining the geometry of the respiratory tract. The model created here representing an ideal HRT up to the first two generations of the bronchi are based on the dimensions cited. We assume here that there is a variation due to the shape of the HRT. The length and diameter for HRT were referred from the literature cited and the Pro-E model generated showed some variation in dimensions when performing a sweep function where the diameter of one cross section changes for example there is a variation in diameter when the length of the Trachea at the start is of 21 mm and gradually reduces to 20 mm as designed in the 3D drafting software.

Thus, a simplified model having a smooth internal surface and cylindrical cross-section with different diameters for each of the identified portions in the human upper respiratory tract is used for simulation. The value of the thickness of tissue is referred to

CHAPTER 4. CFD SIMULATION

The studies carried out to study the heat and mass transfer characteristics in the human respiratory tract at present has witnessed increase in usage of Computational Fluid Dynamics software. Once these measurements of the heat and water transport were carried out by the use of thermocouples, mathematical models depicting the heat and water transport phase was developed by some authors, and these models were used for the purpose of numerical simulation and to study the heat transfer characteristics. Recent trends used to generate the three dimensional model of the respiratory tract using any 3D modeling software and import into software's specifically for CFD like Ansys or Fluent. The HRT model generation was based on the MRI or CT scan of the respiratory tract obtained from a healthy volunteer. The CFD simulations studying the heat and mass transfer in the HRT have been previously performed using different geometric models. Idealized geometry and CT scan images have been used in past for performing simulation.

Computational Fluid Dynamics (CFD) software enables us to study the fluid flow characteristics, and performs calculations using the numerical formulas/equations based on the laws of physics. The CFD simulation is based on the Navier-Stokes equation for three dimensional incompressible flows. The CFD software used here for simulation is by using the software Ansys CFX 12. The solution methodology used by Ansys CFX is Finite Volume technique. The procedure to use the CFD software generally consists of four major steps; first the geometry is created using a three dimensional modeling software, after developing the model is imported into the CFD software that constitute the second step where parameters are defined followed by the third step of simulation run. The fourth step consists of the post processing of the results. Three dimensional model developed

using 3D modeling software is shown in Figure 18. Geometry of the upper HRT for 3D analysis and this is imported into the Ansys CFX. Figure 19 shows the imported geometry with mesh constructed for the simulation run. The mesh generation process here is determined by the value of the Reynolds number and the Reynolds number used here is 4130 (See Appendix 1) based on the diameter of the trachea and k- ϵ turbulence model is used for turbulent flow of low Reynolds number.

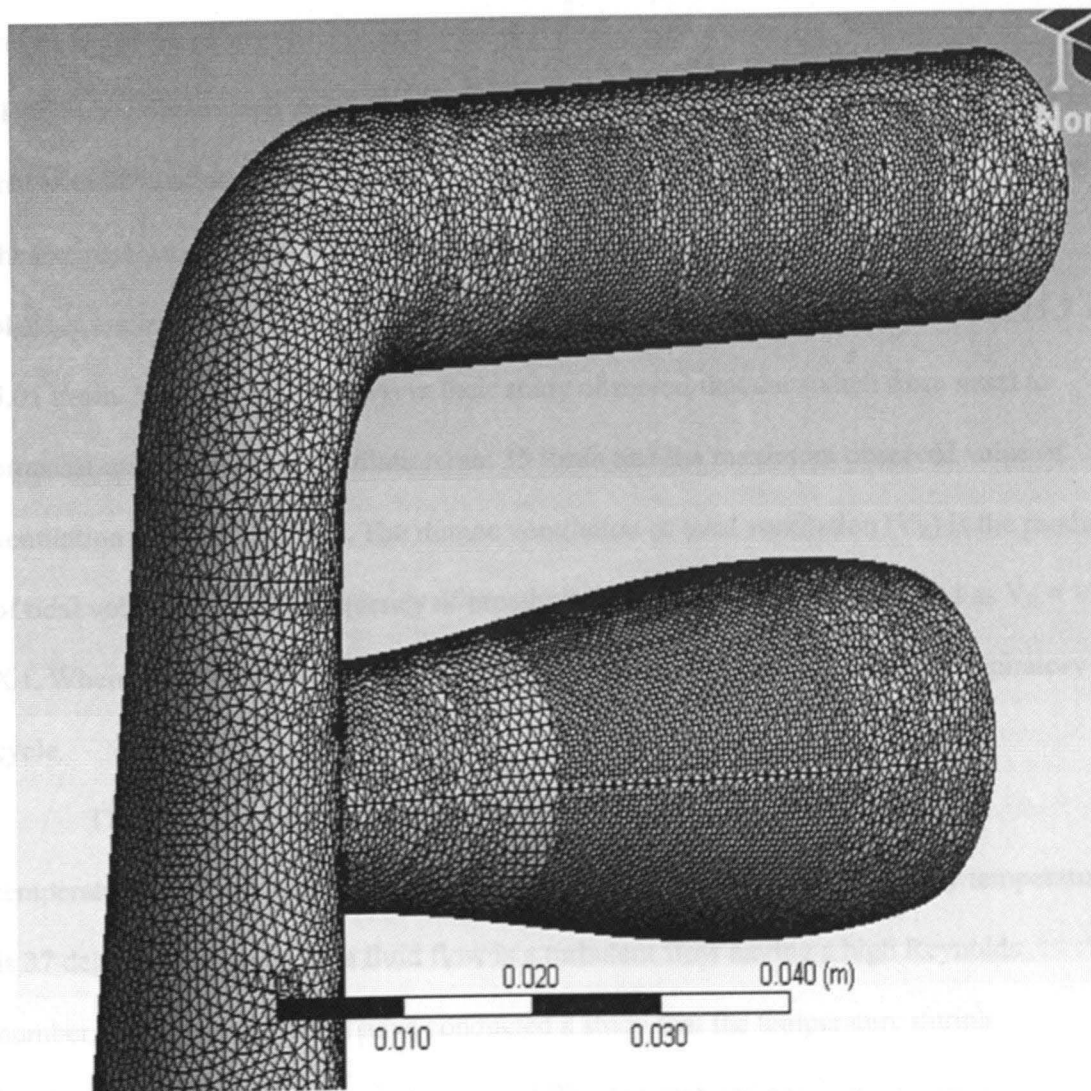


Figure 19. Mesh generation

4.1. Boundary Conditions

The 3-D model for the Human Respiratory Tract developed in this section is based on the data available in the literature. Due to the complex structure of the respiratory tract, the tract is modeled as a circular conduit having varying diameter D and varying length L . The volume of air intake in the respiratory tract will be in the case of an excited condition where oronasal breathing takes place in emergency situations. The volume of air intake in this case will be subject to oronasal breathing during heavy exercise. Wheatley et al. (1991) have determined the airflow characteristics during heavy exercises and have stated that over 80% of normal subjects breathe oronasally. The minute ventilation (V_E) before the exercise was 10.7 ± 1.01 l/min. The switch from nasal to oronasal breathing took place at a minute Ventilation of 22.3 ± 3.5 l/min and the final value obtained was 75.7 ± 5.01 l/min. Malarbet et al. (1994) in their study observed that the switch from nasal to oronasal was made at the ventilation rate 35 l/min and the maximum observed value of ventilation rate was 90 l/min. The minute ventilation or total ventilation (V_E) is the product of tidal volume (V_T) and frequency of breathing (f). Mathematically expressed as $V_E = V_T \times f$. Where V_T = tidal volume, which is the volume of air exhaled during one respiratory cycle.

The fluid in the human respiratory tract is assumed to be hot air having a temperature of 100 degrees centigrade. Density of air 1.165 kg/m^3 . The body temperature is 37 degrees centigrade. The fluid flow is a turbulent flow having a high Reynolds number. Varene et al. (1986) have conducted a study that the temperature during inspiration (T_I) and during expiration (T_E) differs for oral and nasal cavity, oral cavity having the higher temperature rate than the nasal cavity. But this was concluded by the fact

that no large differences exist from an energetic point of view between nasal and oral cavity as the difference in heat exchange were found to be very less and the total power loss was only 7 % lower during the nasal breathing than during mouth breathing.

4.2. Simulation Run Setup

The Input for Simulation:

Input Parameters: Ansys Set-up for simulation (Using the Quick set up mode)

Problem type: Single phase

Working Fluid: Air

Temperature of working Fluid: $100^{\circ}\text{C} = 373^{\circ}\text{K}$

Wall temperature is maintained at Body Temperature: $37^{\circ}\text{C} = 310^{\circ}\text{K}$

Analysis type: Steady state

Reference Pressure: 1 ATM

Heat Transfer: Thermal Energy

Turbulence model: k- ϵ

Defining Boundaries: Nasal Inlet, Oral Inlet, Outlet 1 and Outlet 2.

Density of Air at $100^{\circ}\text{C} = 0.946\text{ kg/m}^3$

The flow rate i.e. the max ventilation of about 90 liters/minute is considered for simulation purpose. Becquemin et al. (1999) reported an average value for percentage for oral breathing during oronasal breathing to be 50.13 % \approx 50 %. Hence we have the flow rate for Nasal inlet and oral inlet to be 45 liters/minute. The airway conduit was assumed to be a smooth wall so as to have a no slip condition imposed on airway walls.

4.3. Scenarios Considered for Simulation

The simulation is performed for the following scenarios. This is done in order to study the impact created at the two temperature levels. Further independent simulation is also run for nasal breathing and oral breathing.

- Oronasal breathing with inlet air temperature of 373 ° K (100° C)
- Oronasal breathing with inlet air temperature of 423 ° K (150° C)
- Nasal only breathing with inlet air temperature of 373 ° K (100° C)
- Oral only breathing with inlet air temperature of 373 ° K (100° C)

4.4. Simulation Results and Discussion

The results from the simulation are obtained for temperature distribution along the flow for the nasal cavity, oral cavity and Trachea. Velocity contours, temperature contours, pressure contour and streamlines path along the human respiratory tract is observed for the two different mesh configurations. The inlet air temperature decreases gradually as it passes through the bronchi and to the lungs. This phenomenon is observed due to the fact that body absorbs much of the heat from the inlet air if the inlet air temperature is higher body temperature. As it is assumed that the body temperature is constant throughout and less than the inlet air temperature, it is expected that there will be a decrease in the air temperature as it reaches the bronchi.

A cross-sectional view showing the temperature variation inside the respiratory tract up to the tracheal region is shown in Figure 20. The temperature variations can be observed here, at the inlet the temperature is the air temperature (surrounding temperature) and the air temperature increases or decreases as it flows through the tract.

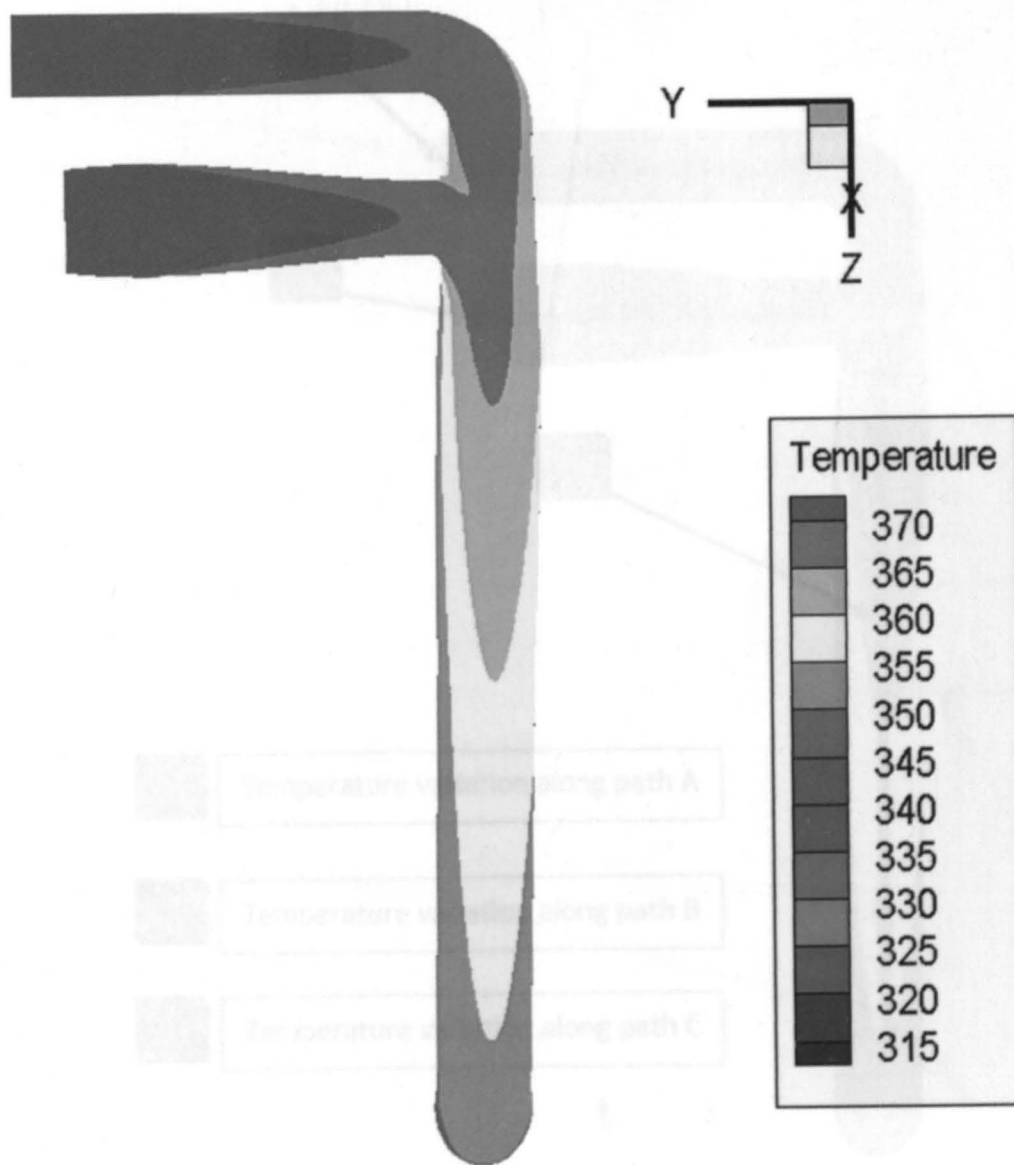


Figure 20. Temperature (K) variation inside the tract (A cross-sectional view)

This is due to the heat exchange between the inlet air and the respiratory tract. Temperature profiles for the portion of nasal cavity, oral cavity and the tracheal region along the centre as the path along which temperature variation shown is identified as A for nasal cavity, B for oral cavity and C for tracheal region in Figure 21.

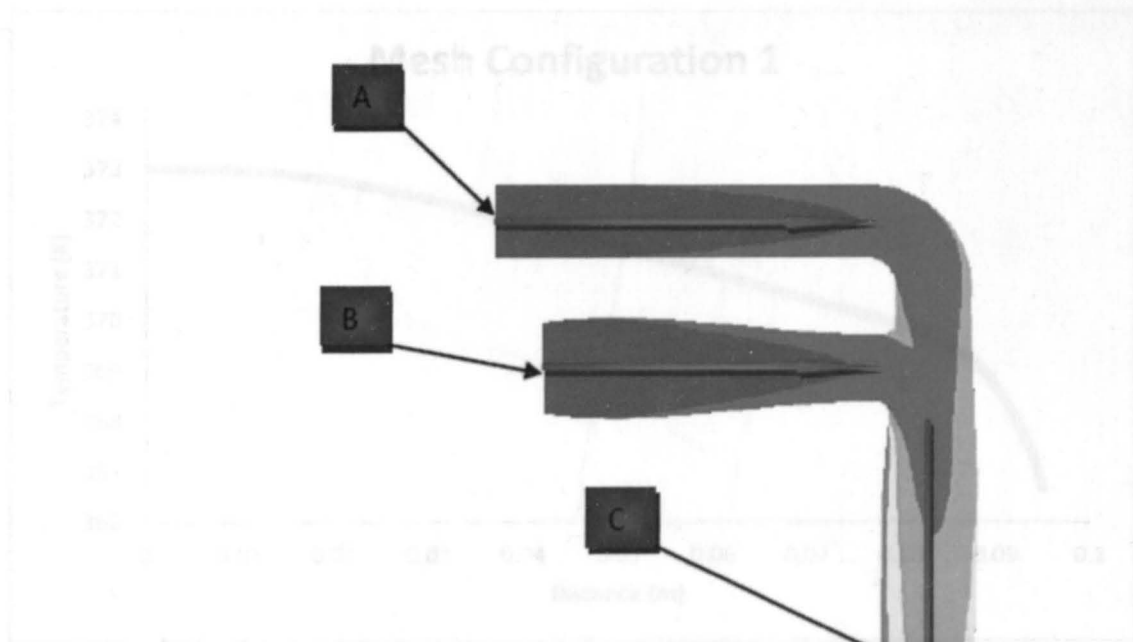


Figure 21. Nasal temperature profile for mesh configuration 1.

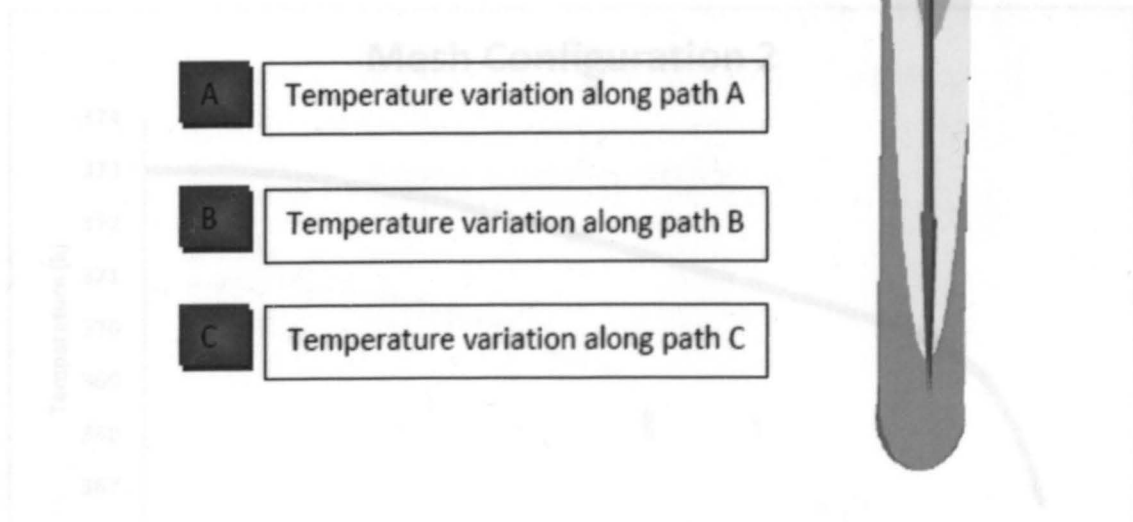


Figure 21. Temperature profile along the nasal, oral and tracheal region.

Figure 22 and Figure 23 gives the variation in the temperature along the center path of the nasal cavity up to a distance of 100 mm in horizontal direction i.e. the path A in Figure 21. The variations in the temperature can be seen for the two different mesh configurations. A decrease in the temperature is observed right from the inlet point.

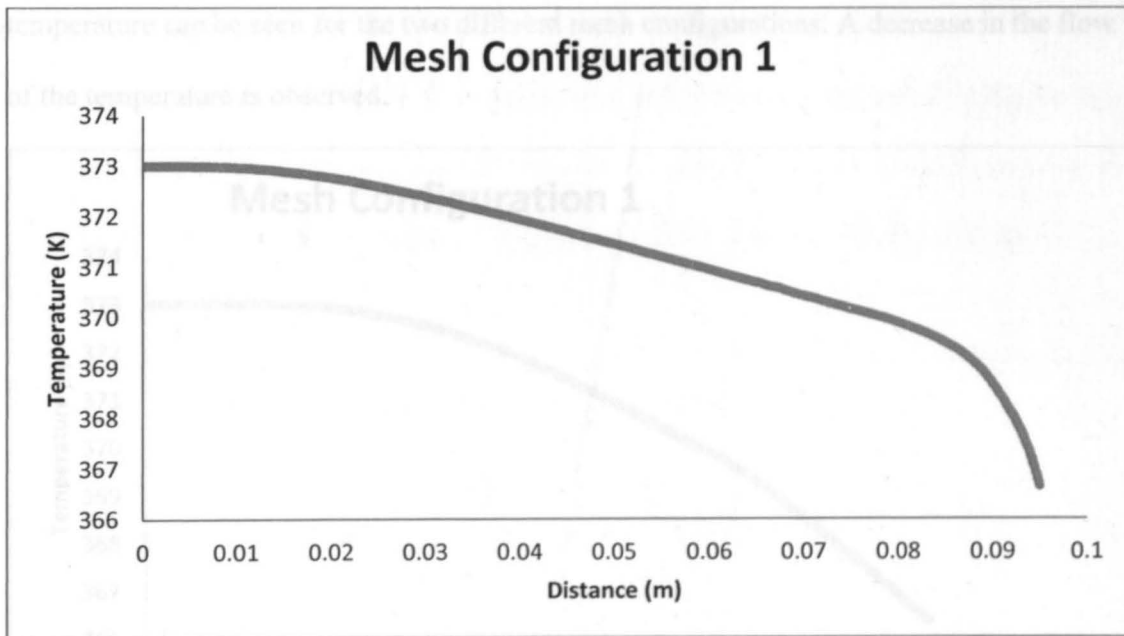


Figure 22. Nasal temperature profile for mesh configuration 1

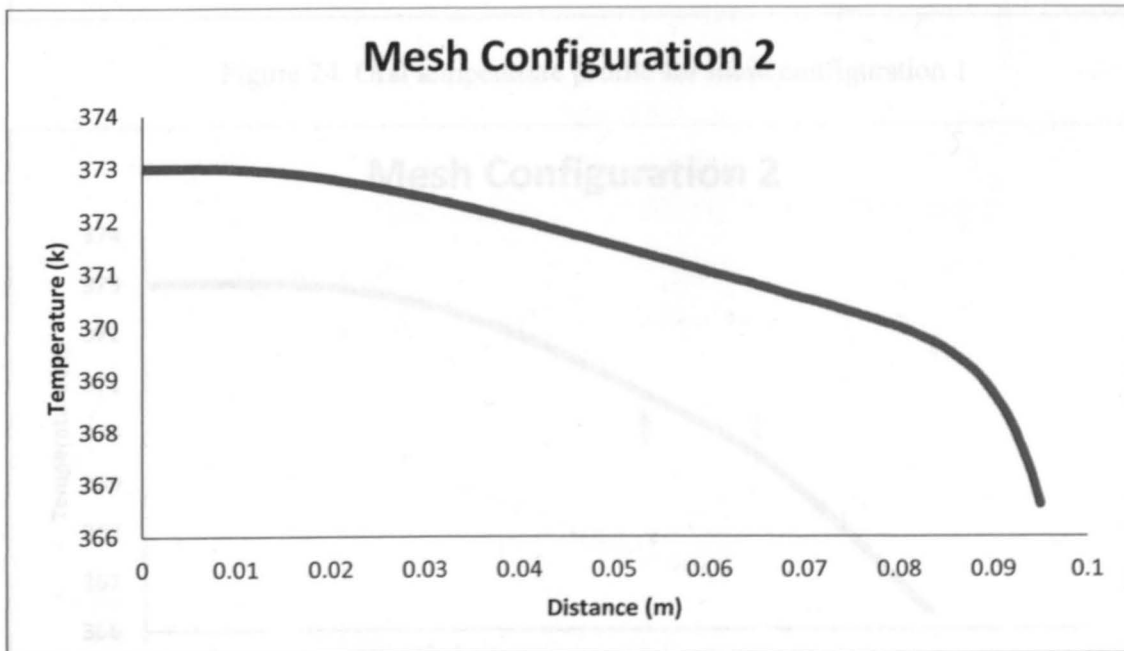


Figure 23. Nasal temperature profile for mesh configuration 2

Figure 24 and Figure 25 gives the variation in the temperature along the center path of the oral cavity in horizontal direction i.e. the part B in Figure 21. The variations in the

temperature can be seen for the two different mesh configurations. A decrease in the flow of the temperature is observed.

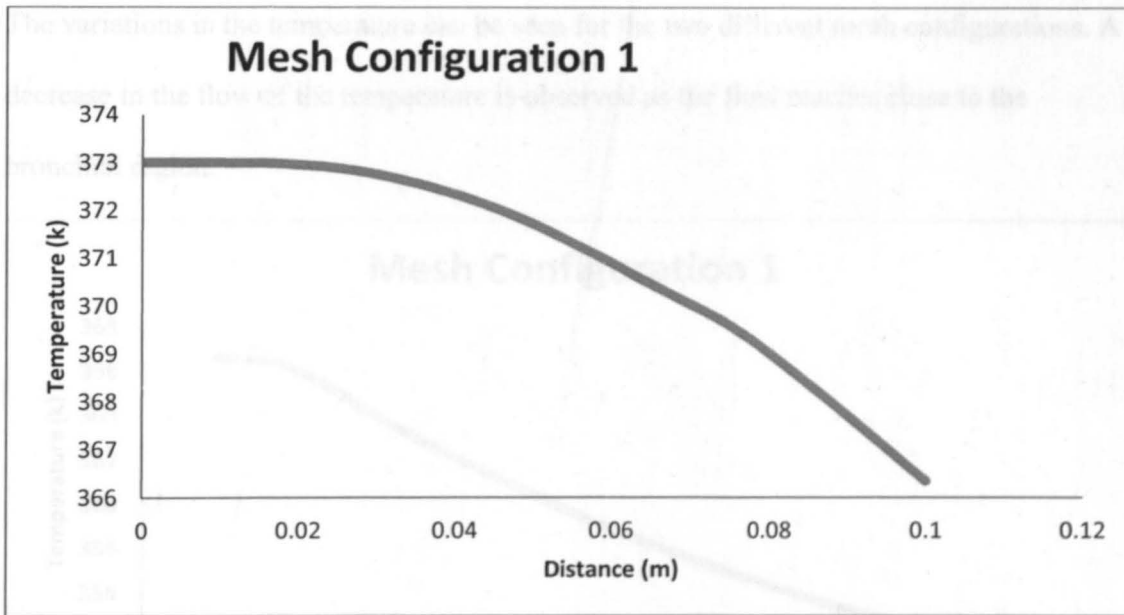


Figure 24. Oral temperature profile for mesh configuration 1

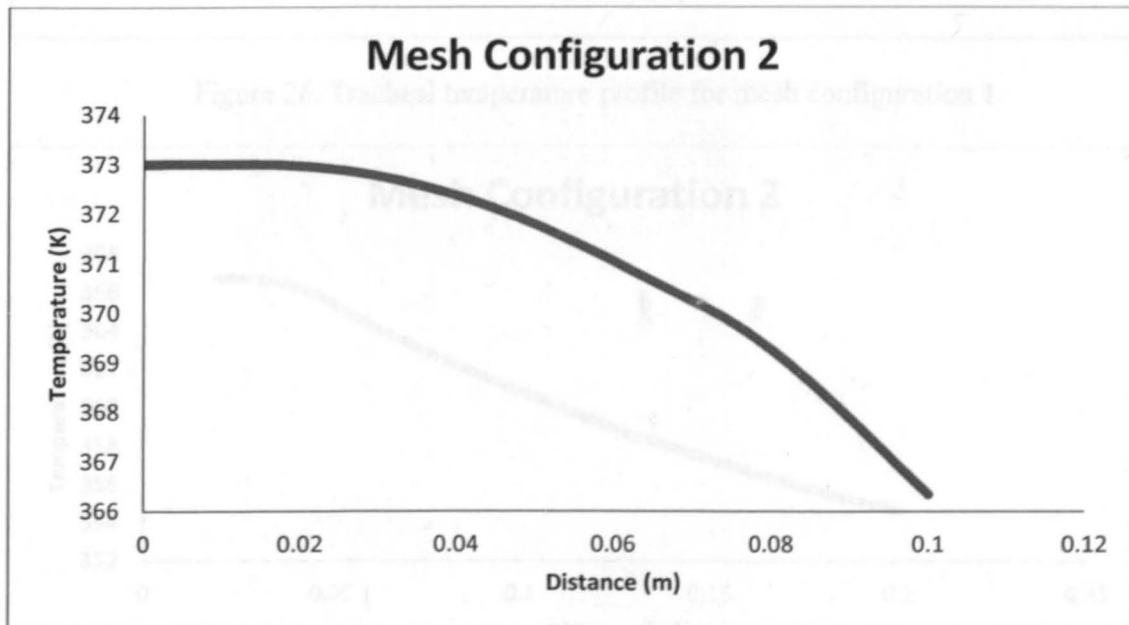


Figure 25. Oral temperature profile mesh configuration 2

Figure 26 and Figure 27 gives the variation in the temperature along the center path of the trachea up to a distance of 200 mm in vertical direction i.e. the part C in Figure 21. The variations in the temperature can be seen for the two different mesh configurations. A decrease in the flow of the temperature is observed as the flow reaches close to the bronchial region.

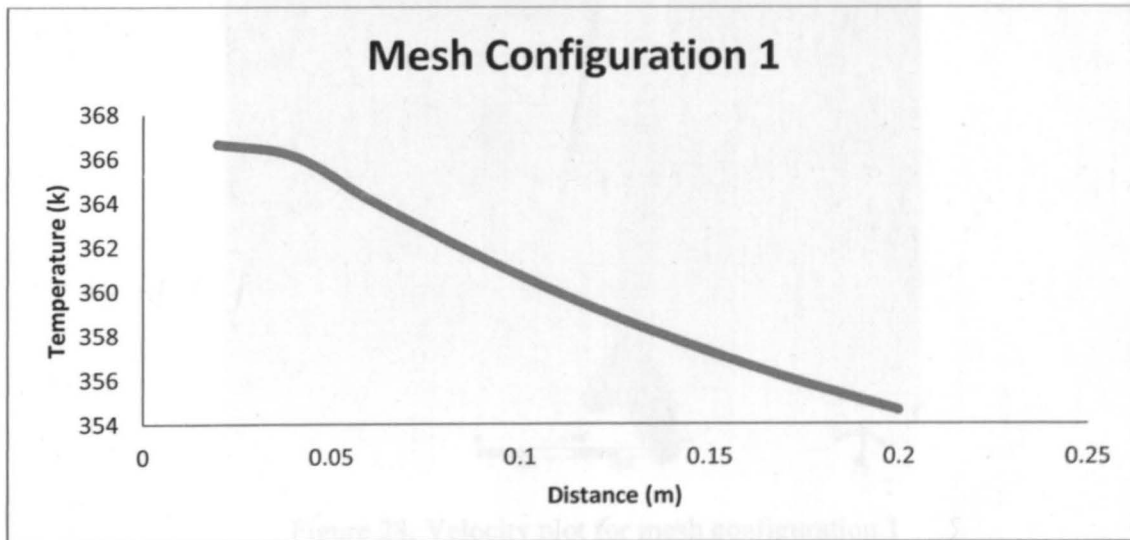


Figure 26. Tracheal temperature profile for mesh configuration 1

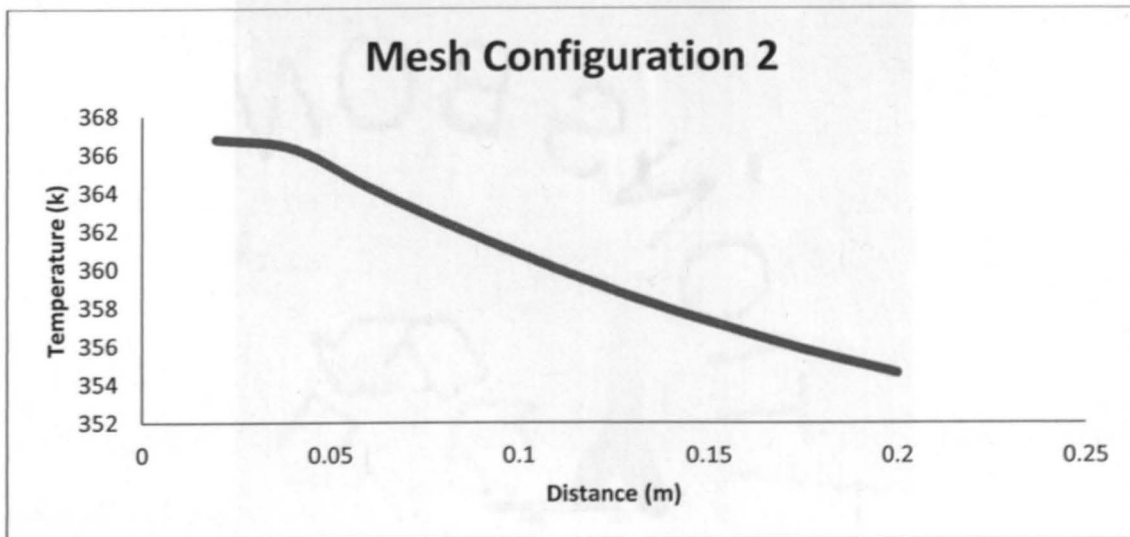


Figure 27. Tracheal temperature profile for mesh configuration 2

The velocity contours are shown in Figure 28 and Figure 29 for the two different meshes showing the velocity variations along the human respiratory tract. It is observed that the intersection point for the nasal and oral tract forms the high velocity region.

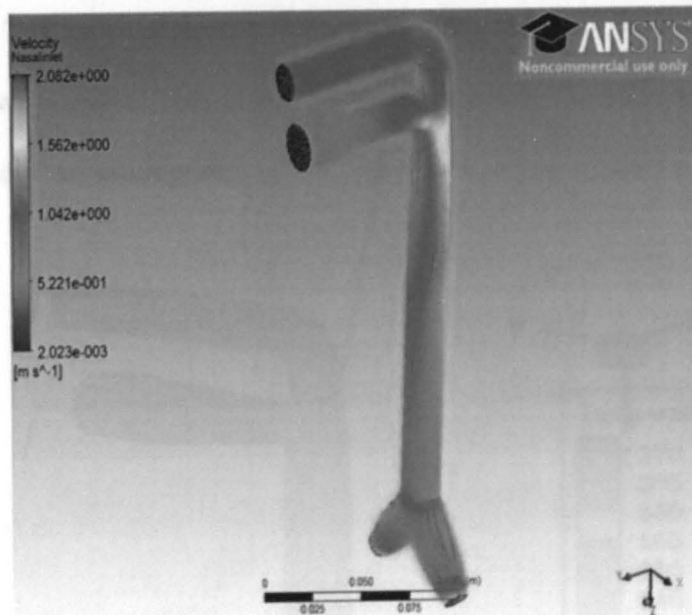


Figure 28. Velocity plot for mesh configuration 1

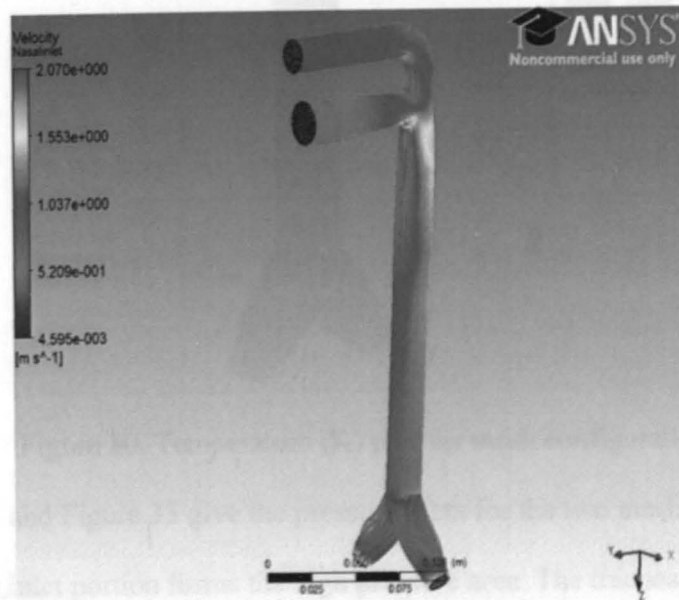


Figure 29. Velocity plot for mesh configuration 2

Figure 30 and Figure 31 gives the temperature plots for the two mesh configurations, it can be inferred from the plot that the center temperature is high at the inlet in the range of 373 degree K gradually decreasing through its flow as observed in Figures 22 - 27. The temperature due to the flow along the wall surface being in range of 315 K for the two meshes. This is due to the reason that the body temperature is kept constant throughout, an assumption.

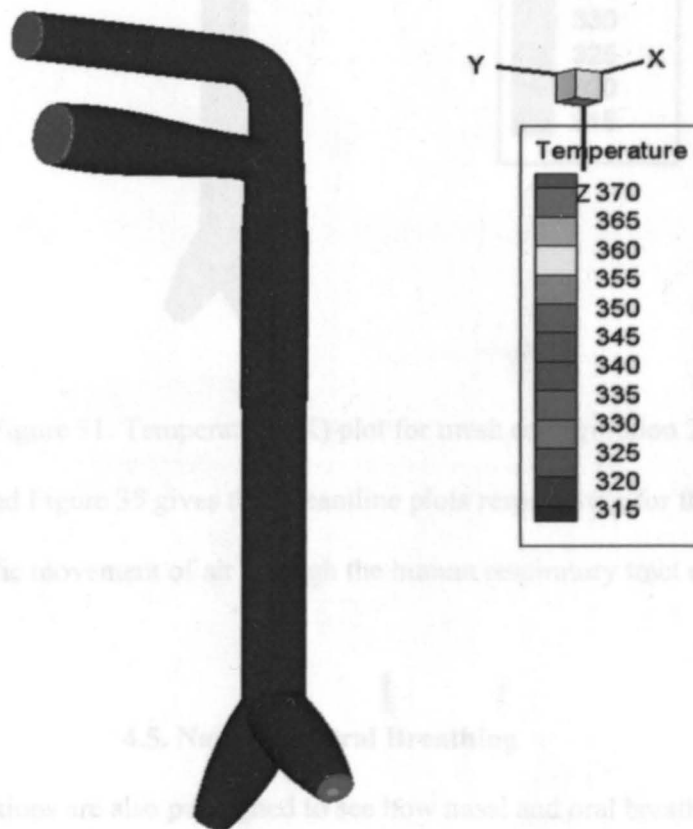


Figure 30. Temperature (K) plot for mesh configuration 1

Figure 32 and Figure 33 give the pressure plots for the two mesh configuration. It is observed that the inlet portion forms the high pressure area. The tracheal region maintains a average pressure throughout the trachea.

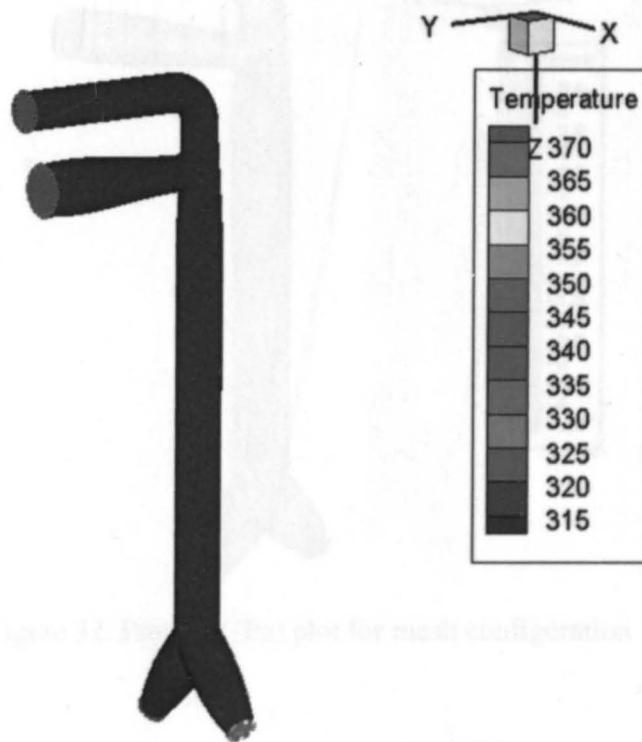


Figure 31. Temperature (K) plot for mesh configuration 2

Figure 34 and Figure 35 gives the streamline plots respectively for the human respiratory tract. The movement of air through the human respiratory tract can be observed.

4.5. Nasal and Oral Breathing

CFD simulations are also performed to see how nasal and oral breathing during the inspiration phase affects the HRT. For this case the mesh configuration having total number of elements of 3003027 is used and the flow rate of 45 L/min for nasal and oral only breathing conditions are used as input. The results of these simulations are plotted down.

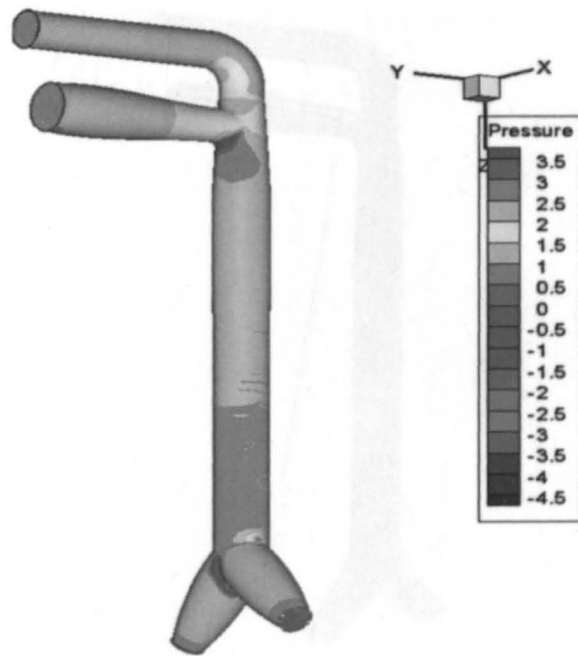


Figure 32. Pressure (Pa) plot for mesh configuration 1

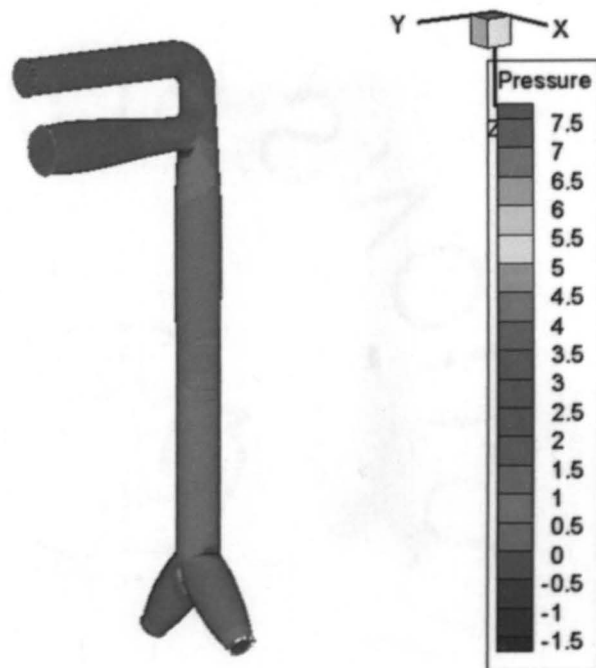


Figure 33. Pressure (Pa) plot for mesh configuration 2

The velocity plot for both mesh configurations is shown in Figure 36 and Figure 37. The velocity at the inlet for both mesh configurations is approximately equal when compared to the velocity of exposed breathing shown in Figure 38 and Figure 39.

Need breathing

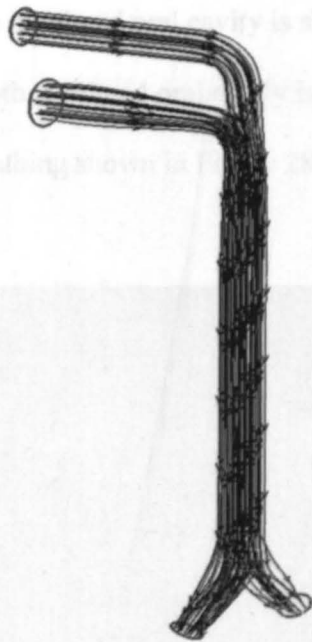


Figure 34. Streamline plot for mesh configuration 1

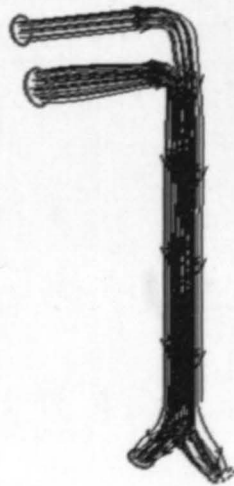


Figure 35. Streamline plot for mesh configuration 2

Figure 36. Velocity profiles for need breathing

Oral The velocity plot for both nasal and oral cavity is shown in Figure 36 and Figure 37, the velocity at the inlet for both nasal and oral cavity is approximately same when compared to that of oronasal breathing shown in Figure 28 and Figure 29.

Nasal breathing

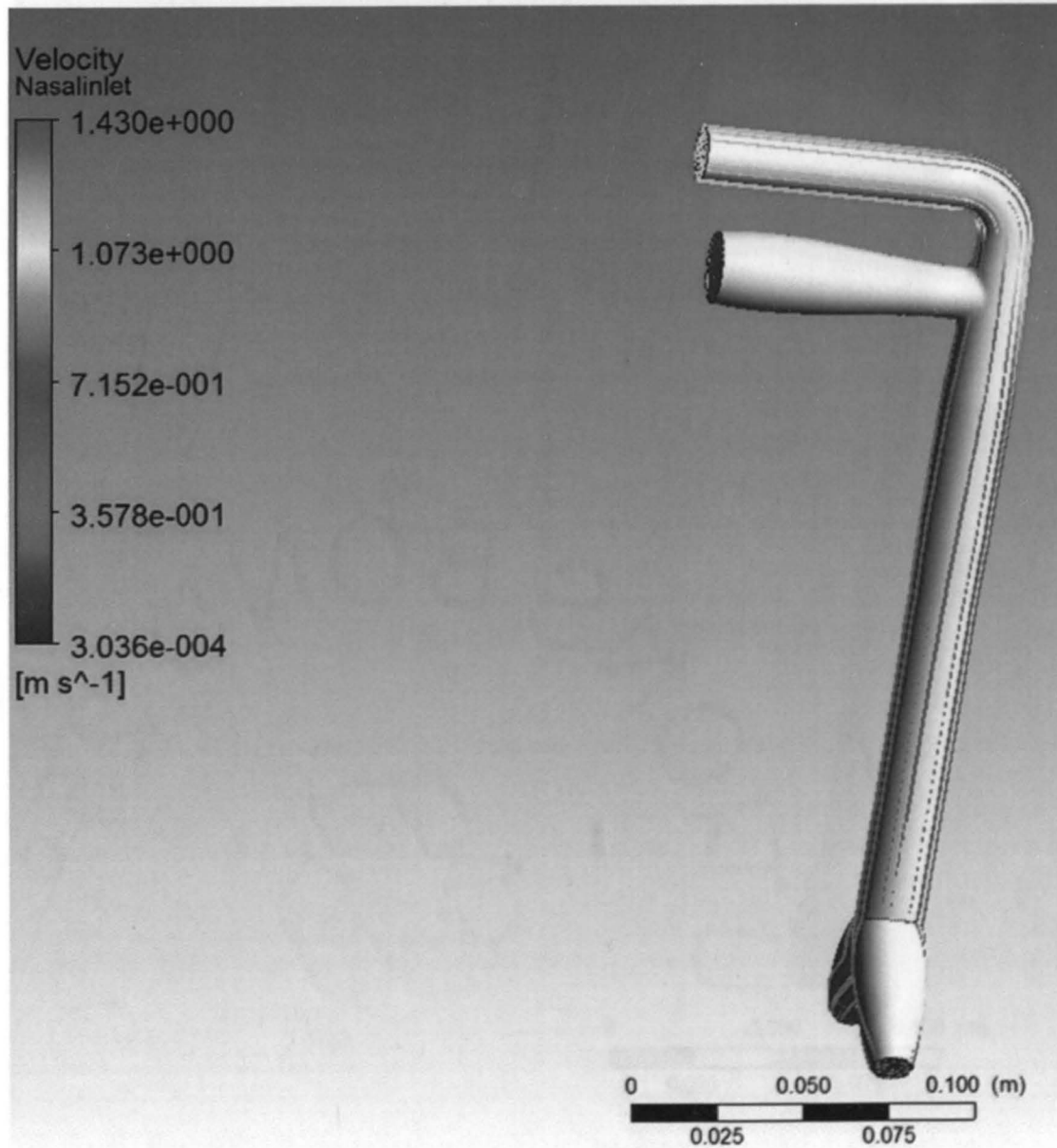


Figure 37. Velocity profiles for oral breathing

Figure 36. Velocity profiles for nasal breathing

Oral breathing

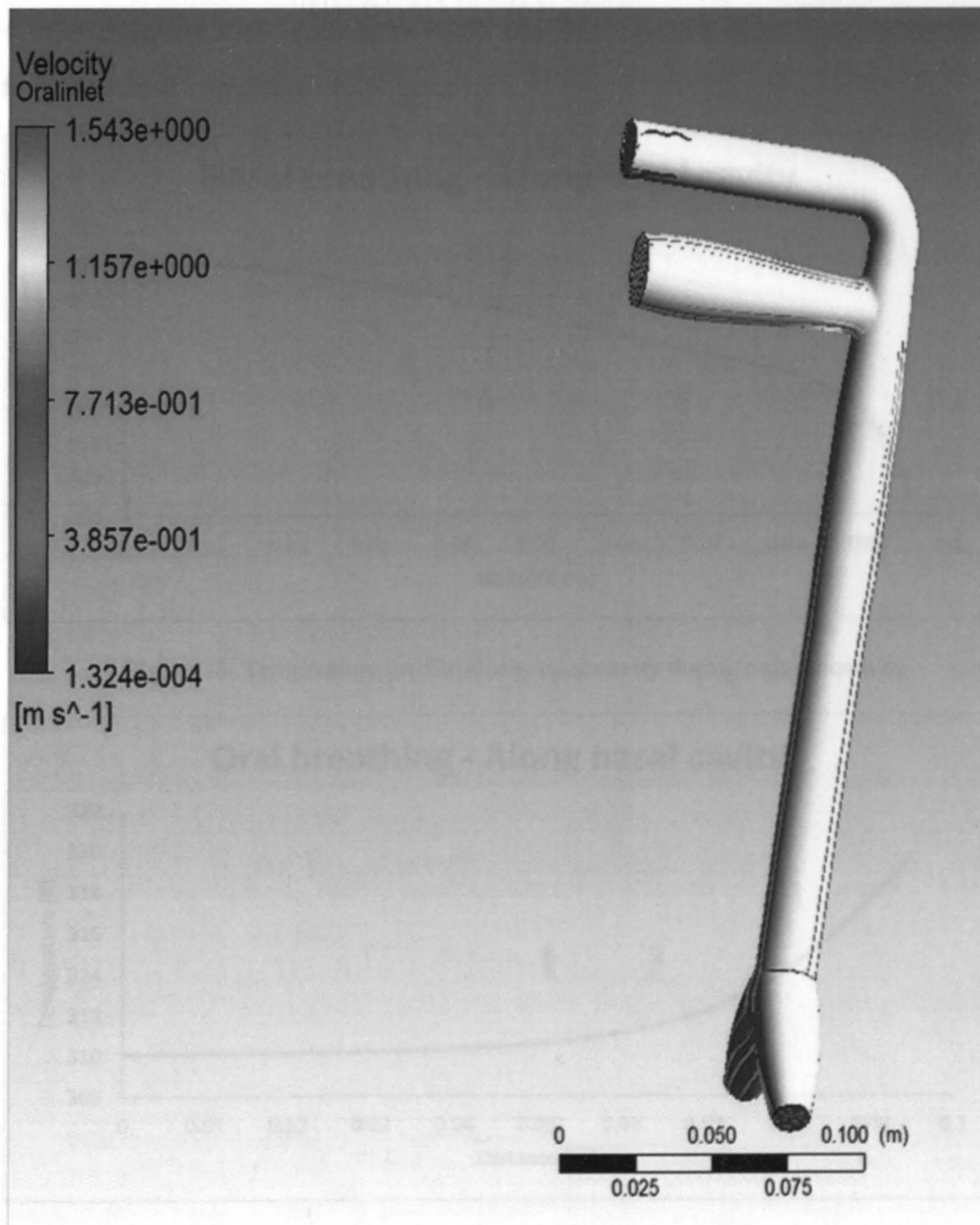


Figure 37. Velocity profiles for oral breathing

Figure 38 and Figure 39 shows the temperature profile for the nasal cavity portion A as identified in Figure 21. For nasal breathing, a decrease in the temperature is observed from the inlet up to a distance of 100 mm.

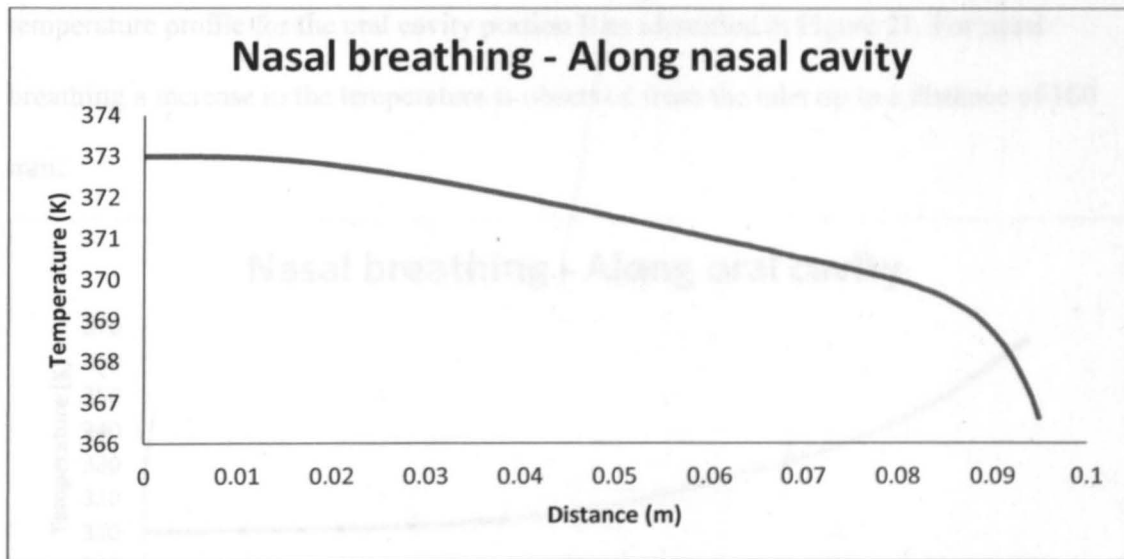


Figure 38. Temperature profile along nasal cavity during nasal breathing

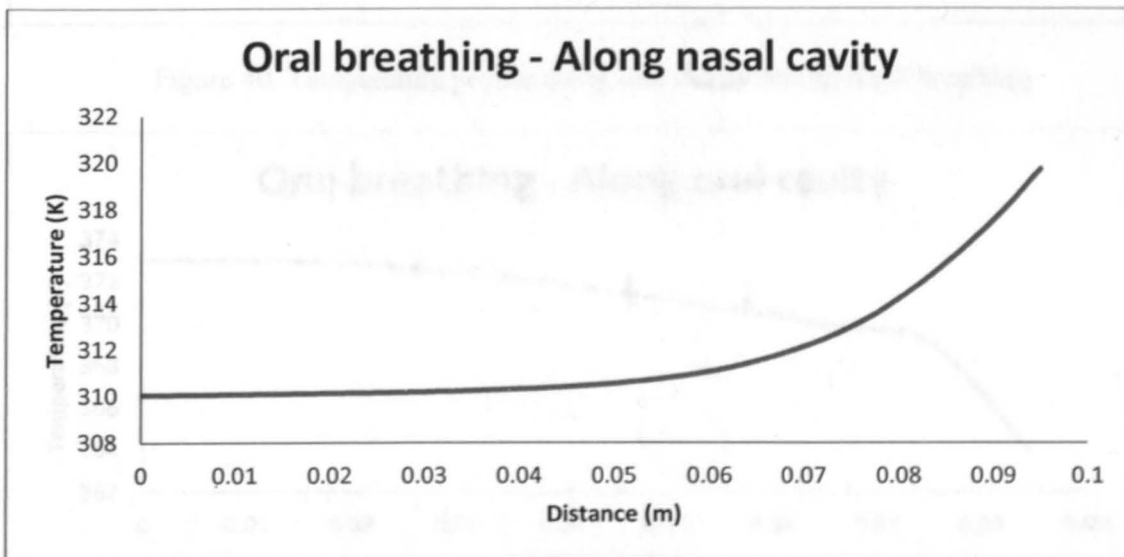


Figure 39. Temperature profile along nasal cavity during oral breathing

For the oral breathing, a increase in temperature is observed along the nasal cavity. This can be justified by the fact that the inhaled air through nasal cavity causes an increase in temperature inside the human respiratory tract. Figure 40 and Figure 41 shows the temperature profile for the oral cavity portion B as identified in Figure 21. For nasal breathing a increase in the temperature is observed from the inlet up to a distance of 100 mm.

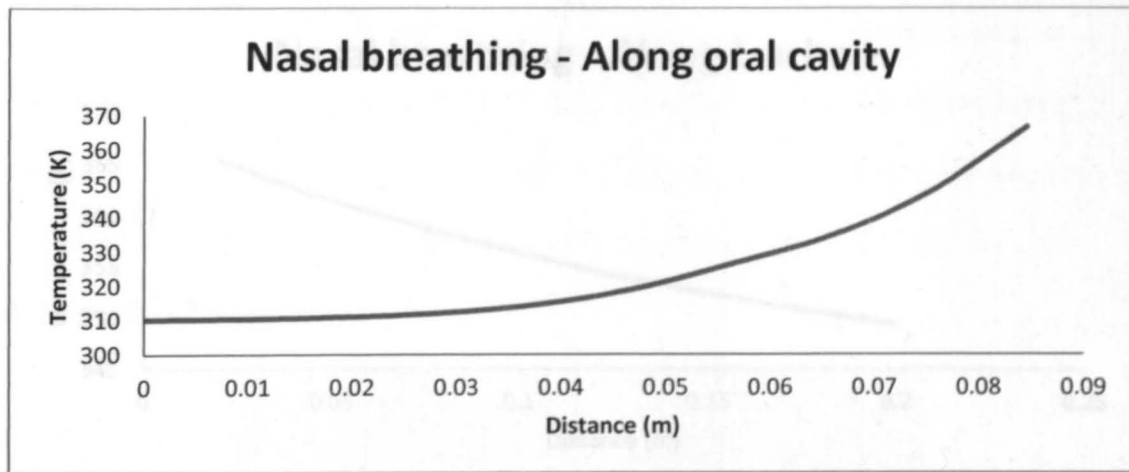


Figure 40. Temperature profile along oral cavity during nasal breathing

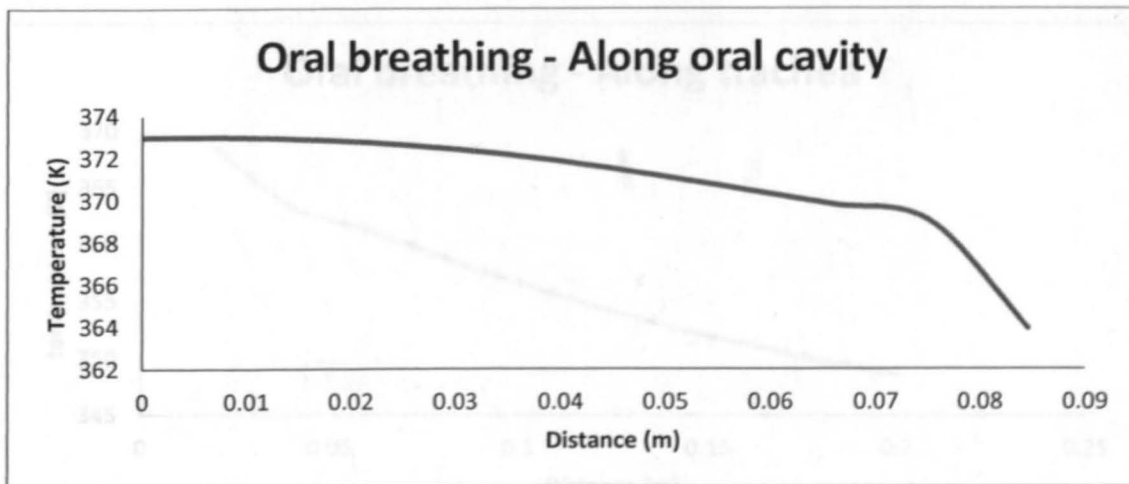


Figure 41. Temperature profile along oral cavity during oral breathing

This can be justified by the fact that the inhaled air through oral cavity causes an increase in temperature inside the human respiratory tract. For the oral breathing, a decrease in temperature is observed along the oral cavity. Figure 42 and Figure 43 shows the temperature profile for the nasal cavity portion C as identified in Figure 21. For both breathing conditions, a decrease in the temperature is observed from the inlet up to a distance of 100 mm.

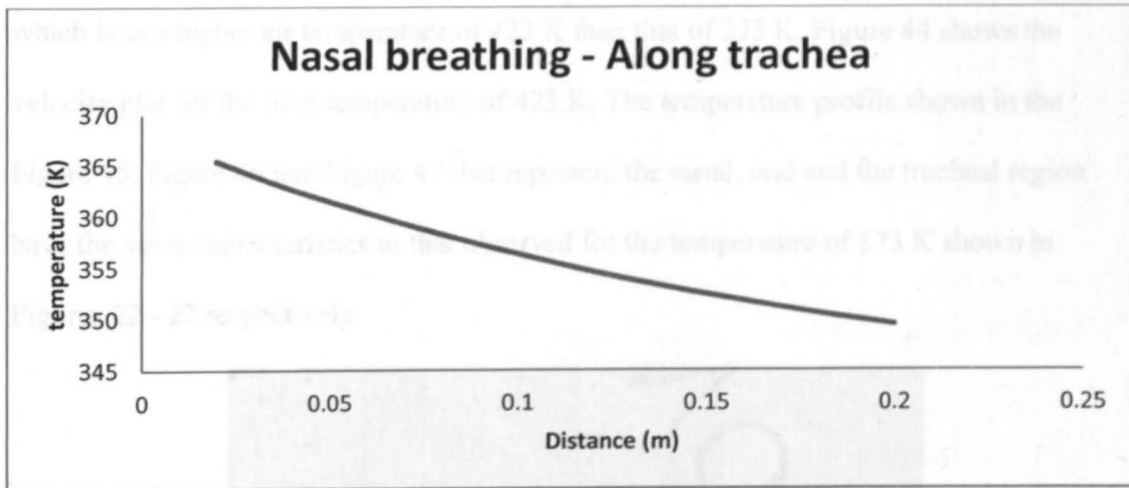


Figure 42. Temperature profile along trachea during nasal breathing

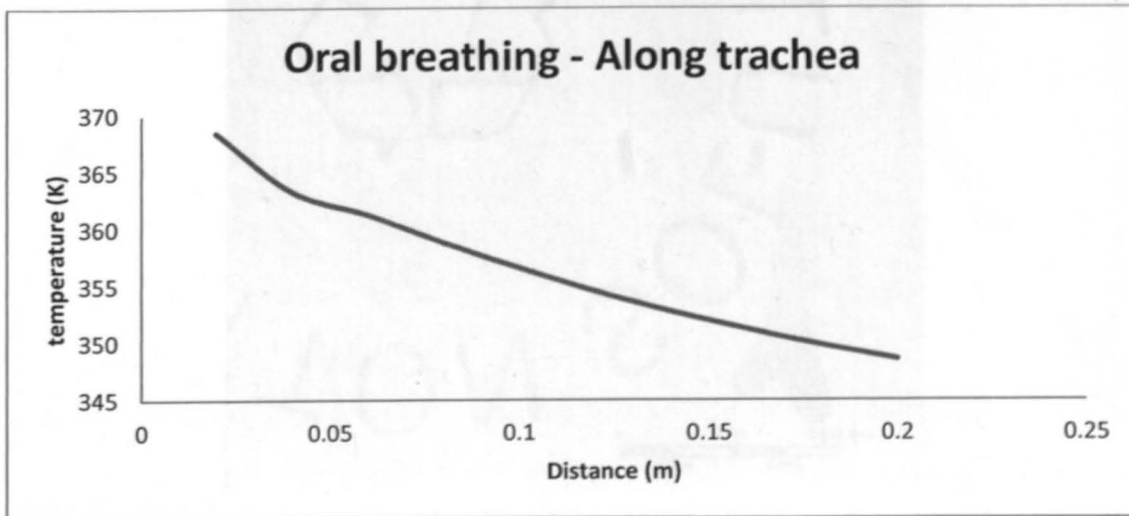


Figure 43. Temperature profile along trachea during oral breathing

4.6. Higher Temperature Inlet of 423 K.

A CFD simulation is also performed here to study the effect of higher air temperature of 150 degrees Celsius or 423 K. For this case the mesh configuration having total number of elements of 3003027 is used and the flow rate of 45 L/min for nasal and oral only breathing conditions are used as input. The results of these simulations are plotted down. The results given in this section give the temperature profile of the inlet air which is at a higher air temperature of 423 K than that of 373 K. Figure 44 shows the velocity plot for the inlet temperature of 423 K. The temperature profile shown in the Figure 45, Figure 46 and Figure 47 that represent the nasal, oral and the tracheal region have the same characteristics to that observed for the temperature of 373 K shown in Figures 22 - 27 respectively.

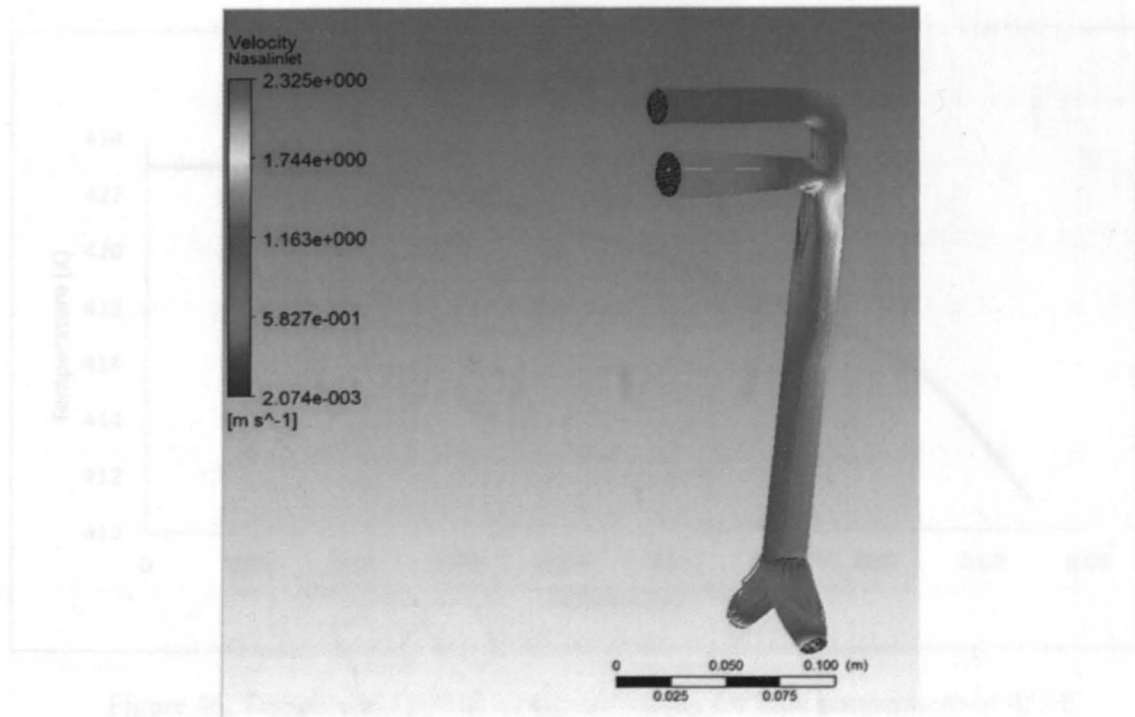


Figure 44. Velocity profile for inlet temperature of 423 K

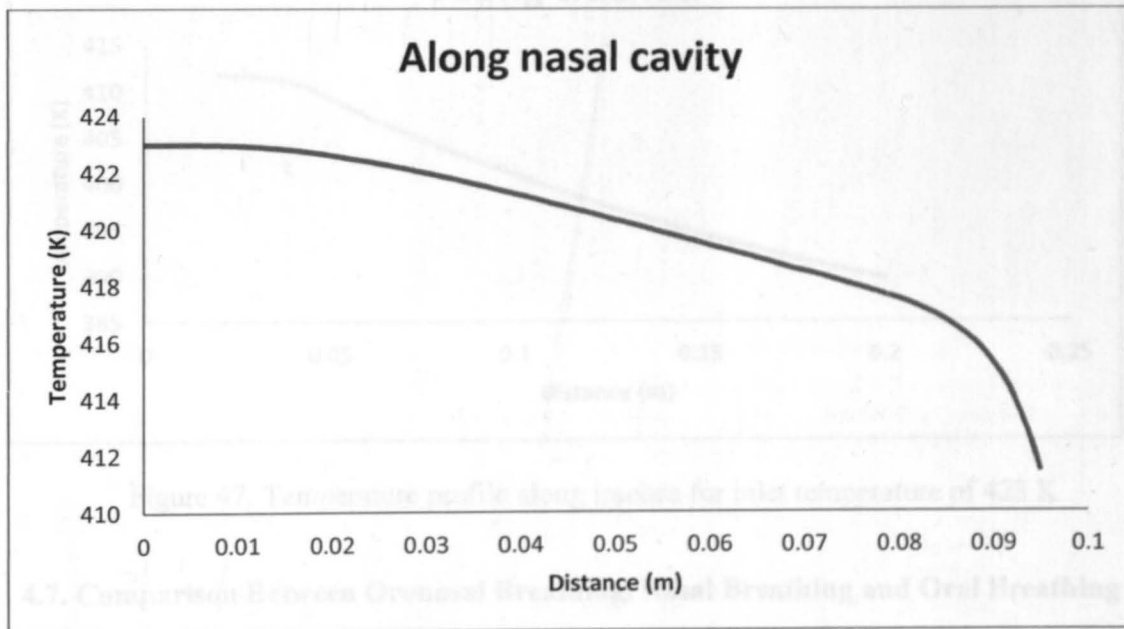


Figure 45. Temperature profile along nasal cavity for inlet temperature of 423 K

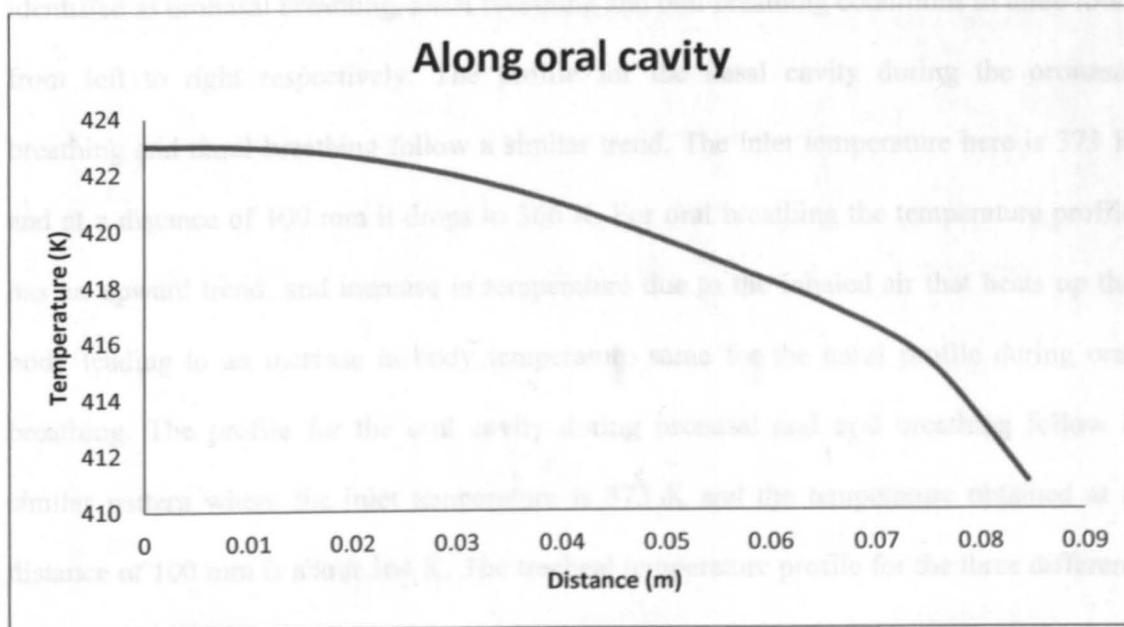


Figure 46. Temperature profile along oral cavity for inlet temperature of 423 K

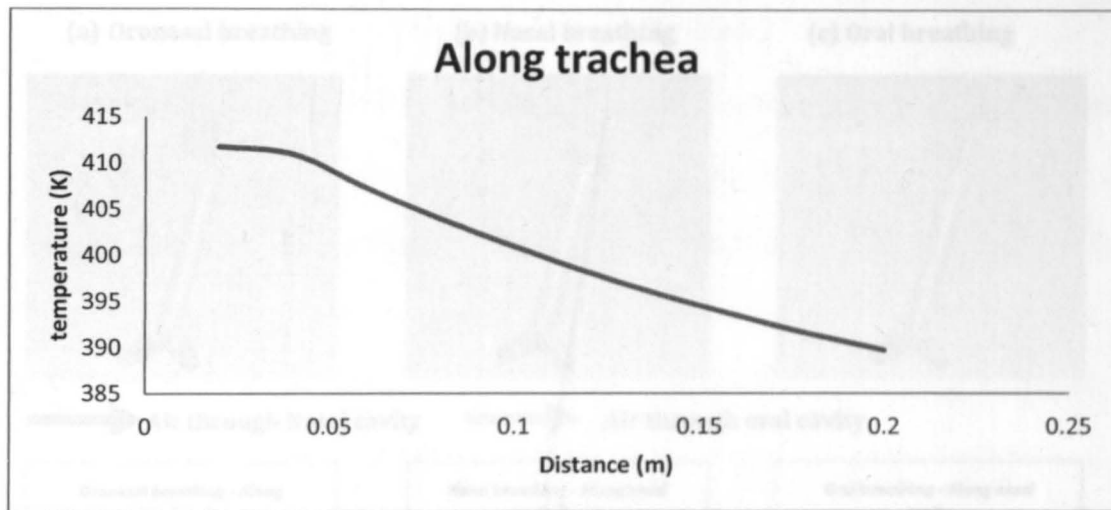


Figure 47. Temperature profile along trachea for inlet temperature of 423 K

4.7. Comparison Between Oronasal Breathing, Nasal Breathing and Oral Breathing

Figure 48 compares the temperature profile along the three different types identified as oronasal breathing, nasal breathing and oral breathing conditions in three rows from left to right respectively. The profile for the nasal cavity during the oronasal breathing and nasal breathing follow a similar trend. The inlet temperature here is 373 K and at a distance of 100 mm it drops to 366 K. For oral breathing the temperature profile has an upward trend, and increase in temperature due to the inhaled air that heats up the body leading to an increase in body temperature same for the nasal profile during oral breathing. The profile for the oral cavity during oronasal and oral breathing follow a similar pattern where the inlet temperature is 373 K and the temperature obtained at a distance of 100 mm is about 364 K. The tracheal temperature profile for the three different breathing conditions has a similar trend. The temperature at the inlet point of the path being about 365 K – 368 K and decreasing up to 350 – 355 K for a distance of 200 mm as defined in the model.

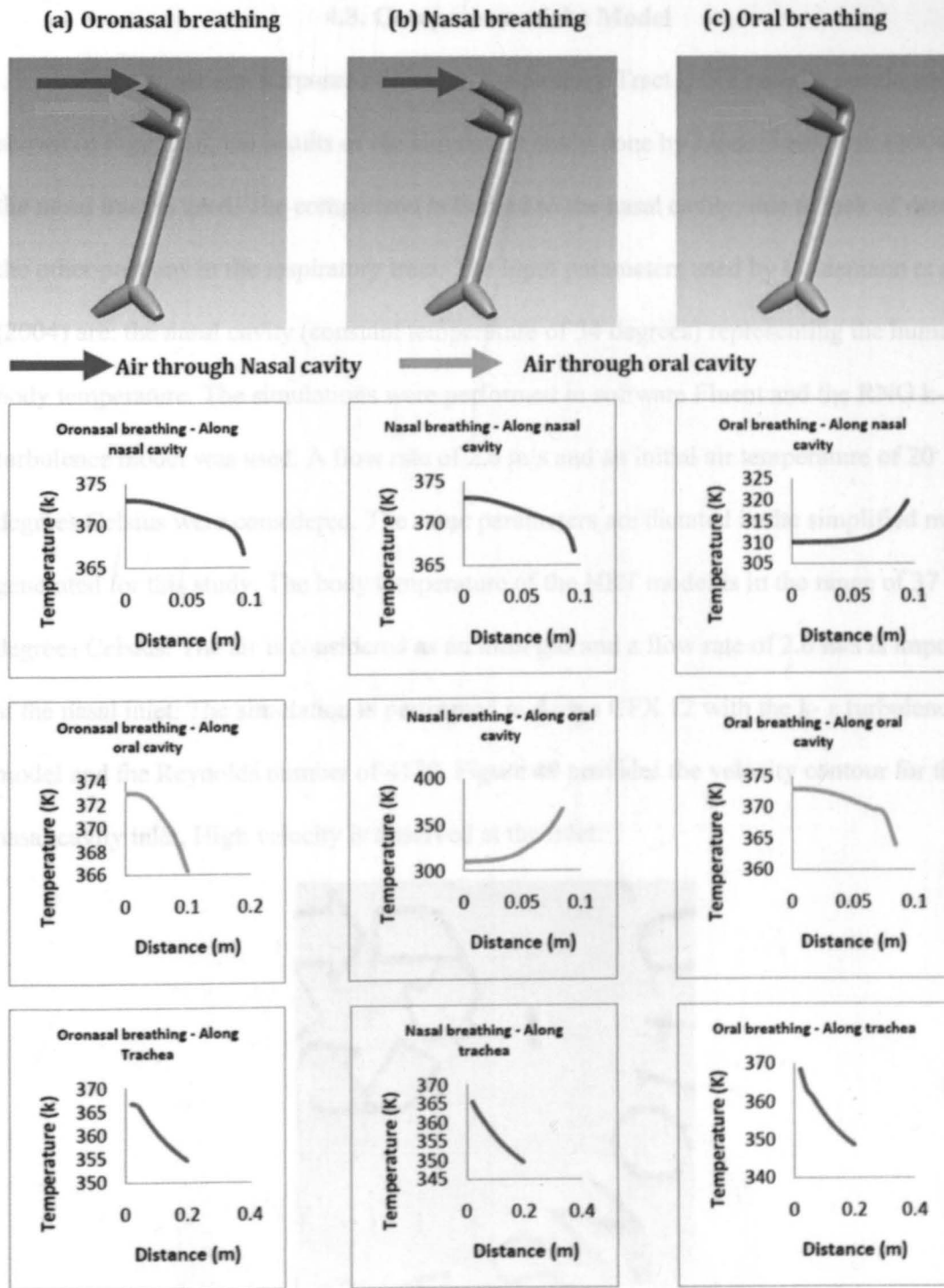


Figure 48. Comparison between oronasal breathing, nasal breathing and oral breathing

4.8. Comparison of the Model

For comparison purposes of Human Respiratory Tract (HRT) model developed and shown in Figure 18, the results of the simulation study done by Lindemann et al. (2004) for the nasal tract is used. The comparison is limited to the nasal cavity, due to lack of data for the other portions in the respiratory tract. The input parameters used by Lindemann et al. (2004) are: the nasal cavity (constant temperature of 34 degrees) representing the human body temperature. The simulations were performed in software Fluent and the RNG k- ϵ turbulence model was used. A flow rate of 2.6 m/s and an initial air temperature of 20 degrees Celsius were considered. The same parameters are dictated in the simplified model generated for this study. The body temperature of the HRT model is in the range of 37 degrees Celsius. The air is considered as an ideal gas and a flow rate of 2.6 m/s is imposed at the nasal inlet. The simulation is performed in Ansys CFX 12 with the k- ϵ turbulence model and the Reynolds number of 4130. Figure 49 provides the velocity contour for the nasal cavity inlet. High velocity is observed at the inlet.

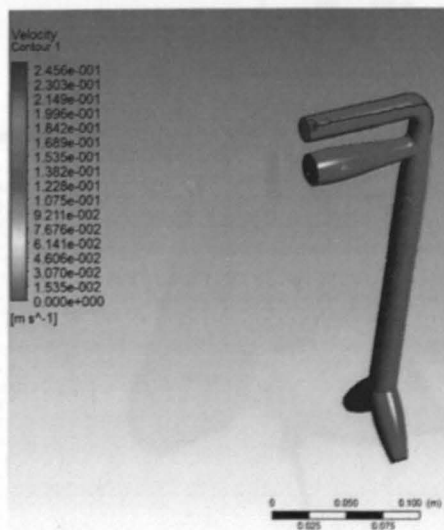


Figure 49. Velocity contour at nasal inlet

Figure 50 shows the temperature distribution for the results of the simplified model and that of Lindemann et al. (2004). The temperature at the surface of the simplified model is in the range of 293 K to 295 K whereas in that of Lindemann et al. (2004) it varies from 292 K to 307 K, but at the anterior portion where the cross section is small low temperature range is observed from 292 K to 298 K.

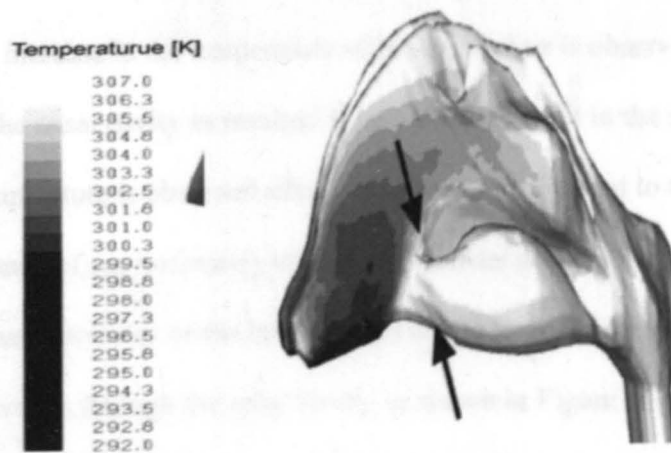
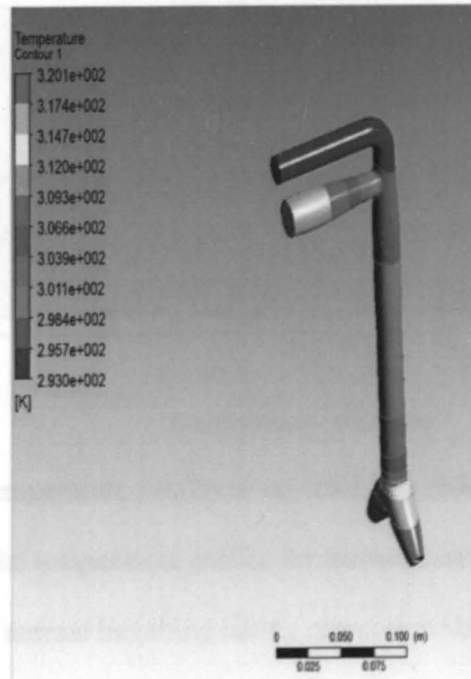


Figure 50. Comparison between current simulation model and Lindemann et al. (2004)

Figure 51 shows the logarithmic curve of temperature of air passing through the heated tube with steady wall temperature an experimental finding reported by Lindemann et al. (2004). The values of the temperature range and the length of the nasal cavity are estimated. The highest temperature increase is observed at the inlet of the tube.

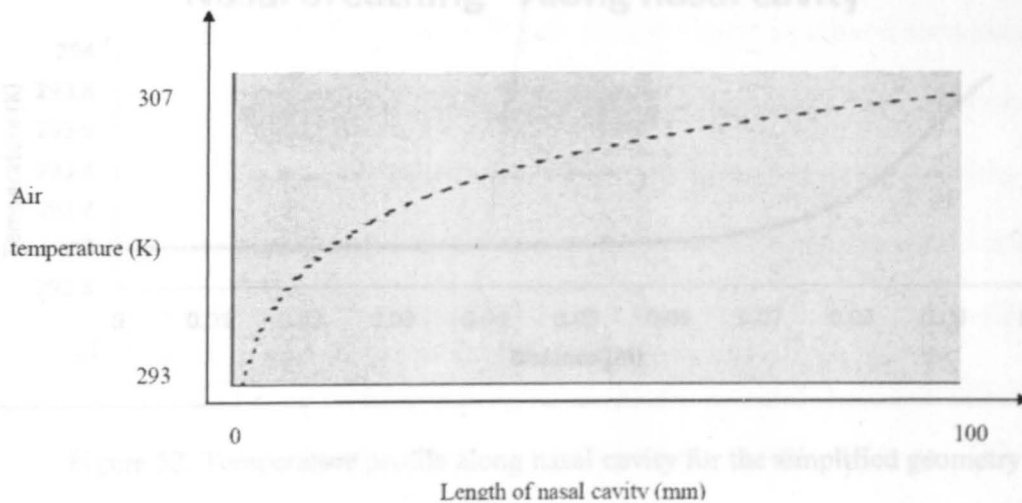


Figure 51. Temperature profile as reported by Lindemann et al. (2004)

Figure 52 shows the temperature profile for the nasal cavity in the simplified geometry. In the event of normal breathing taking place, it is observed during the inspiration phase that the temperature of inhaled air increases as observed in the above two cases. A steep increase in the temperature of the inhaled air is observed at the point where the air enters the nasal cavity as resulted from Lindemann but in the simplified model the increase in temperature is observed after a time period equivalent to the time taken to travel the distance of approximately 60 mm. The model used by Lindemann et al. (2004) depicts the actual geometry of the human nasal cavity where the cross-sectional area right from the inlet varies through the nasal cavity as shown in Figure 53 whereas the developed simplified model for the HRT has a circular cross-section and of a constant diameter for

the nasal cavity. More over the simplified model until the first two generation of the bronchi was taken into account for this simulation whereas the model used by Lindemann at al. (2004) considers the portion until the nasopharynx region.

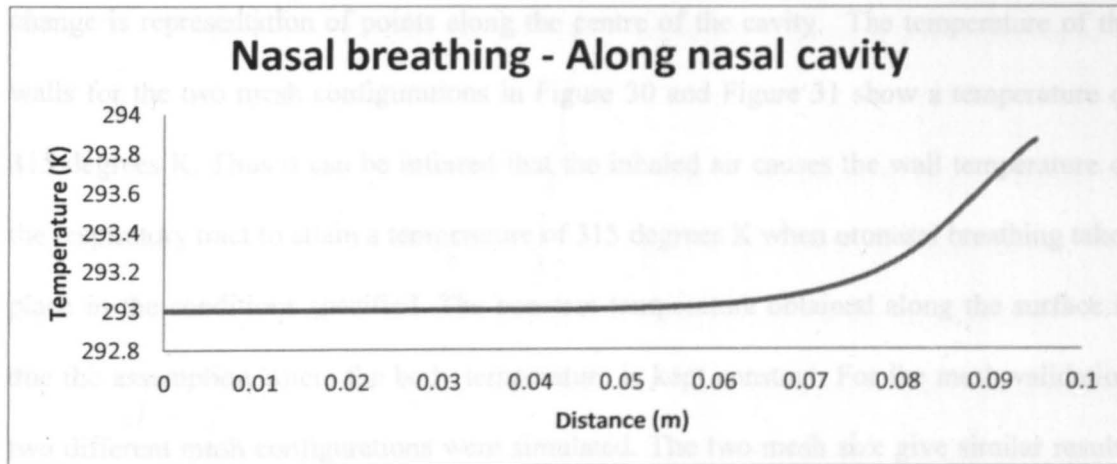


Figure 52. Temperature profile along nasal cavity for the simplified geometry

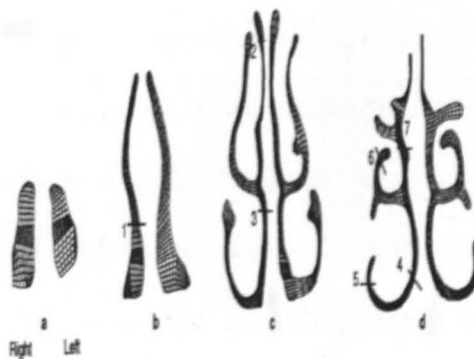


Figure 53. Cross-section at inlet (a) and towards the center (c, d), Subramanian et al.

(1997)

The temperature plots shown in Figures 22 - 27 give the temperature variations along the nasal cavity, oral cavity and the tracheal region. For the nasal and oral cavity the

temperature variation shown is starting from the inlet portion up to a distance of 100 mm inside the cavity. The temperature variation for the tracheal cavity is from the start of the oropharynx region up to a distance of 200 mm close to the bronchi. This temperature change is representation of points along the centre of the cavity. The temperature of the walls for the two mesh configurations in Figure 30 and Figure 31 show a temperature of 315 degrees K. Thus it can be inferred that the inhaled air causes the wall temperature of the respiratory tract to attain a temperature of 315 degrees K when oronasal breathing takes place in the conditions specified. The constant temperature obtained along the surface is due the assumption where the body temperature is kept constant. For the mesh validation two different mesh configurations were simulated. The two mesh size give similar results hence we can conclude that the results are independent of the grid size. This wall temperature will be temperature obtained at the surface of the tissue leading to a possible injury to the respiratory tract.

CHAPTER 5. BURN EVALUATION

Burn injury is one of the most serious injuries caused to the human body. It requires proper medication along with specialist treatment by a team of providers and nurses. Burn injury is also considered to be more catastrophic in nature and expensive to treat with prolonged recovery.

The injury to the human body extremities or skin is considered to begin with the burning sensation at a temperature of 44°C. The impact the temperature makes on the human tissue is dependent on two factors; the heat transfer rate and the time duration human tissue is in contact with the high temperature. The time factor which is the duration of time the tissue is exposed to high temperature more prominently determines the degree of the injury. Burn injuries are categorized in three levels based on severity. First, second, or third-degree burns depend on how badly the skin is damaged. First-degree burn which is considered the mildest of the three is limited to the top layer of human tissue internal to the body and the skin external to the body. The first-degree burns produce redness, pain, and minor swelling and externally the skin is dry and red. Internally, the tissue becomes dry and red as well with light swelling. Second-degree burns are more serious and impact the skin layers beneath the top layer of external skin and produces blisters externally with higher degree of pain and redness. Internally, the top tissue layer will be covered with bubbly blisters and will turn red and black. It will also be quite painful and will take much longer to heal. Third-degree burns are the most severe type of burn and involve all the layers of the skin and underlying tissue externally and internally could affect tissue and surrounding muscles. The surfaces will look charred and dry with a waxy white, leathery, brown, or charred look. Since the nerves are damaged or burned, there may be little or no

pain or the area may feel numb at first. The burn injuries caused can be due to radiation, convection and conduction.

Inhaled hot air can cause external and internal respiratory tract and lungs burn injuries. The burn injury caused in the human respiratory tract due to the inhalation of the hot gases is caused by heat transfer by convection. The majority of fire-related deaths (70 percent) are caused by smoke inhalation of the toxic gases produced by fires. Actual flames and burns only account for about 30 percent of fire-related deaths and injuries. The amount of injury or the damage occurred inside the human respiratory tract is dependent on the duration of the exposure, temperature of air exposed to, and finally the portion of the respiratory tract impacted.

Quantitative burn evaluation was first proposed by Henriques. The burn evaluation is performed by the use of Henriques's burn integration model given in equation 1.

$$\Omega = \int_0^t P \exp\left(-\frac{\Delta E}{RT}\right) \cdot dt \quad (\text{Eq. 1})$$

Where,

P = constant that varies with tissue and local temperature

ΔE = activation energy

R = ideal gas constant

Ω = dimensionless Henriques' burn integral

T = Temperature (K)

5.1. Fire and Fire Injury Statistics

According to Lafferti and Goet, burns and fires are considered to be the third leading cause of injuries among the human population. The injuries due to fire and burns

are stated as the second leading cause for death in homes for all age group and leading cause of injury in case of children and young adults. In 1998, approximately 381,500 residential fires occurred in the US, resulting in 3,250 non firefighter deaths, 17,175 injuries, and nearly \$4.4 billion in property loss. It is also stated that an estimated 90% of fires not reported to fire departments. More than half of all fatal residential fires started between the hours of 11 pm and 7 am. As quoted by Lafferti and Goet "Incidence of smoke inhalation increases from less than 10% in patients with a mean total body surface area (TBSA) burn size of 5% to more than 80% in patients with a mean TBSA burn size of 85% or more. Smoke inhalation is present in one third of patients treated at burn centers. The magnitude of smoke inhalation is devastating, as the presence of an inhalation injury has a greater effect on mortality than either patient age or surface area burned". According to the National Fire Protection Association survey, in 1997, 4,675 Firefighters suffered burn injuries as a result of performing their assigned duties, of which 3,770 also suffered inhalation injuries.

5.2. Thermal Impact

Lv et al (2006) has concluded that at the nasal surface the first degree burn occurs only after 230 seconds and for the deeper tissue it takes more than 900 seconds for a first degree burn to occur. The minimum temperature for the first degree burn to occur is 44° C (317° K). The burn evaluation performed here was based on the Henrique's model where the tissue damage is represented as an integral of a chemical rate process.

A first-degree and second-degree of burn is said to occur if both conditions 1 and 2 below are satisfied.

1. $T > 44^{\circ}\text{C}$ (317°K)
2. $\Omega > 0.53$ (First degree burn)
3. $\Omega > 1$ (Second degree burn)

Temperature for degree of burns:

A first degree burn involves damage to the epidermis, second-degree burn involves the epidermis and a part of the dermis, whereas the third-degree burns involves deeper tissue. The temperature range is provided in Table 3. Temperature range for degree of burn to occur. Temperature obtained at the skin surface for simulating inlet air temperature of 100°C and 150°C is given Table 4. Temperature obtained at respiratory tract surface.

Table 3. Temperature range for degree of burn to occur

Degree of Burn	Temperature ($^{\circ}\text{C}$)	Temperature ($^{\circ}\text{K}$)
First degree	44	317
Second degree	51	324
Third degree	71	344

Table 4. Temperature obtained at respiratory tract surface

Temperature of inlet air ($^{\circ}\text{C}$)	Temperature of inlet air ($^{\circ}\text{K}$)	Temperature obtained at respiratory tract surface ($^{\circ}\text{C}$)	Temperature obtained at respiratory tract surface ($^{\circ}\text{K}$)
100	373	42	315
150	423	47	320

5.3. Time for Thermal Injury to Occur in the Upper Human Respiratory Tract

Lv et al (2006) have outlined that the temperature increases with the distance away from the nose and at the main Bronchial generation at about 180 mm where the temperature reaches 90% of the body temperature during normal breathing conditions. Mucosal temperature is assumed to be constant. For the temperature of 150° C, the temperature of tissues at a length of 80 mm and for a radius of 0.635 cm will be 48° C at 300 seconds. When surrounding air temperature is 70° C the temperature of tissues at 80 mm will be 39° C.

From the simulation, for the two temperatures of 100° C and 150° C we determine the time required for the first and second degree using values provided in Table 5. Values for Henriques' constant (Lv et al. (2006)).

Table 5. Values for Henriques' constant (Lv et al. (2006))

Epidermis	Henriques' constant	Weaver's constant	Mehta's constant
P (s ⁻¹)	3.1 X 10 ⁹⁸	3.1 X 10 ⁹⁸ , 44° C < T ≤ 50° C 1.823 X 10 ⁵¹ , T ≥ 50° C	1.43 X 10 ⁷²
ΔE/R (K)	75000	93534.9, 44° C < T ≤ 50° C 39109.8, T ≥ 50° C	55000

A first-degree burn is experienced if both conditions, $T > 44^{\circ}\text{C}$ (317° K) and $\Omega > 0.53$ are satisfied. For the inlet air temperature 100° C we have the temperature obtained at the surface < 44° C hence we can conclude that no internal burn injury takes place. When the inlet air temperature is 150° C we observe that the temperature obtained at the surface

of the skin is $> 44^{\circ}\text{C}$, hence we perform a burn evaluation to predict the time required for first and second-degree burn using equation 1.

Table 6. Results solving equation 1 with respect to time shows the results obtained from the calculations for two inlet temperatures. First-degree burn occurs at a time of 1050 seconds after exposure where $\Omega > 0.53$ and second-degree burn occurs at 2000 seconds after exposure where $\Omega > 1$ at the skin surface. Figure 54 gives the burn integral values for various time steps.

Table 6. Results solving equation 1

Parameter	Inlet 100°C	Inlet 150°C
$P\ (\text{s}^{-1})$	$3.1\text{E}+98$	$3.1\text{E}+98$
$\Delta E/R$	75000	75000
T	315	320
$\Delta E/RT$	/	234.375
	/	-234.375
Exp	/	$1.63\text{E}-102$
Function	/	0.0005054

5.4. Injury as a Result of Inhaling Hot Gas or Steam

A Fire smoke is a mixture toxic substances and of high temperature. This mixture of smoke and toxic substance when inhaled causes burn injury inside the Human Respiratory Tract, and at times becomes fatal to human life. Fire has been associated with 3 different types of inhalation injuries that cause damage to the human body.

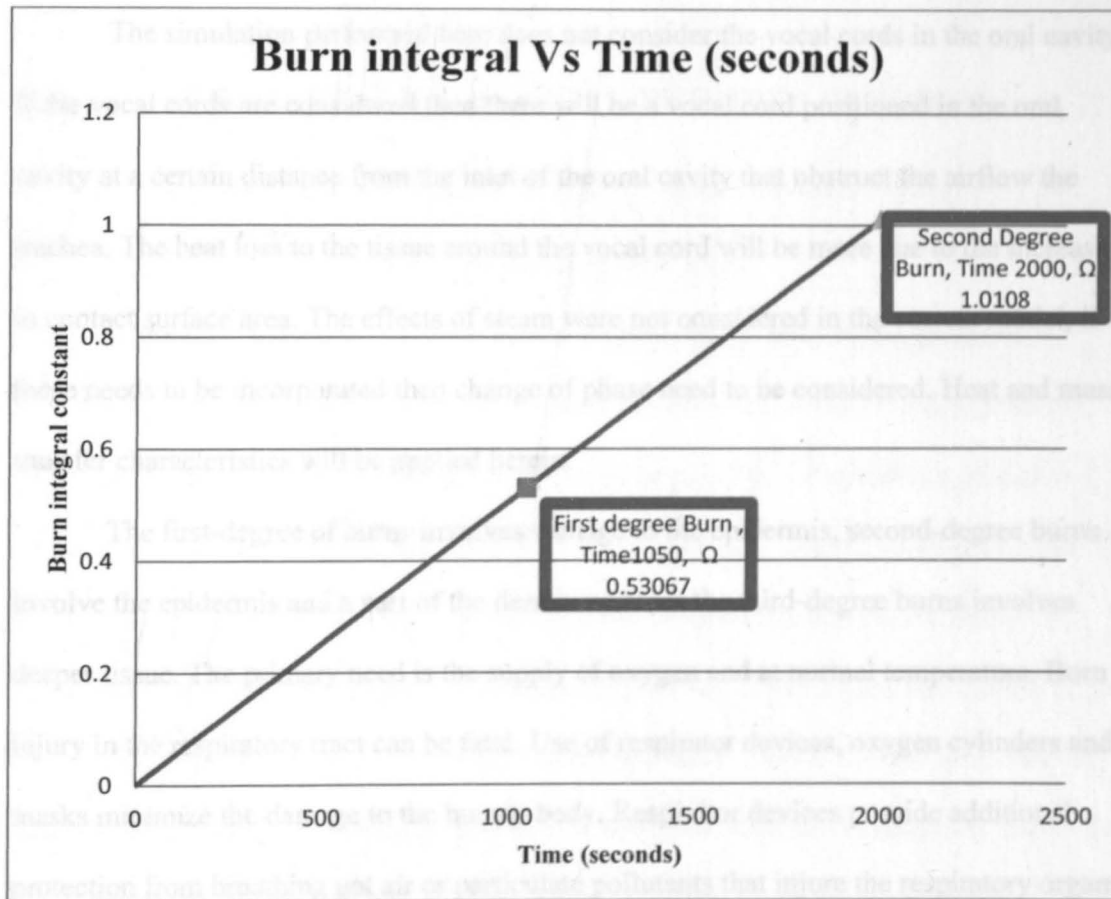


Figure 54. Ω (Burn value) value at various time (seconds) level

Inhalation of high temperature gas causes burns inside the Human Respiratory Tract. During inhalation of hot gas the portion of the upper Human Respiratory Tract gets affected to a vast extent protecting the lungs. The inhaled fluid if consists of toxic substances included in it also proves fatal to human life. Toxic substances are readily absorbed into oxygen and can cause damage to the human organs including brain. Carbon Monoxide poisoning can appear symptomless up until the point where the victim falls into a coma. Lastly, during situation of fire hazard, smoke inhalation is more likely resulting into burn injury into the Human Respiratory Tract. 60% to 80% of fatalities resulting from burn injuries can be attributed to smoke inhalation.

The simulation performed here does not consider the vocal cords in the oral cavity. If the vocal cords are considered then there will be a vocal cord positioned in the oral cavity at a certain distance from the inlet of the oral cavity that obstruct the airflow the trachea. The heat loss to the tissue around the vocal cord will be more due to the increase in contact surface area. The effects of steam were not considered in the current model, if these needs to be incorporated then change of phase need to be considered. Heat and mass transfer characteristics will be applied herein.

The first-degree of burns involves damage to the epidermis, second-degree burns involve the epidermis and a part of the dermis whereas the third-degree burns involves deeper tissue. The primary need is the supply of oxygen and at normal temperature. Burn injury in the respiratory tract can be fatal. Use of respirator devices, oxygen cylinders and masks minimize the damage to the human body. Respirator devices provide additional protection from breathing hot air or particulate pollutants that injure the respiratory organs. Respirator devices can be classified as face masks or respirators with oxygen supplies. A respirator is designed as an enclosure that covers the nose and mouth or the entire face or head. Some respirators are also assisted with oxygen cylinders. A higher air velocity is said to increase the tissue temperature absurdly, hence decreasing the air velocity and increasing the respiratory rate is helpful for minimizing the thermal injury in respiratory tract.

CHAPTER 6. PROPOSED METHODOLOGY FOR ANTHROPOMETRIC DATA COLLECTION

6.1. Anthropometric Data

Anthropometric data collection is a tool widely used today in design and development of a product. The use of the Anthropometric data during the design stage assists in the optimum use of the product by target population for intended application. National institute for occupational safety and health (NIOSH) conducted an anthropometric study of the facial measurements. The safety of the population using the respirators is addressed by the NIOSH and it is the responsibility of NIOSH to ensure that quality of the respirators is maintained and it fits to the target population. Hence NIOSH conducted an anthropometric survey of sample population depicting the diverse US respirator users. The manufactures also followed the guidelines given by NIOSH. An overview of the airway geometry is needed by many for the purpose of studying the airflow dynamics involved. The volume of intake air first comes in contact with the anterior portion of the nasal cavity and oral cavity. These two regions get first affected by the fluid intake. The geometry of the nasal cross section is very complex and asymmetric in nature. These dimensions are measured using scanning and imaging methods for measuring the cross-section in the middle region consisting of the turbinates and the posterior region connecting to the Nasopharynx. The Anterior portion as highlighted in Figure 55 can be measured using the available device patented (US6659963) shown in Figure 56. The Oral cavity when compared to the nasal cavity is convenient to measure until the throat region.

Data collections for the anthropometric measurements are usually related to the measurements externally and not internally due to the complexity of the human body. The anthropometric data measured for the external body comprise of number of subjects up to 4000 in number and more. The morphometric studies conducted for the internal body consisted of approximately 100 subjects at the maximum. The reason here is that the internal studies need sophisticated equipments like CT or MRI scans etc whereas the external anthropometric measurements need basic measuring instruments like calipers and measuring tape. The usage of the imaging devices is a complicated procedure and needs to be done by medical providers. The use of these equipments could be complicated, time consuming and cost will be staggering for a large population sample size. The same when performed by the use of the measuring devices for external anthropometric measurements will not be as expensive and complicated as for example the use of imaging devices.

The anthropometric data related to the volume of the nasal and oral cavity has been measured using imaging devices using small sample size. A measuring technique is proposed here in to measure the dimensions of the nasal and oral cavity with help of measuring instrument. The instrument could be used for measuring the inside dimensions of the nasal and oral cavity. This process of collecting anthropometric data for the human nasal and the oral cavity will provide the much needed data to help with the treatment of injuries, design of the respirator systems and other respiratory devices.

6.2. Current Methodology

A number of approaches are in the literature that study the characteristics related to heat and mass transfer along the HRT, deposition of particles, drug therapy applications and injury analysis. These studies do involve taking measurements of the various portions

of the upper (nasal and oral) respiratory tract. The Human body does show a high degree of variation between different Human races around the world. The Anthropometric data collection for the human respiratory tract can be identified in two different categories, first in which the measurements for the internal portion of the HRT are taken into consideration for the analysis of the process of heat transfer characteristics, burn injury and or aerosol deposition taking place and in the second category the facial dimensions are noted down to assist fitting of the respirator device on the human face for full-facepiece respirators or half-facepiece respirators. The categories when analyzed are from a completely different point of view but when the functionality is taken into account; the facial characteristics and the inlet portion of the nasal and oral cavity are directly related to the effective functioning of the human being using the respirator device. The current methodology of gathering the anthropometric data are limited in both the cases. For the category 1 the inlet dimensions of the HRT are identified using the process of CT scan, MRI and Acoustic Rhinomanometry which is a costly process and can be performed on a limited number of subjects. The use of scale, calipers and tape for the category 2 type has been extensively used. This method has been performed on a number of subjects but it has its limitations as it can measure only the facial dimensions from outside.

6.3. Proposed Methodology

The Nasal cavity geometry follows a highly complex and asymmetric shape after a length of about 30 mm from the nasal inlet. The process of capturing the characteristics of this region is challenging task. The first 30 mm length of the Nasal cavity is the anterior portion which first comes in contact with the flow during inlet as shown in Figure 55 (During a hazardous situation if hot air is inhaled then degree of burn injury suffered could

be very high). The dimensions can be measured if an appropriate measuring device is designed for this particular task. The procedure for using this type of tool which penetrates into anterior portion of the nasal cavity must be performed under medical supervision. Figure 57 shows a measuring device (patent number US6659963) designed to measure the cavity in the anterior portion of the nasal cavity in between the inlet and the nasal turbinates.

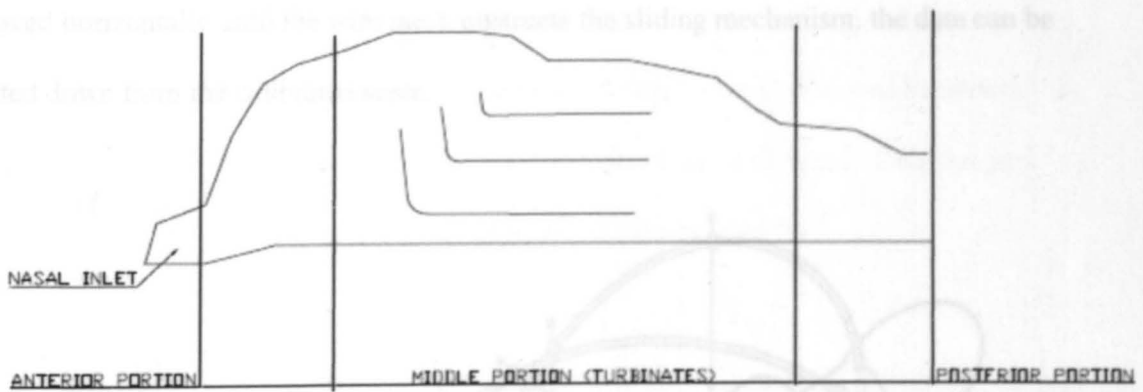


Figure 55. Anterior portion of the Nasal cavity

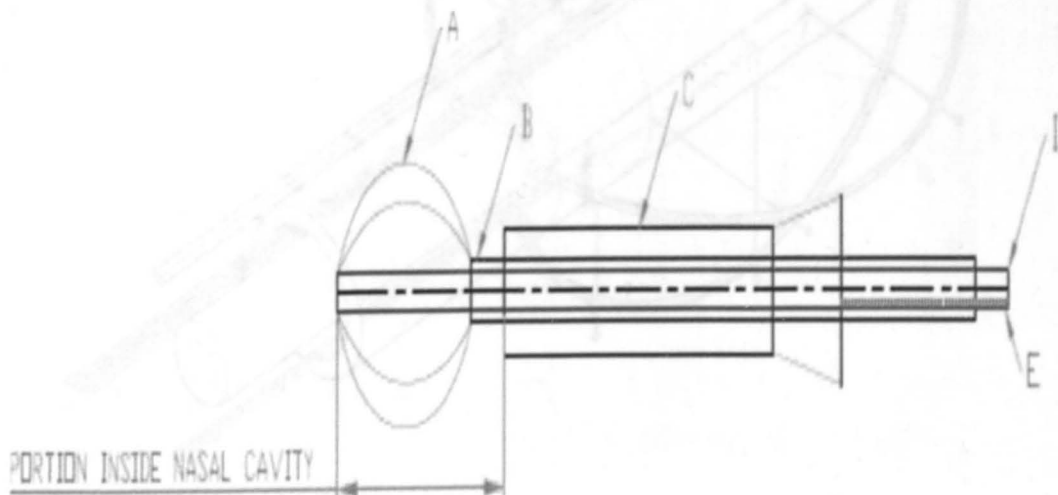


Figure 56. Tool for measuring Nasal cavity dimension. (Patent number US6659963)

The device consists of three different tubes of varying length and diameter. The tube E has a calibrated scale shown in red color. The tube B and D are connected by a wire mesh A. The wire mesh A expands or contracts when the tube D is moved in the horizontal direction i.e. inwards or outwards. The outer tube C acts as support for the two sliding tubes within. The portion of the tool that penetrates into anterior portion of the nasal cavity is highlighted in Figure 56. When the portion is inserted into the cavity and the tube is moved horizontally until the wire mesh obstructs the sliding mechanism, the data can be noted down from the calibrated scale.

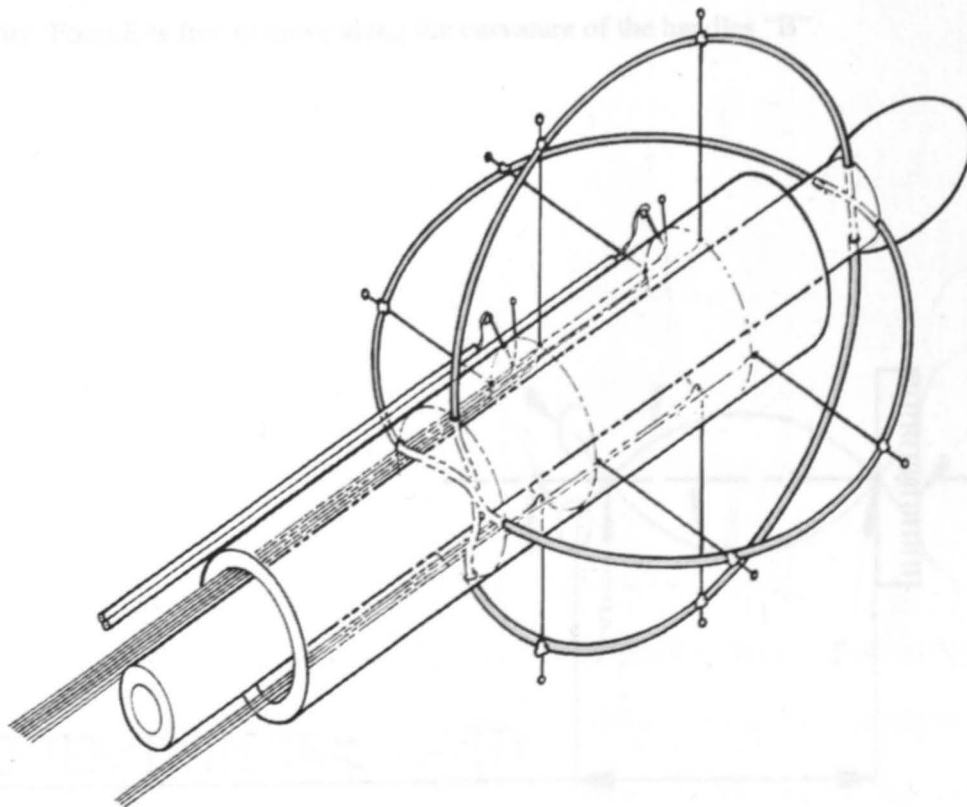


Figure 57. Pictorial view of the tool (Patent number US6659963)

The dimensions of the Oral cavity can also be measured internally. A measuring instrument similar to a caliper can be used to measure distance in 2 or 4 or 8 directions. This procedure might not need the degree of medical supervision as in the case of the Nasal cavity measurement but it is advisable to have a guidance of a medical practitioner.

Figure 58 shows an arrangement of the instrument designed to measure the oral cavity dimensions. The end portion A is inserted into the mouth while the handle D is manipulated. The ends "A" are placed against the wall of the oral cavity and the displacement of ends "A" is measured from the calibrated scale C. The two handles B pivot about the point F to place the two ends "A" against the wall tissue inside the oral cavity. Point E is free to move along the curvature of the handles "B".

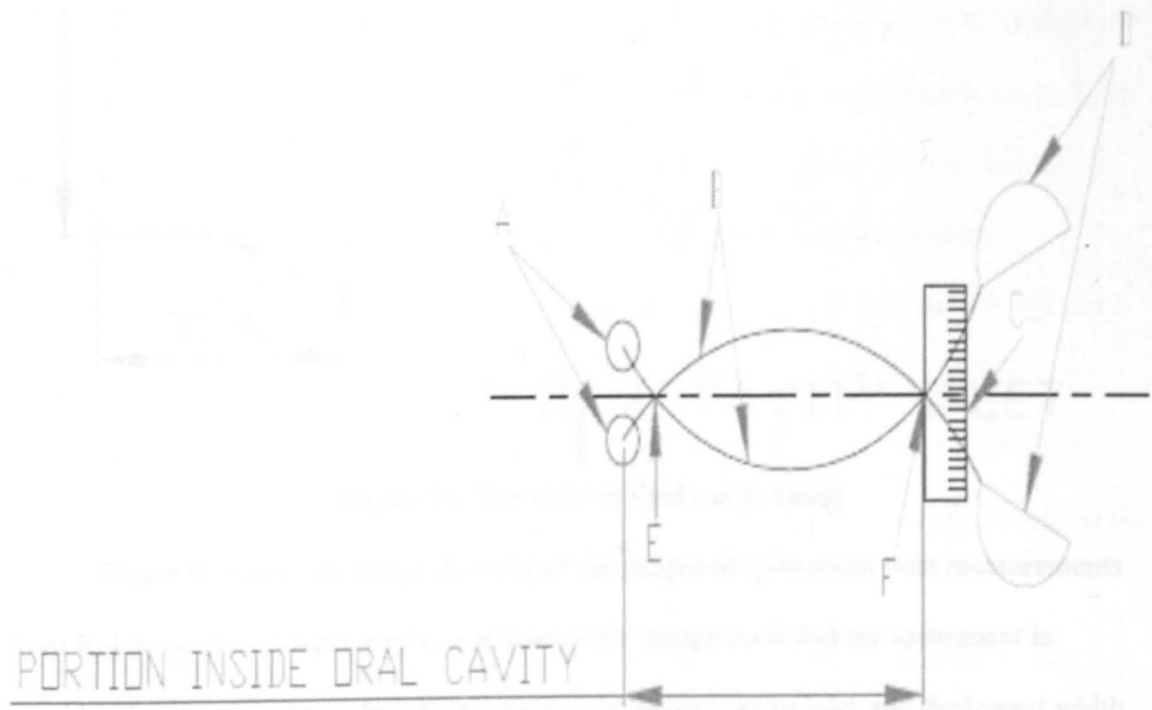


Figure 58. Tool for measuring Oral cavity dimension

The instrument shown in the Figure 58 is proposed using the dimensions of the oral cavity as identified in Robinson et al. (2009) as a guideline. The inlet of the oral cavity is the widest and follows a tapering cross-section as it advances horizontally towards the Oropharynx. The outermost width being 30.9 mm and approximately 20 mm in width when measured 54 mm deep within the oral cavity as shown in Figure 59.

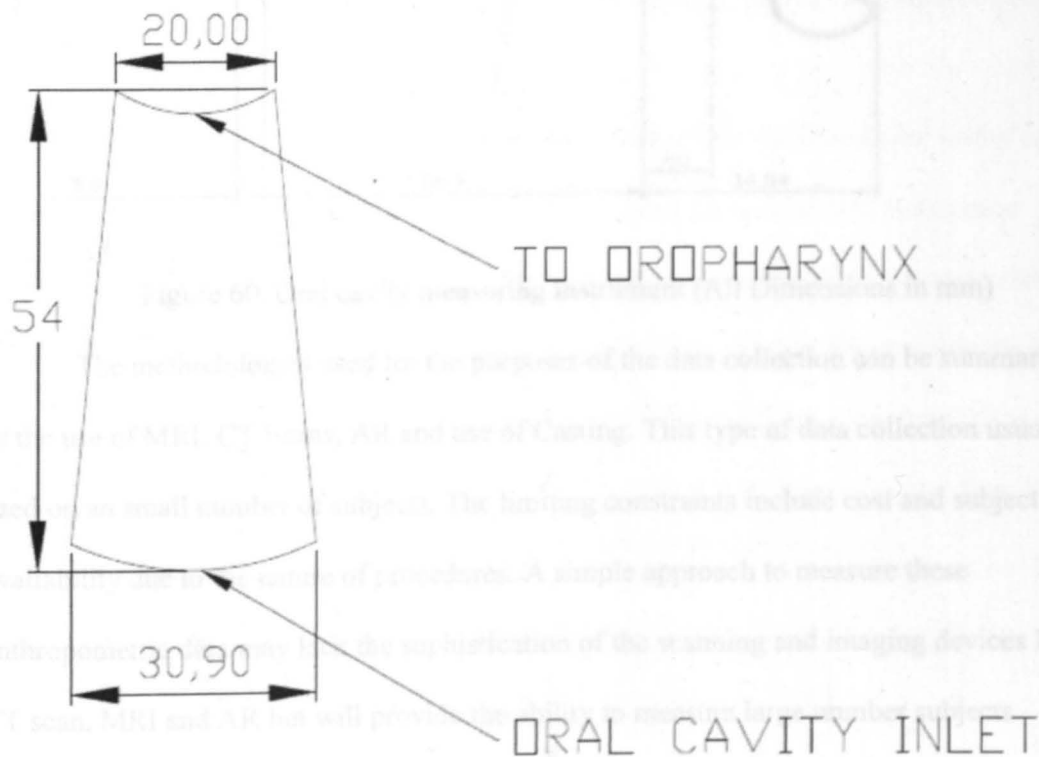


Figure 59. Top view of Oral cavity (mm)

Figure 60 shows the actual drawing of the proposed instrument with measurements from Robinson et al. (2009) used as a reference for design such that the instrument is capable of measuring the widest distance close to the oral cavity inlet and the lowest width which is at a distance of 54 mm from the opening.

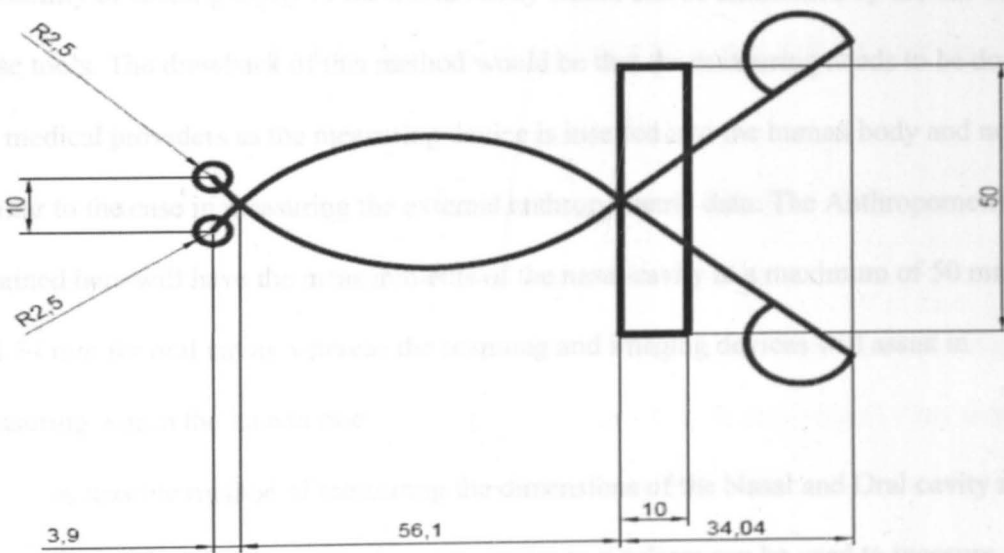


Figure 60. Oral cavity measuring instrument (All Dimensions in mm)

The methodologies used for the purposes of the data collection can be summarized as the use of MRI, CT Scans, AR and use of Casting. This type of data collection usually is used on a small number of subjects. The limiting constraints include cost and subject availability due to the nature of procedures. A simple approach to measure these anthropometric data may lack the sophistication of the scanning and imaging devices like CT scan, MRI and AR but will provide the ability to measure large number subjects leading to more statistically usable data. The usages of the MRI, CT scan and AR have disadvantages of being unsafe from ionizing radiation or high costs of using the equipment and use.

The advantages of using this process of identifying the internal nasal and cavity dimensions can be attributed to the fact that this process can be applied to a large sample group. The cost involved with the use of the scanning and imaging devices will also be eliminated by this process. Exposure to the scanning and imaging devices also has a

possibility of causing injury to the human body which can be eliminated by the use of these tools. The drawback of this method would be that the measuring needs to be done by the medical providers as the measuring device is inserted into the human body and not similar to the case in measuring the external anthropometric data. The Anthropometric data obtained here will have the measurements of the nasal cavity at a maximum of 50 mm deep and 54 mm for oral cavity whereas the scanning and imaging devices will assist in measuring within the human body.

A feasible method of measuring the dimensions of the Nasal and Oral cavity needs to be developed. A measuring instrument similar to a caliper can be used to measure the distance and or volume within the cavity. The process of measuring the anthropometric data here first starts with defining the landmarks in the human body, for example the tip of the nasal or oral inlet being one of the landmarks in the data collection process followed by the data analysis

CHAPTER 7. CONCLUSION AND FUTURE RESEARCH

7.1. Conclusion

A heat transfer study along the Human Respiratory Tract (HRT) provides the temperature distribution and variation along the surface of the respiratory tract for the given length during oronasal breathing conditions. The temperatures obtained along the surface of the tissue walls help in assessing the internal burn injury caused. This study will assist in developing safe and effective preventive measures and treatments to the injuries caused in the respiratory tract. Design of respirator devices and safety features for the occupations that involve an exposure to extreme and unfavorable conditions to the human health can be well implemented by knowing the level of injury caused in the HRT. A comparison of the differences in the temperature profile in the HRT considering variations in breathing pattern and the implementation of respiratory devices to cool the inhaling air temperature to normal range will be quite effective in preventing any injury. An approach of measuring the nasal and oral cavity dimensions is outlined above. The proposed approach is in reference to the Anthropometric data collected for the use of the respiratory device design and treatment of the respiratory tract during injury. The process of collection is challenging if a large sample size has to be used in the Anthropometric data collection process both using scanning/imaging devices and manually.

7.2. Future Research

Future studies could include the use of hazardous particle deposition along the respiratory tract during oronasal breathing, simulating various adverse conditions. Extreme temperatures, hot or cold do affect the human being and to evaluate the extent such

simplified models can be used for CFD simulations. The effect of cold inhaled air, the temperature variation along the HRT can also be studied. The deposition phenomenon of the drug can also be simulated in order to observe the drug deposition pattern.

Cheng, K. H., Cheng, T. S., Chen, J. and Hoff, D. L. (1997). "Measurements of airway cross-sections and estimation of steady-state transfer characteristics of human oral passage." *Journal of Aerosol Medicine*, 10(2), 129-142.

Cheng, K. H., Cheng, T. S., Chen, J., Hoff, D. L., Simpson, S. Q., Yang, Y. and Nath, P. (2001). "The measurement of nasal airway dimensions and relationship to dimensions of the human nasal and oral airways." *Journal of Aerosol Medicine*, 27, 105-110.

Cheng, K. H., Cheng, T. S. (1998). "Mathematical modeling of heat and water transport in human respiratory tract." *Journal of Aerosol Physiology* 69(1): 362-372.

DeLoraine, D., Malmgren, B., Smed, M. "An anthropometric face modeling using variational techniques." *Journal of Aerosol Medicine* 15(2): 105-115.

Du, L., et al. (2008). "Nasal and oral anthropometric survey of Chinese workers." *Annals of Occupational Hygiene* 52(5): 771-777.

Elmehrik, G., et al. and Hoff, M. (2001). "Anatomically-based three-dimensional model of airway resistance, flow and particle transport using computational fluid dynamics." *Journal of Aerosol Medicine* 14(4): 289-300.

Evans, G. W. and Whitaker, W. S. (1961). "Measurement of Time Constant of Wet-Bulb Thermometer in Air." *Journal of Heat Transfer* 19(3): 165-180.

REFERENCES

- Bubb, H. (2004). "Challenges in application of anthropometric measurements." Theoretical issues in Ergonomical Science. **5**(2):154-168.
- Cheng, K. H., Cheng, Y. S., Yeh, H. and Swift, D.L., (1997). "Measurements of airway dimensions and calculation of mass transfer characteristics of human oral passage." Transactions of the ASME. **119**: 476-482.
- Cheng, K. H., Cheng, Y. S., Yeh, H., Guilmette, R. A., Simpson, S. Q., Yang, Y. and Swift, D. L., (1996). "In VIVO measurement of nasal airway dimensions and ultrafine aerosol deposition in the human nasal and oral airways." Journal of Aerosol Science. **27**: 785-801.
- Daviskas, E., Gonda, I., et al. (1990). "Mathematical modeling of heat and water transport in human respiratory tract." Journal of Applied Physiology **69**(1): 362-372.
- DeCarlo, D., Metaxas, D., Stone, M., "An Anthropometric face modeling using variational techniques."
- Du, L., et al. (2008). "Head-and-face anthropometric survey of Chinese workers." Annals of Occupational Hygiene. **52**(8):773-782.
- Erthbruggen, C., Hirsch, C. and Paiva, M. (2005). "Anatomically based three dimensional model of airways to simulate flow and particle transport using computational fluid dynamics." Journal of Applied physiology. **98**:970-980.
- Farahmand, K. and Kaufman, J.W. (2006). "Measurement of Time Constant of Wet-Bulb Thermocouple in Air." Experimental Heat Transfer **19**(3): 165 - 180.

- Farahmand, K. and Kaufman, J.W. (2001). "Experimental measurement of fine thermocouple response times in air." Experimental Heat Transfer **14**(2): 107 - 118.
- Farahmand, K. and Kaufman, J.W. (2006). "In vivo measurements of human oral cavity heat and water vapor transport." Respiratory Physiology & Neurobiology, **150**(2-3): 261-277.
- Saidel, G. M., et al. (1985). "Model Simulation of Heat and Water Transport Dynamics in an Airway." Journal of Biomechanical engineering **105**(2): 188.
- Yu, G., Zhang, Z. and Lessmann, R. (1998). "Fluid flow and Particle Deposition in the human upper respiratory system" Aerosol Science and Technology **28**: 146-158
- Gemci, T., Ponyavin, V., Chen, Y., Chen, H. and Collins, R. (2007). "Computational model of airflow in upper 17 generations of human respiratory tract." Journal of Biomechanics **41**: 2047 - 2054.
- Gemci, T., Corcoran, T.E. and Chigier, N. (2002) "A numerical and experimental study of spray dynamics in a simple throat model." Aerosol Science and Technology. **36**:18 - 38 (2002).
- Gomes, A.O.C., Claudia, A., Teixeira, M.S., Henrique, S., Trindade, K., Trindade, I.E.K., (2008). "Nasal cavity geometry of healthy adults assessed using acoustic rhinometry." Rev Bras Otorrinolaringol. **74**(5):746-754.
- Grgic, B., Finlay, W.H., Heenan, A.F., 2004. "Regional aerosol deposition and flow measurements in an idealized mouth and throat." Journal of Aerosol Science. **35**. 21-32.

- Grgic, B., Finlay, W.H. and Heenan, A.F. (2004). "In vitro intersubject and intrasubject deposition measurements in realistic mouth-throat geometries." Journal of Aerosol Science. **35**:1025-1040.
- Hack, A. L. and McConville, J.T. (1978). "Respirator protection factors: Part 1 – Development of an anthropometric test panel". American Industrial Hygiene Association. **39**:970-975.
- Hanna et al. (1986). "A theoretical model of localized heat and water vapor transport in the human respiratory tract." Journal of Biomechanical engineering **108**(1): 19-27.
- Harber, H., Beck, J. and Luo, J., (1997). "Study of Respirator Effect on Nasal-Oral flow partition". American Journal of Industrial Medicines. **32**:408-412.
- Hilberg, O., Jackson, A. C., Swift, D. L., Pedersen, O. F., (1989). "Acoustic rhinometry: evaluation of nasal cavity geometry by acoustic reflection". Journal of Applied Physiology. **66**(1):295-303.
- Hlastlala and Berger (2001), "Physiology of respiration." Oxford University press.
- Incropera, F. P. and DeWitt, D. P. (2002). "Fundamentals of heat and mass transfer". New York. J. Wiley.
- Ingenito et al. (1986). "Finite difference analysis of respiratory heat transfer." Journal of Applied Physiology **61**(6): 2252-2259.
- Institute of Medicine (IOM). (2007). "Assessment of the NIOSH Head-and-Face anthropometric survey of US respirator users." Washington, DC: The National Academies Press.

- Inthavong, K., Tian, Z.F., Li, H.F., Tu, J.Y., Yang, W., Xue, C.L. and Li, C.G. (2006). A numerical study of spray particle deposition in a human nasal cavity. Aerosol Science and Technology. **40** (11): 1034-1045.
- Joerg, L., et al. (2004). "A Numerical Simulation of Intranasal Air Temperature during Inspiration." The Laryngoscope. **114**(6): 1037-1041.
- Johnstone, A., Uddin, M., Pollard, A., Heenan, A. and Finlay, W.H. (2004) "The flow inside an idealized form of the human extra-thoracic airway." Experiments in fluids. **37**:673-689.
- Kaufman, J.W., Askew, G.K., Farahmand, K. (2003). "Apparatus for obtaining temperature and humidity measurements". United States, The United States of America as represented by the Secretary of the Navy (Washington, DC), Patent Number 6659963.
- Keck, T., Leiacker, R., Heinrich, A., Kühnemann, S. and Rettinger, G. (2001). "Humidity and temperature profile in the nasal cavity." Rhinology. **38**(4): 167-171.
- Kjaergaard, T., Cvancarova, M. and Steinsvag, S. K. (2009). "Relation of nasal air flow to nasal cavity dimensions." Arch Otolaryngol Head Neck Surg. **135**(6):565-570.
- Kothandaraman, C. P. and Subramanyan, S. (1975). Heat and mass transfer data book. Wiley Publications, New York.

- Lindemann, J., Keck, T., Wiesmiller, K., Sander, B., Brambs, H. J., Rettinger, G. and Daniela, P. (2004). "A numerical simulation of intranasal air temperature during inspiration." Laryngoscope. **114**:1037-1041.
- Liu, Y., Johnson, M. R., Matida, E. A., Kherani, S., Marsan, J. (2009). "Creation of standardized geometry of the human nasal cavity." Journal of Applied Physiology. **106**:784-795.
- Luo, X. Y., Hinton, J. S., Liew, T.T. and Tan, K. K. (2004). "LES modeling of flow in a simple airway model." Medical Engineering and Physics. **26**:403 – 413.
- Lv, Y. G., Liu, J., Zhang, J. (2006). "Theoretical evaluation of burns to the human respiratory tract due to inhalation of hot gas in the early stage of fires." Journal of the international society for the burn injuries. **32**:436-446.
- Malarbet, J. L., Bertholon, J. F., Becquemin, M. H., Taieb, G., Bouchikhi, A. and Roy, M. (1994). "Oral and nasal flowrate partitioning in healthy subjects performing graded exercise." Radiation Protection Dosimetry. **53**:179-182.
- Malkoc, S., Usumez, S., Nur, M. and Donaghy, C.E. (2005). "Reproducibility of airway dimension and tongue and hyoid positions on lateral cephalograms." AmJ Orthod Dentofacial Orthop. **128**:513-516.
- Tsu et al. (1988). "Dynamics of heat, water and soluble gas exchange in the human airways: 1. A model study." Annals of Biomedical engineering **16**: 547-571.

- McCutchan, J. W. and Taylor, C. L. (1951). "Respiratory Heat Exchange with Varying Temperature and Humidity of Inspired Air." Journal of Applied Physiology. 4(2): 121-135.
- McFadden, E. R., Jr., B. M. Pichurko, et al. (1985). "Thermal mapping of the airways in humans." Journal of Applied Physiology. 58(2): 564-570.
- Mohebbi, A., Farhadi, M. and Erfan, A. (2008). "Assesment of Nasal volume and cross-sectional area by acoustic rhinometry in a sample of normal adult Iranians." Archives of Iranian Medicine. 11(5):555-558.
- Musante, J., Martonen, T.B., Quan, L. and Zhang, Z. (2002). "Flow simulation in the human upper respiratory tract." Cell Biochemistry and Biophysics 37: Cell Biochemistry and Biophysics.
- Naftali, S., Schroter, R.C., Shiner, R.J. and Elad, D. (1998). "Transport Phenomena in the Human Nasal Cavity: A Computational Model." Annals of Biomedical Engineering. 26(5): 831-839.
- Niinimaa, V., Cole, P., Mintz, S. and Shephard, R.J. (1981). "Oronasal distribution of respiratory airflow." Respiration Physiology 43: 69-75
- Pless, D., T. Keck, et al. (2004). "Numerical simulation of air temperature and airflow patterns in the human nose during expiration." Clinical Otolaryngology 29(6): 642-647.
- Robinson, J.R., Russo, J. and Doolittle, R. (2009). "3D Airway reconstruction using visible human data set and human casts with comparison to morphometric data." The Anatomical record. 292:1028-1044.

- Srinivasan, R., Farahmand, K. and Hamidi, M. (2011). "CFD heat transfer simulation for the Human upper Respiratory Tract for oronasal breathing condition." IAJC conference (paper accepted)
- Tang, H., Tu, J. Y., Li, H. F., Au-Hijleh, B., Xue, C. C. and Li, C. G. (2004). "Dynamic analysis of airflow features in a 3D real-anatomical geometry of the human nasal cavity". 15th Australian Fluid Mechanics Conference.
- Technical report (1988). "Anthropometric survey of U.S. army personnel: methods and summary statistics." NATICK/TR-89/044
- Terheyden, H., Maune, S., Mertens, J. and Hilberg, O. (2000). "Acoustic rhinometry: validation by three-dimensionally reconstructed computer tomographic scans." Journal of Applied physiology. **89**:1013-1021.
- Tilman, K., et al. (2000). "Temperature Profile in the Nasal Cavity." The Laryngoscope. **110**(4): 651-654.
- Tsai, C.L., Saidel, G.M., McFadden, E.R., and Fouke, J.M. (1990) "Radial heat and water transport across the airway wall." The American Physiological Society. **69**:222-231.
- Tsu, M., Babb, A. L., Ralph, D. D. and Hlastala, M. P. (1988). "Dynamics of heat, water and soluble gas exchange in the human airways: 1. A model study." Annals of Biomedical engineering. **16**:547-571.

- Varene, P., Ferrus, L., Manier, G. and Gire, J. (1986). "Heat and water respiratory exchanges: comparison between mouth and nose breathings in humans." Clinical Physiology. **6**:405-414 (1986).
- Wang, Y., Liu, Y., Sun, X., Yu, S. and Gao, F. (2009). "Numerical analysis of respiratory flow patterns within human upper airway." Acta Mech Sin 10.1007/s10409-009-0283-1
- Webb, P. (1951). "Air Temperatures in Respiratory Tracts of Resting Subjects in Cold." J Appl Physiol. **4**(5): 378-382.
- Weibel, E. R. (1963). "Morphometry of Human lung". Academic, New York.
- Wen, J., Inthavang, K., Tu, J and Wang, S. (2008). "Numerical simulations for detailed airflow dynamics in a human nasal cavity." Respiratory Physiology and Neurobiology **161**: 125-135
- Wheatley, J.R., Amis, T. C. and Engel, L.A. (1991). "Oronasal partitioning of ventilation during exercise in humans." The American Physiological Society. **71**:546-551.
- X. Sun, C. Yu, Y. Wang and Y. Liu (2007). "Numerical simulation of soft palate and airflow in human upper airway by fluid-structure interaction method." Acta Mech Sin **23**: 359-367.
- Xi, J., Longest, P.W. (2008). "Effects of oral airway geometry characteristics on the diffusional deposition of inhaled nanoparticles." Journal of Bio-mechanical engineering. **130**:1-16.

- Yu, G., Zhang, Z., and Lessman, R. (1996). "Computer simulation of the flow field and particle deposition by diffusion in a 3-D human airway bifurcation." Aerosol science and Technology. **25**:338 – 352.
- Zhang, J., Liu, Y., Sun, X., Yu, S. and Yu, C. (2008). "Computational fluid dynamics simulations of respiratory airflow in human nasal cavity and its characteristic dimension study" Acta mech sin **24**: 223-228.
- Zhang, Z., C. Kleinstreuer, et al. (2003). "Species heat and mass transfer in a human upper airway model." International Journal of heat and mass transfer. **46**: 4755 - 4768.
- Zhang, J., Liu, Y., Sun, X., Yu, S. and Yu, C: Computational fluid dynamics simulations of respiratory airflow in human nasal cavity and its characteristic dimension study. Acta mech sin. **24**:223-228 (2008).
- Zhuang, Z. and Bradtmiller, B. (2005). "Head-and-face anthropometric survey of U.S. respirator users". Journal of Occupational and Environmental Hygiene. **2**:567-576.
- Zhuang, Z., Coffey, C.C. and Roland, B.A. (2005). "The effect of subject characteristics and respirator feature on respirator fit." Journal of Occupational and Environmental Hygiene. **2**:641-649.

APPENDIX-1

The Calculation of the Reynolds number:

The Reynolds number is calculated at the inlet for the Nasal and Oral Cavity:

$$Re = \rho VD / \mu \text{ or } \rho QD / \mu A = VD / \nu$$

Where ρ = density of the fluid (kg/m^3)

V = fluid velocity (m/s)

L = length of tract (m)

μ = dynamic viscosity ($\text{kg/m}\cdot\text{s}$)

Q = volumetric flow rate (m^3/s)

D = diameter of the pipe (m)

A = cross-sectional area (m^2)

ν = kinematic viscosity (m^2/s)

For the dry air at the temp of 100°C (373°K), we have the following values (Heat and mass transfer data book / C. P. Kothandaraman and S. Subramanyan. New York : Wiley, [1975])

$$\rho = 0.946 \text{ kg/m}^3$$

$$\mu = 21.87 \text{ kg/m}\cdot\text{s}$$

$$\nu = 23.13 \times 10^{-6} \text{ m}^2/\text{s}$$

The volumetric flow rate here is $Q = 90$ liters/minute

$$1 \text{ m}^3/\text{s} = 1.5850 \times 10^4 \text{ gal/min (Fundamentals of heat and mass transfer / Frank P.$$

Incropera, David P. DeWitt. New York : J. Wiley, c2002.)

$$90 \text{ liters/min} = 23.775 \text{ gal/min} = 0.0015 \text{ m}^3/\text{s}$$

Velocity = 7.144 m/s (<http://www.1728.com/flowrate.htm>, Volumetric flow rate = Area X

Velocity)

Nasal Cavity:

For a $D = 0.01635$ m, $Q = 0.00075$ m³/s

Velocity = 3.5722 m/s (<http://www.1728.com/flowrate.htm>, Volumetric flow rate = Area X

Velocity)

$$Re = VD/\nu = (3.5722 \times 0.01635) / 23.13 \times 10^{-6} = 2525.09 \approx 2525$$

Oral Cavity:

For a $D = 0.021$ m, $Q = 0.00075$ m³/s

Velocity = 2.1653 m/s (<http://www.1728.com/flowrate.htm>, Volumetric flow rate = Area X

Velocity)

$$Re = (2.1653 \times 0.021) / 23.13 \times 10^{-6} = 1965.90 \approx 1966$$

Tracheal Region:

For a $D = 0.02$ m, $Q = 0.0015$ m³/s

Velocity = 2.3873 m/s (<http://www.1728.com/flowrate.htm>, Volumetric flow rate = Area X

Velocity)

$$Re = (4.7746 \times 0.02) / 23.13 \times 10^{-6} = 4129.70 \approx 4130$$

The Reynolds number here is observed to vary from 1966 to 4130 for the three different portions in the conduit. We here perform the CFD simulation using the Reynolds number based on for trachea using the k- ϵ turbulence model.

APPENDIX-2

MESH 1

File report

File Information for CFX

Case	CFX
File Path	F:\HRT4130_11\HRT_files\dp0\CFX\CFX\CFX_009.res
File Date	05 May 2010
File Time	04:54:52 PM
File Type	CFX5
File Version	12.0

Mesh report

Mesh Information for CFX

Domain	Nodes	Elements
Default Domain	605856	2546507

Physics report

Domain Physics for CFX

Domain - Default Domain	
Type	Fluid
Location	B71
<i>Materials</i>	
Air Ideal Gas	
Fluid Definition	Material Library
Morphology	Continuous Fluid
<i>Settings</i>	
Buoyancy Model	Non Buoyant
Domain Motion	Stationary

Reference Pressure	1.0000e+00 [atm]
Heat Transfer Model	Thermal Energy
Turbulence Model	k epsilon
Turbulent Wall Functions	Scalable

Boundary Physics for CFX

Domain	Boundaries	
Default Domain	Boundary - NasalInlet	
	Type	INLET
	Location	NasalInlet
	<i>Settings</i>	
	Flow Direction	Normal to Boundary Condition
	Flow Regime	Subsonic
	Heat Transfer	Static Temperature
	Static Temperature	3.7300e+02 [K]
	Mass And Momentum	Mass Flow Rate
	Mass Flow Rate	2.0000e-01 [g s ⁻¹]
	Turbulence	Medium Intensity and Eddy Viscosity Ratio
	Boundary - OralInlet	
	Type	INLET
	Location	OralInlet
	<i>Settings</i>	
	Flow Direction	Normal to Boundary Condition
	Flow Regime	Subsonic
	Heat Transfer	Static Temperature
	Static Temperature	3.7300e+02 [K]

Mass And Momentum	Mass Flow Rate
Mass Flow Rate	2.0000e-01 [g s ⁻¹]
Turbulence	Medium Intensity and Eddy Viscosity Ratio
Boundary - Outlet 1	
Type	OUTLET
Location	Outlet1
<i>Settings</i>	
Flow Regime	Subsonic
Mass And Momentum	Average Static Pressure
Pressure Profile Blend	5.0000e-02
Relative Pressure	0.0000e+00 [Pa]
Pressure Averaging	Average Over Whole Outlet
Boundary - Outlet2	
Type	OUTLET
Location	Outlet2
<i>Settings</i>	
Flow Regime	Subsonic
Mass And Momentum	Average Static Pressure
Pressure Profile Blend	5.0000e-02
Relative Pressure	0.0000e+00 [Pa]
Pressure Averaging	Average Over Whole Outlet
Boundary - Default Domain Default	

Type	WALL
Location	F100.71, F101.71, F102.71, F103.71, F73.71, F74.71, F76.71, F77.71, F78.71, F79.71, F80.71, F81.71, F82.71, F84.71, F85.71, F86.71, F87.71, F88.71, F90.71, F91.71, F92.71, F93.71, F94.71, F95.71, F96.71, F97.71, F98.71, F99.71
<i>Settings</i>	
Heat Transfer	Fixed Temperature
Fixed Temperature	3.1000e+02 [K]
Mass And Momentum	No Slip Wall
Wall Roughness	Smooth Wall

MESH 2

File report

File Information for CFX

Case	CFX
File Path	F:\HRT4130_33\HRT_files\dp0\CFX\CFX\CFX_010.res
File Date	06 May 2010
File Time	04:48:12 AM
File Type	CFX5
File Version	12.0

Mesh report

Mesh Information for CFX

Domain	Nodes	Elements
Default Domain	711240	3003027

Physics report

Domain Physics for CFX

Domain - Default Domain	
Type	Fluid
Location	B71
<i>Materials</i>	
Air Ideal Gas	
Fluid Definition	Material Library
Morphology	Continuous Fluid
<i>Settings</i>	
Buoyancy Model	Non Buoyant
Domain Motion	Stationary
Reference Pressure	1.0000e+00 [atm]
Heat Transfer Model	Thermal Energy
Turbulence Model	k epsilon
Turbulent Wall Functions	Scalable

Boundary Physics for CFX

Domain	Boundaries	
Default Domain	Boundary - NasalInlet	
	Type	INLET
	Location	NasalInlet
	<i>Settings</i>	
	Flow Direction	Normal to Boundary Condition
	Flow Regime	Subsonic
	Heat Transfer	Static Temperature
	Static Temperature	3.7300e+02 [K]
	Mass And	Mass Flow Rate

Momentum	
Mass Flow Rate	2.0000e-01 [g s ⁻¹]
Turbulence	Medium Intensity and Eddy Viscosity Ratio
Boundary - OralInlet	
Type	INLET
Location	OralInlet
<i>Settings</i>	
Flow Direction	Normal to Boundary Condition
Flow Regime	Subsonic
Heat Transfer	Static Temperature
Static Temperature	3.7300e+02 [K]
Mass And Momentum	Mass Flow Rate
Mass Flow Rate	2.0000e-01 [g s ⁻¹]
Turbulence	Medium Intensity and Eddy Viscosity Ratio
Boundary - Outlet 1	
Type	OUTLET
Location	Outlet1
<i>Settings</i>	
Flow Regime	Subsonic
Mass And Momentum	Average Static Pressure
Pressure Profile Blend	5.0000e-02
Relative Pressure	0.0000e+00 [Pa]
Pressure Averaging	Average Over Whole Outlet
Boundary - Outlet2	

Type	OUTLET
Location	Outlet2
<i>Settings</i>	
Flow Regime	Subsonic
Mass And Momentum	Average Static Pressure
Pressure Profile Blend	5.0000e-02
Relative Pressure	0.0000e+00 [Pa]
Pressure Averaging	Average Over Whole Outlet
Boundary - Default Domain Default	
Type	WALL
Location	F100.71, F101.71, F102.71, F103.71, F73.71, F74.71, F76.71, F77.71, F78.71, F79.71, F80.71, F81.71, F82.71, F84.71, F85.71, F86.71, F87.71, F88.71, F90.71, F91.71, F92.71, F93.71, F94.71, F95.71, F96.71, F97.71, F98.71, F99.71
<i>Settings</i>	
Heat Transfer	Fixed Temperature
Fixed Temperature	3.1000e+02 [K]
Mass And Momentum	No Slip Wall
Wall Roughness	Smooth Wall

NASAL

File report

File Information for CFX

Case	CFX
------	-----

File Path	F:\HRT3Nasal\HRT_files\dp0\CFX\CFX\CFX_011.res
File Date	16 July 2010
File Time	05:36:58 PM
File Type	CFX5
File Version	12.0

Mesh report

Mesh Information for CFX

Domain	Nodes	Elements
Default Domain	711240	3003027

Physics report

Domain Physics for CFX

Domain - Default Domain	
Type	Fluid
Location	B71
<i>Materials</i>	
Air Ideal Gas	
Fluid Definition	Material Library
Morphology	Continuous Fluid
<i>Settings</i>	
Buoyancy Model	Non Buoyant
Domain Motion	Stationary
Reference Pressure	1.0000e+00 [atm]
Heat Transfer Model	Thermal Energy
Turbulence Model	k epsilon
Turbulent Wall Functions	Scalable

Boundary Physics for CFX

Domain	Boundaries	
Default Domain	Boundary - NasalInlet	
	Type	INLET
	Location	NasalInlet
	<i>Settings</i>	
	Flow Direction	Normal to Boundary Condition
	Flow Regime	Subsonic
	Heat Transfer	Static Temperature
	Static Temperature	3.7300e+02 [K]
	Mass And Momentum	Mass Flow Rate
	Mass Flow Rate	2.0000e-01 [g s ⁻¹]
	Turbulence	Medium Intensity and Eddy Viscosity Ratio
	Boundary - Outlet 1	
	Type	OUTLET
	Location	Outlet1
	<i>Settings</i>	
	Flow Regime	Subsonic
	Mass And Momentum	Average Static Pressure
	Pressure Profile Blend	5.0000e-02
	Relative Pressure	0.0000e+00 [Pa]
	Pressure Averaging	Average Over Whole Outlet
	Boundary - Outlet2	
	Type	OUTLET

Location	Outlet2
<i>Settings</i>	
Flow Regime	Subsonic
Mass And Momentum	Average Static Pressure
Pressure Profile Blend	5.0000e-02
Relative Pressure	0.0000e+00 [Pa]
Pressure Averaging	Average Over Whole Outlet
Boundary - Default Domain Default	
Type	WALL
Location	F100.71, F101.71, F102.71, F103.71, F73.71, F74.71, F76.71, F77.71, F78.71, F79.71, F80.71, F81.71, F82.71, F83.71, F84.71, F85.71, F86.71, F87.71, F88.71, F90.71, F91.71, F92.71, F93.71, F94.71, F95.71, F96.71, F97.71, F98.71, F99.71
<i>Settings</i>	
Heat Transfer	Fixed Temperature
Fixed Temperature	3.1000e+02 [K]
Mass And Momentum	No Slip Wall
Wall Roughness	Smooth Wall

ORAL

File report

File Information for CFX

Case	CFX
File Path	F:\HRT3Oral\HRT_files\dp0\CFX\CFX\CFX_011.res

File Date	16 July 2010
File Time	11:42:44 PM
File Type	CFX5
File Version	12.0

Mesh report

Mesh Information for CFX

Domain	Nodes	Elements
Default Domain	711240	3003027

Physics report

Domain Physics for CFX

Domain - Default Domain	
Type	Fluid
Location	B71
<i>Materials</i>	
Air Ideal Gas	
Fluid Definition	Material Library
Morphology	Continuous Fluid
<i>Settings</i>	
Buoyancy Model	Non Buoyant
Domain Motion	Stationary
Reference Pressure	1.0000e+00 [atm]
Heat Transfer Model	Thermal Energy
Turbulence Model	k epsilon
Turbulent Wall Functions	Scalable

Boundary Physics for CFX

Domain	Boundaries

Default Domain	Boundary - OralInlet	
	Type	INLET
	Location	OralInlet
	<i>Settings</i>	
	Flow Direction	Normal to Boundary Condition
	Flow Regime	Subsonic
	Heat Transfer	Static Temperature
	Static Temperature	3.7300e+02 [K]
	Mass And Momentum	Mass Flow Rate
	Mass Flow Rate	2.0000e-01 [g s ⁻¹]
	Turbulence	Medium Intensity and Eddy Viscosity Ratio
	Boundary - Outlet 1	
	Type	OUTLET
	Location	Outlet1
	<i>Settings</i>	
	Flow Regime	Subsonic
	Mass And Momentum	Average Static Pressure
	Pressure Profile Blend	5.0000e-02
	Relative Pressure	0.0000e+00 [Pa]
	Pressure Averaging	Average Over Whole Outlet
	Boundary - Outlet2	
	Type	OUTLET
	Location	Outlet2
	<i>Settings</i>	

Flow Regime	Subsonic
Mass And Momentum	Average Static Pressure
Pressure Profile Blend	5.0000e-02
Relative Pressure	0.0000e+00 [Pa]
Pressure Averaging	Average Over Whole Outlet
Boundary - Default Domain Default	
Type	WALL
Location	F100.71, F101.71, F102.71, F103.71, F73.71, F74.71, F76.71, F77.71, F78.71, F79.71, F80.71, F81.71, F82.71, F84.71, F85.71, F86.71, F87.71, F88.71, F89.71, F90.71, F91.71, F92.71, F93.71, F94.71, F95.71, F96.71, F97.71, F98.71, F99.71
<i>Settings</i>	
Heat Transfer	Fixed Temperature
Fixed Temperature	3.1000e+02 [K]
Mass And Momentum	No Slip Wall
Wall Roughness	Smooth Wall

Higher temperature of 423K

File report

File Information for CFX

Case	CFX
File Path	F:\HRT423K\HRT_files\dp0\CFX\CFX\CFX_011.res
File Date	17 July 2010

File Time	08:18:46 PM
File Type	CFX5
File Version	12.0

Mesh report

Mesh Information for CFX

Domain	Nodes	Elements
Default Domain	711240	3003027

Physics report

Domain Physics for CFX

Domain - Default Domain	
Type	Fluid
Location	B71
<i>Materials</i>	
Air Ideal Gas	
Fluid Definition	Material Library
Morphology	Continuous Fluid
<i>Settings</i>	
Buoyancy Model	Non Buoyant
Domain Motion	Stationary
Reference Pressure	1.0000e+00 [atm]
Heat Transfer Model	Thermal Energy
Turbulence Model	k epsilon
Turbulent Wall Functions	Scalable

Boundary Physics for CFX

Domain	Boundaries
Default	Boundary - NasalInlet

Domain	Type	INLET
	Location	NasalInlet
	<i>Settings</i>	
	Flow Direction	Normal to Boundary Condition
	Flow Regime	Subsonic
	Heat Transfer	Static Temperature
	Static Temperature	4.2300e+02 [K]
	Mass And Momentum	Mass Flow Rate
	Mass Flow Rate	2.0000e-01 [g s ⁻¹]
	Turbulence	Medium Intensity and Eddy Viscosity Ratio
	Boundary - OralInlet	
	Type	INLET
	Location	OralInlet
	<i>Settings</i>	
Flow Direction	Normal to Boundary Condition	
Flow Regime	Subsonic	
Heat Transfer	Static Temperature	
Static Temperature	4.2300e+02 [K]	
Mass And Momentum	Mass Flow Rate	
Mass Flow Rate	2.0000e-01 [g s ⁻¹]	
Turbulence	Medium Intensity and Eddy Viscosity Ratio	
Boundary - Outlet 1		
Type	OUTLET	
Location	Outlet1	
<i>Settings</i>		

Flow Regime	Subsonic
Mass And Momentum	Average Static Pressure
Pressure Profile Blend	5.0000e-02
Relative Pressure	0.0000e+00 [Pa]
Pressure Averaging	Average Over Whole Outlet
Boundary - Outlet2	
Type	OUTLET
Location	Outlet2
<i>Settings</i>	
Flow Regime	Subsonic
Mass And Momentum	Average Static Pressure
Pressure Profile Blend	5.0000e-02
Relative Pressure	0.0000e+00 [Pa]
Pressure Averaging	Average Over Whole Outlet
Boundary - Default Domain Default	
Type	WALL
Location	F100.71, F101.71, F102.71, F103.71, F73.71, F74.71, F76.71, F77.71, F78.71, F79.71, F80.71, F81.71, F82.71, F84.71, F85.71, F86.71, F87.71, F88.71, F90.71, F91.71, F92.71, F93.71, F94.71, F95.71, F96.71, F97.71, F98.71, F99.71
<i>Settings</i>	
Heat Transfer	Fixed Temperature
Fixed Temperature	3.1000e+02 [K]

Mass And Momentum		No Slip Wall
Wall Roughness	Stationary	Smooth Wall

HRT comparison

File report

File Information for CFX

Case	CFX
File Path	F:\HRTverification\HRT_files\dp0\CFX\CFX\CFX_012.res
File Date	19 July 2010
File Time	04:42:28 PM
File Type	CFX5
File Version	12.0

Mesh report

Mesh Information for CFX

Domain	Nodes	Elements
Default Domain	707648	2982411

Physics report

Domain Physics for CFX

Domain - Default Domain	
Type	Fluid
Location	B71
<i>Materials</i>	
Air Ideal Gas	
Fluid Definition	Material Library
Morphology	Continuous Fluid

<i>Settings</i>	
Buoyancy Model	Non Buoyant
Domain Motion	Stationary
Reference Pressure	1.0000e+00 [atm]
Heat Transfer Model	Thermal Energy
Turbulence Model	k epsilon
Turbulent Wall Functions	Scalable

Boundary Physics for CFX

Domain	Boundaries	
Default Domain	Boundary - NasalInlet	
	Type	INLET
	Location	NasalInlet
	<i>Settings</i>	
	Flow Direction	Normal to Boundary Condition
	Flow Regime	Subsonic
	Heat Transfer	Static Temperature
	Static Temperature	2.9300e+02 [K]
	Mass And Momentum	Mass Flow Rate
	Mass Flow Rate	2.6800e-03 [g s ⁻¹]
	Turbulence	Medium Intensity and Eddy Viscosity Ratio
	Boundary - Outlet 1	
	Type	OUTLET
	Location	Outlet1
	<i>Settings</i>	
	Flow Regime	Subsonic

Mass And Momentum	Average Static Pressure
Pressure Profile Blend	5.0000e-02
Relative Pressure	0.0000e+00 [Pa]
Pressure Averaging	Average Over Whole Outlet
Boundary - Outlet2	
Type	OUTLET
Location	Outlet2
<i>Settings</i>	
Flow Regime	Subsonic
Mass And Momentum	Average Static Pressure
Pressure Profile Blend	5.0000e-02
Relative Pressure	0.0000e+00 [Pa]
Pressure Averaging	Average Over Whole Outlet
Boundary - Default Domain Default	
Type	WALL
Location	F100.71, F101.71, F102.71, F103.71, F73.71, F74.71, F76.71, F77.71, F78.71, F79.71, F80.71, F81.71, F82.71, F83.71, F84.71, F85.71, F86.71, F87.71, F88.71, F90.71, F91.71, F92.71, F93.71, F94.71, F95.71, F96.71, F97.71, F98.71, F99.71
<i>Settings</i>	
Heat Transfer	Adiabatic
Mass And Momentum	No Slip Wall
Wall Roughness	Smooth Wall